Nagra
Nationale
Genossenschaft
für die Lagerung
radioaktiver Abfälle

Cédra
Société coopérative
nationale
pour l'entreposage
de déchets radioactifs

Cisra
Società cooperativa
nazionale
per l'immagazzinamento
di scorie radioattive

TECHNICAL REPORT 86-12 E

Bentonite as a backfill material in the high-level waste repository: chemical aspects

R. Grauer

January 1986

Swiss Federal Institute for Reactor Research, Würenlingen

Parkstrasse 23 5401 Baden/Schweiz Telephon 056/20 55 11

Nagra
Nationale
Genossenschaft
für die Lagerung
radioaktiver Abfälle

Cédra
Société coopérative
nationale
pour l'entreposage
de déchets radioactifs

Cisra
Società cooperativa
nazionale
per l'immagazzinamento
di scorie radioattive

TECHNICAL REPORT 86-12 E

Bentonite as a backfill material in the high-level waste repository: chemical aspects

R. Grauer

January 1986

Swiss Federal Institute for Reactor Research, Würenlingen

Parkstrasse 23 5401 Baden/Schweiz Telephon 056/20 55 11

FOREWORD

This report was prepared as an account of work sponsored by Nagra. The viewpoints presented and conclusions reached are those of the author(s) and do not necessarily represent those of Nagra.

SUMMARY

The present Nagra concept for disposal of high-level waste foresees emplacing the steel canisters enclosing the borosilicate glass in tunnels of 3.7 m diameter at a depth of 1000 to 1500 m. These tunnels are to be backfilled with compacted bentonite, a clay with a high montmorillonite content. Bentonites are suitable as a backfill due to, inter alia, their swelling capability, their low hydraulic conductivity and their sorption properties.

This report is restricted to those chemical aspects of the backfill material which can affect the behaviour of a repository system: swelling capability, sorption properties and long-term stability.

Under repository conditions, the swelling of montmorillonite upon water inflow is primarily innercrystalline. At present, there is no microscopic model which gives a quantitative description of this process. However, on the basis of equilibrium thermodynamics, relationships can be deduced between swelling pressure and experimentally more easily determinable water vapour sorption isotherms and heats of immersion.

Cation adsorption, which is important for nuclide retention in the repository, can be described by appropriate models. However, for various reasons, interpretation of published sorption data is rarely possible from a theoretical viewpoint and direct diffusion measurements on compacted bentonite are therefore preferable to the use of sorption data.

It can be concluded from natural analogue studies and from laboratory experiments that the properties of the backfill material will not alter significantly over a period of 10^6 years. Nevertheless, in the long term, the formation of mixed-layer illite/montmorillonite cannot be ruled out. Such mixed-layer clays still have good swelling and sorption properties. Given the quantity ratios foreseen, no adverse changes due to radioactive decay are to be expected.

The interactions between the bentonite and the container corrosion products must, in the absence of literature data, be investigated experimentally. The type of reaction products expected (iron-containing clay minerals) and the high bentonite/iron ratio lead to the conclusion that the function of the backfill need not be impaired by these processes.

Because of its better stability, a calcium bentonite is preferable to the sodium variant. A low iron content is desirable because, under reducing conditions, the surface charge of the montmorillonite is increased by reduction of iron (III). Organic and sulphidic contaminants should also be kept to a minimum.

TABLE OF CONTENTS PAGE

1 THE REPOSITORY CONCEPT AND THE REQUIREMENTS ON THE BACKFILL MATERIAL

1.1 The high-level waste repository concept

The current Swiss concept for disposal of high-level radioactive waste is described in detail in the Nagra Project "Gewähr" reports /102/. The planned multiple safety barrier principle is therefore only summarised in Figure 1.

The waste is immobilised in a borosilicate glass matrix and then emplaced in a self-supporting steel canister with a wall thickness of 25 cm. The canister is designed to have a lifetime of at least 1000 years. After this time, the concentration of the two critical nuclides Sr-90 and Cs-137 has dropped to a negligible level and the temperature in the repository has reached the ambient temperature of around 55°C.

The steel canisters are emplaced at a depth of 1000 to 1500 m in the host rock (granite or gneiss) in tunnels with a diameter of 3.7 m. These tunnels are to be backfilled with bentonite, i.e. a material with a high content of the clay mineral montmorillonite.

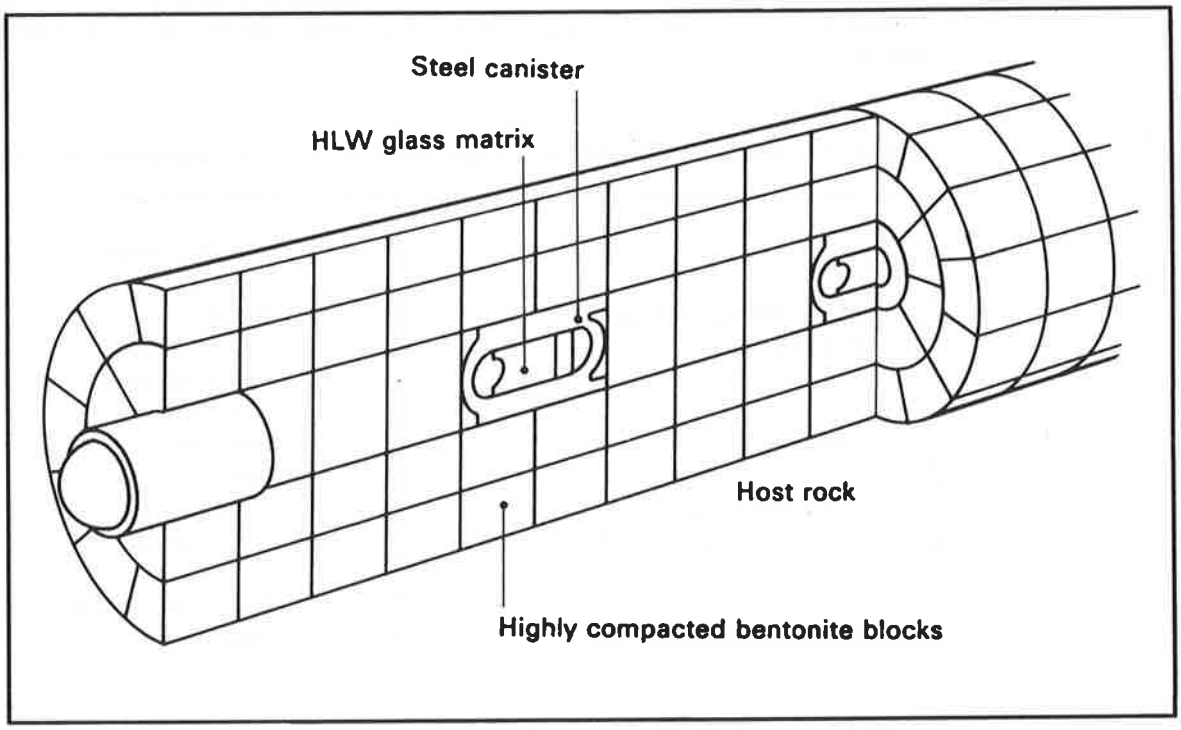

Fig. 1: The technical safety barrier system in a high-level waste repository. The tunnel diameter is 3.7 m (Nagra).

1.2 Requirements on the backfill material

The backfill material in a repository is an important link in the safety barrier chain and has to fulfil certain physical/ mechanical and chemical requirements. The most important of these are (cf. also /128, 133, 185, 187/):

- low water permeability compared to the host rock
- high radionuclide retention capacity
- compatibility with other repository components
- the ability to swell and seal voids caused by construction and rock fissures
- plasticity to absorb rock displacements and to allow homogeneous pressure distribution
- sufficient loading capacity to prevent the canister sinking
- stability over a period of at least 10^6 years
- sufficient availability and economic viability

This list of requirements is fulfilled more or less successfully by a number of materials or compounds. Table 1 gives a selection of suggested backfill materials. A compilation of material properties is given in /105/.

Bentonite was selected as a tunnel backfill material in Project "Gewähr" /102/ and fulfils the requirements to a very large extent.

Table 1: Suggested backfill materials for a repository /25/

Clays	Minerals, rocks
Na- and Ca-bentonite	Pyrite
Illite	Glauconite
	Serpentine
Zeolites	Anhydrite
	Basalt
Clinoptilolite	Tuff
Synthetic products	
	Drying agents
Silica sand	Calcium oxide
	Magnesium oxide
Metal powders and compounds	
Iron	Activated carbons
Aluminium	
Lead oxide	

Sweden also plans to use bentonite as a backfill material. Numerous reports have been produced in this connection, the more general ones being /128, 129, 133/. Further works which concern themselves exclusively or partly with bentonite as a backfill material are /103, 105, 158, 187/. Brookins /25/ gives a summary mainly of American work. The investigations of bentonites carried out at the request of Nagra are mentioned later in the text.

1.3 Aim of this report

As there are already numerous publications on the use of bentonites as a backfill material, this report is not intended to give yet another summary overview but rather to deal with the important chemical aspects which determine or influence the behaviour of bentonite in a repository system. The main emphasis is therefore on swelling behaviour, sorption properties and stability under repository conditions. In the latter connection, the interactions of the bentonite with canister corrosion products and with the glass matrix have to be taken into account, as well as possible diagenetic reactions and resistance to radiation.

Restriction of the report to these selected aspects should not obscure the fact that a repository is a complex system /102/ and that isolated consideration of individual components can sometimes lead to incorrect conclusions.

2 THE STRUCTURE OF CLAY MINERALS AND NATURAL BENTONITES

2.1 The structure of clay minerals

The essential component of bentonites is the clay mineral montmorillonite, the properties of which are closely linked to its structure. The structure of clay minerals is discussed here only in so far as is necessary for the understanding of their chemical and physical properties. More extensive treatment of physical aspects can be found in the monographs /23, 63/ which form the basis for the following information. The "Silicates" /86/ and "Clays and clay minerals" /85/ chapters of Ullmann's Encyclopaedia of Technical Chemistry give a more concise presentation.

2.1.1 Structural principles

The structural components of the layer silicates (phyllosilicates) are $[SiO_4]$-tetrahedrons (T) and $[MO_6]$-octahedrons (O), the metal ion M usually being aluminium or magnesium. The octahedrons form layers from two sheets of close-packed oxygen or hydroxyl ions (Figure 2). With M = Al, only 2/3 of the octahedral positions are occupied (dioctahedral series). With M = Mg, all positions are occupied (trioctahedral series).

The $[SiO_4]$-tetrahedrons are linked together in the form shown in Figure 2: all silicon atoms lie in one plane. This arrangement does not result in close oxygen packing: each set of six tetrahedrons encloses a hexagonal gap.

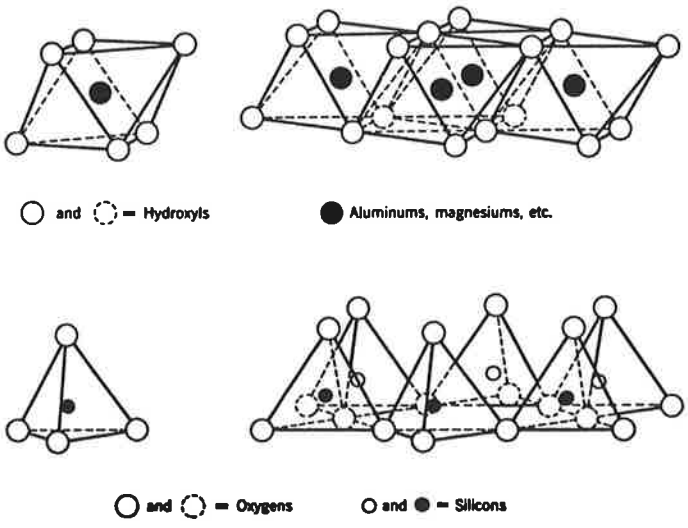

Fig. 2: The structural components of the layer silicates. Above: $[MO_6]$-octahedrons and their arrangement in the O-layer. Below: $[SiO_4]$-tetrahedrons and their arrangement in the T-layer in the form of a hexagonal network /63/.

The large variety of layer silicates is due to the different sequencing of T and O layers. The two-layer silicates such as kaolinite are constructed from T-O stacks while the micaceous three-layer silicates have a T-O-T layer sequence. Further variations are achieved through the isomorphic replacement of metal ions, for example by substitution of Al(III) for an Si(IV) in the T-layer or replacement of octahedral Al(III) by Mg(II). Such substitutions give the layer units a negative charge which is balanced by cations in the interlayer spaces (Figure 3). The charge density of the layers and the hydration behaviour of the interlayer cations are the main parameters influencing the swelling and ion-exchange behaviour of the clay minerals. A high layer charge and low heat of hydration of the interlayer cation (e.g. K^+) result in stable bonding of the layer units in the case of micas. These minerals do not swell in water and the interlayer ions cannot be exchanged. Table 2 gives a systematic overview of the different groups of three-layer silicates.

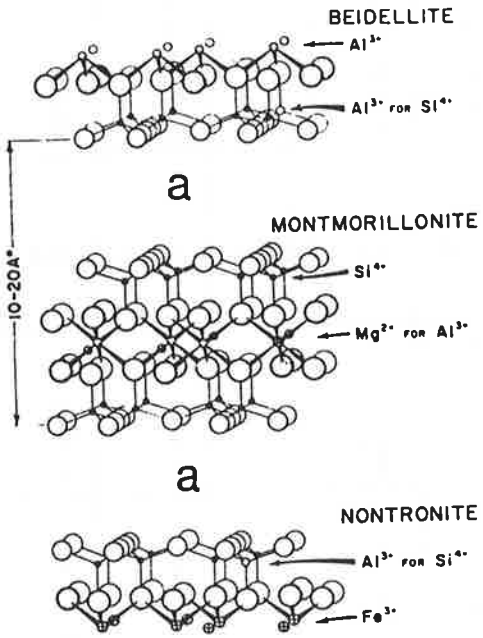

Fig. 3: Smectite structure with the main isomorphic substitutions. The interlayer spaces (a) contain cations and water /132/.

Table 2: Systematics of micaceous layer silicates with the general formula:

$$M^{n+}_{(x+y)/n}(H_2O)_m\,(Al,Mg)^{(6-x)+}_{2\text{ to }3}(OH)_2(Si_{4-y}Al_yO_{10})^{(x+y)-}$$

according to /86/

Layer charge x + y pro $O_{10}(OH)_2$	Group	Main cations in the O-layer	Name of silicate dioct.series	Name of silicate trioct.series	Inner cryst. swelling	Interlayer cations
0	Pyrophillite Talc	Al Mg	Pyrophillite	Talc	- -	- -
0.-2 - 0.6	Smectites x >y x <y	Al Mg Al Fe(III) Mg Zn	Montmorillonite Beidellite Nontronite	Hectorite Saponite Sauconite	 Marked	$Na^+(K^+)$ Ca^{2+}, Mg^{2+}
0.6 - 0.8	Vermiculites	Al Mg Fe	Dioct.vermicul.	Vermiculite Jefferisite	+)*	Mg^{2+}, Ca^{2+} (Na^+)
0.6 - 0.9	Illites	Al Mg Fe(II)	Illite	Tioct.illite Glauconite Seladonite	-	$K^+(Na^+, Li^+)$
0.9 - 1.1	Micas (x ≅ 0)	Al Mg Fe(II)	Moskovite Paragonite	Phlogopite Biotite	-	$K^+(Na^+, Li^+)$
1.8 - 2.0	Brittle Micas (x ≅ 0)	Al Mg	Margarite Ephesite	Xantophyllite	-	Ca^{2+}, (Na^+)

x: charge of the O-layer
y: charge of the T-layer

*) can be blocked with K^+, NH_4^+, Rb^+, Cs^+, Tl^+

2.1.2 Structural models

Kaolinite is a two-layer silicate with the structural formula $Si_4Al_4O_{10}(OH)_8$ (Figure 4). The T-O layer units are uncharged and held together by van der Waals forces. Kaolinite is triclinic with a = 5.155 Å, b = 8.959 Å, c = 7.407 Å, α = 91.68°, β = 104.87°, γ = 89.93°. Halloysite has a similar structure, its layer units being separated by 2 or 4 H_2O per formula unit. Serpentine minerals are trioctahedral variants of the kaolinite structure /86/.

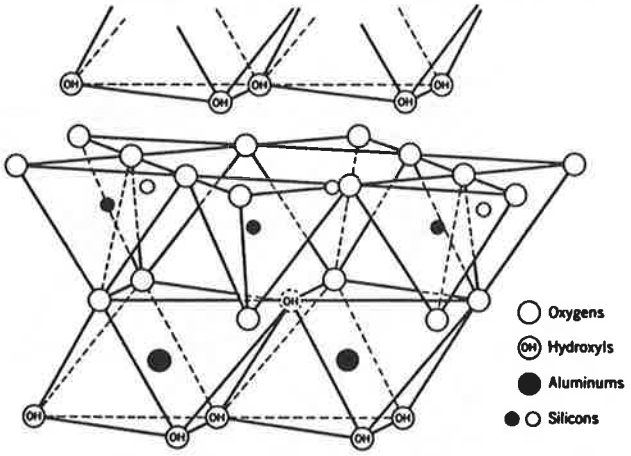

Fig. 4: The structure of kaolinite /63/.

Monoclinic pyrophyllite, $Al_4Si_8O_{20}(OH)_4$, can be considered as a prototype for the three-layer silicates. It is constructed from T-O-T layer units (Figure 5). Because the layers are not charged in this mineral, the individual units are also held together by van der Waals forces in this case. The trioctahedral variant is talc, $Mg_6Si_8O_{20}(OH)_4$.

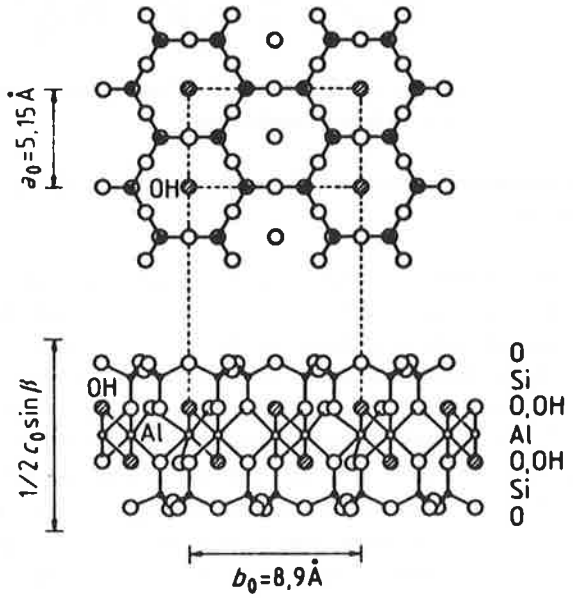

Fig. 5: The structure of pyrophyllite. Projection parallel to the c-axis on (001) and on a plane vertical to the a-axis. c_o = 18.55 Å /86/.

Montmorillonite is derived from pyrophyllite through isomorphic replacement of aluminium with magnesium in the octahedral layer. In the case of beidellite, the layer charge is localised in the tetrahedral layers (replacement of silicon with aluminium). The layer charge of these minerals lies in the range of 0.2 to 0.6 unit charges per $O_{10}(OH)_2$-unit, i.e. per half unit cell. This is balanced by cations in the interlayers (Figure 6). The charge and size of these ions and, therefore, their hydration behaviour determine (with a given layer charge) the spacing of the T-O-T packages, i.e. the crystallographic c-axis.

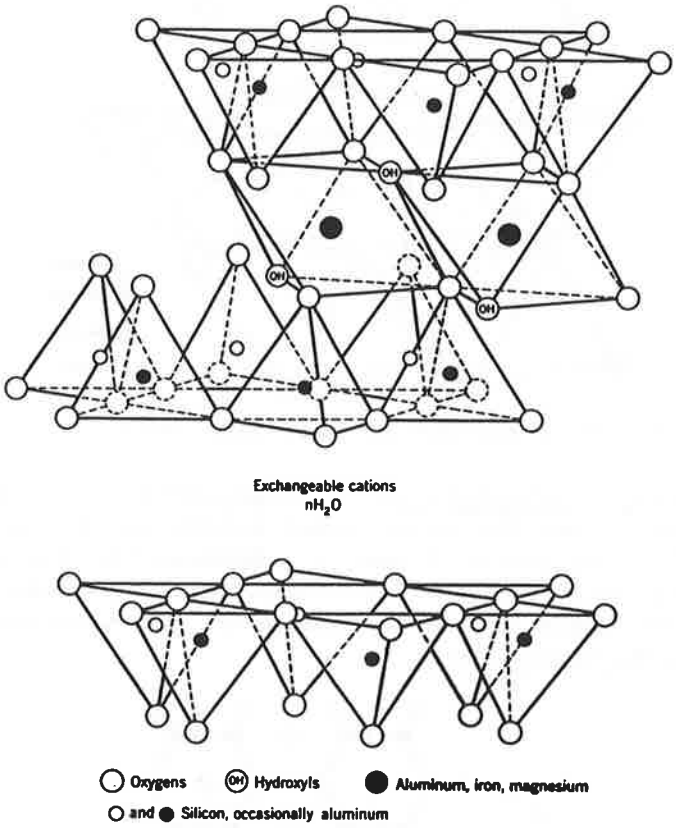

Fig. 6: Montmorillonite structure according to Hofmann et al. /63/.

Edelmann and Favejee /42/ have suggested an alternative structural model for montmorillonite, which should give a better explanation of adsorption behaviour in particular (Figure 7). In contrast with Hofmann's model, every second $[SiO_4]$-tetrahedron is inverted and points in the interlayer direction with an OH instead of an oxygen. For reasons of electro-neutrality, it is necessary to replace oxygen by OH ions in the octahedral layer. The ideal formula is $Al_4Si_8O_{16}(OH)_{12}$. This model is able to explain cation exchange capacity without layer charge by isomorphic replacement because the hydrogen ions of the OH group can be exchanged for cations.

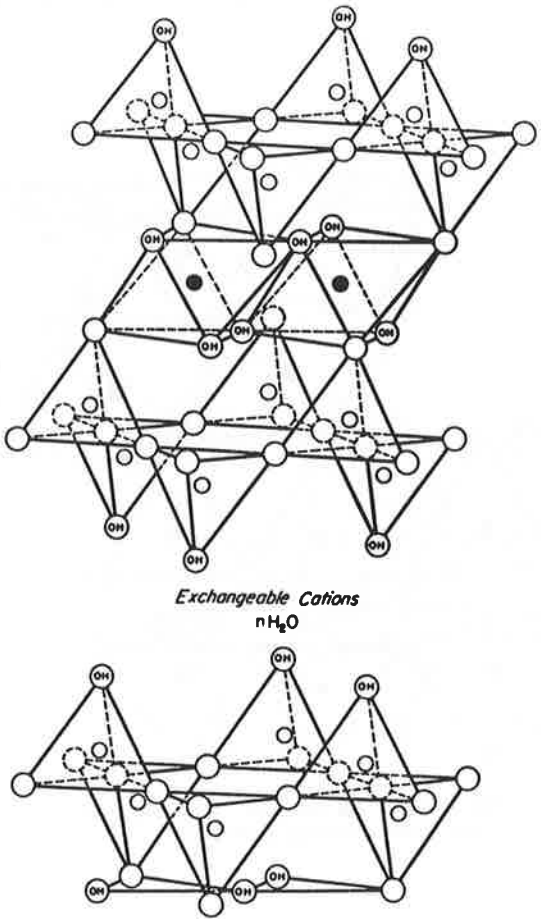

Fig. 7: Modified structural model of montmorillonite according to Edelmann and Favejee /63/.

Although this model gives a better explanation of sorption chemistry than the Hofmann model, its authors have found no conclusive arguments from X-ray investigations against the Hofmann model. An even more modified suggestion /43/ in which only 20% of the tetrahedrons are inverted appears questionable /63, p.89/. For this reason, the structural model in Figure 6 is generally accepted today.

Illite and the micas also have a similar structure to montmorillonite. They differ from the latter in having increased isomorphic replacement of silicon by aluminium and in the layer charge being balanced by non-hydrated potassium ions (Figure 8).

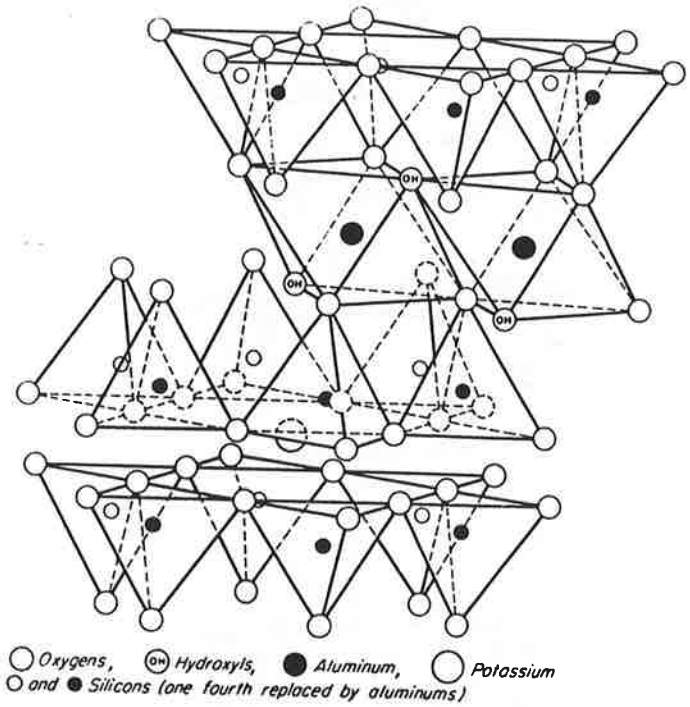

Fig. 8: The structure of muscovite /63/.

In the endmembers of the series, a quarter of the silicon is replaced by aluminium and the layer charge is therefore 2 per unit cell. The dioctahedral endmember is muscovite, $K_2Al_4(Si_6Al_2)O_{20}(OH)_4$. The micas of the biotite group are trioctahedral with magnesium and iron in the octahedral positions (biotite: $K_2(Mg,Fe)_6(Si_6Al_2)O_{20}(OH)_4$.)

Chlorite has a similar structure to the smectites, with the difference that the interlayers are filled with a magnesium hydroxide layer (brucite layer; see Figure 9). Chlorite is trioctahedral ($(Mg,Fe)_6(Si,Al)_8O_{20}(OH)_4$). The negative charge of the T-O-T layer unit is balanced by isomorphic replacement of magnesium with aluminium in the brucite layer. This layer has the general formula $[Mg_{6-x}Al_x(OH)_{12}]^{x+}$.

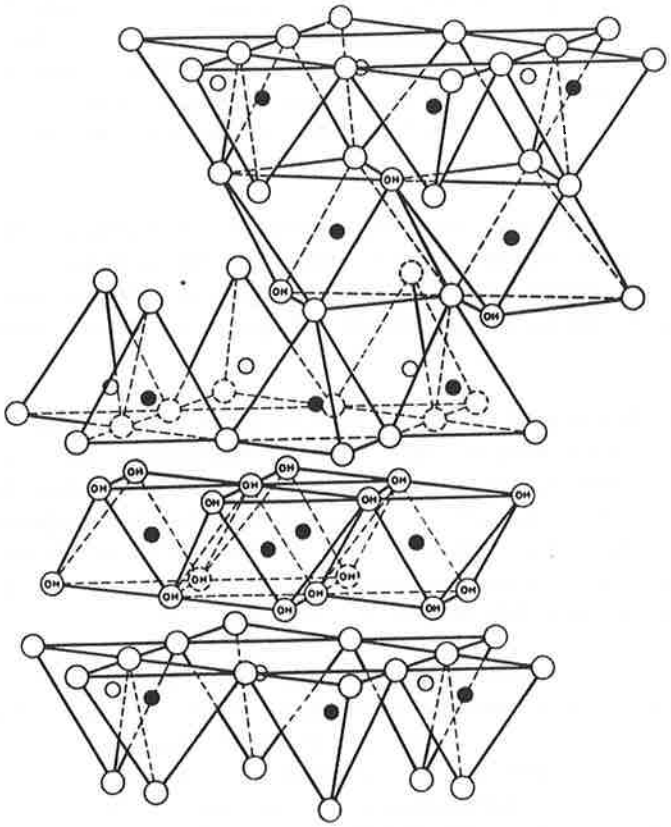

Fig. 9: The structure of chlorite /63/.

Natural clay minerals often do not correspond to ideal compositions and structures. For example, isomorphic replacement in montmorillonites is not restricted solely to the octahedral layer. There are often interstratifications of structural units of different minerals, e.g. illite/smectite or smectite/chlorite. Such interstratifications can be statistical or regular (cf. e.g. p.251 in /23/).

2.2 Natural bentonites

There is a comprehensive monograph on bentonites /64/. Vogt and Köster /175/ have carried out in-depth chemical and mineralogic investigations on 19 bentonite samples. Further reference should be made to the monographs /171, 172/ which deal particularly with the properties of the individual clay minerals.

Bentonites - named after Fort Benton where they were discovered - are plastic clays with a high swelling capacity. Originally, the term bentonite was used only for those products produced in situ by a reaction of volcanic ash with water. However, the term is also used occasionally for clays with "bentonitic" properties formed by hydrothermal alteration of volcanic rock.

The main component of bentonites is montmorillonite, the content of which can range from 65 to 99%. Depending on the composition of the volcanic ash and the formation conditions, bentonites contain varying proportions of quartz, mica, feldspars and other minerals.

The montmorillonite interlayers mostly contain calcium, often together with magnesium. Sodium montmorillonites are rarer, typical ones being the Wyoming bentonites. The nature of the exchangeable cations is determined by the composition of the volcanic ash and there is no correlation with water composition. The montmorillonite in bentonites is unusually finely grained. Most particles are smaller than 0.2 μm.

Bentonites are found world-wide /64/ but often not in workable deposits. The Wyoming bentonites have already been mentioned. There are further deposits in South Dakota and Montana. Significant deposits of Ca-bentonites exist in Bavaria, the montmorillonite containing large quantities of iron in the octahedral layer. The Swiss bentonite at Bischofszell is only a small deposit. Its high layer charge of 0.64 per $O_{10}(OH)_2$-unit and high magnesium content made it unsuitable as a backfill material.

An Na-bentonite (MX-80 from Wyoming) and a Ca-bentonite (Montigel from Bavaria) were investigated more closely in connection with Project Gewähr /106, 107/. Their mineralogic composition is given in Table 3. Noteworthy is the different content of organic carbon which could be important for the complexation of heavy metals.

The mineral formulae and further properties are summarised in Table 4.

Table 3: Mineralogic composition of the bentonites MX-80 and Montigel in percentage of kiln-dried samples /107/.

Mineral	MX-80 %	Montigel %
Montmorillonite	75	66
Quartz	15.2	8.3
Mica	< 1	12-15
Feldspars	5-8	2-4
Carbonates	1.4	3.8
Kaolinite	< 1	2
Pyrite (FeS_2)	0.3	0
Other minerals	2	2-3
Organic carbon	0.4	0.03

Table 4: Mineral formulae and other data for the bentonites MX-80 and Montigel /107/.

Mineral formula of montmorillonite:

MX-80: $(Si_{3.96}Al_{0.04})(Al_{1.55}Fe^{3+}_{0.20}Fe^{2+}_{0.01}Mg_{0.24})O_{10}(OH)_2Na_{0.30}$

Montigel: $Si_{4.00}(Al_{1.36}Fe^{3+}_{0.31}Fe^{2}_{0.01}Mg_{0.35})O_{10}(OH)_2(Ca,Mg)_{0.14}$

	MX-80	Montigel
Montmorillonite content	75%	66%
Molar mass of montmorillonite	372.6 g	375.0 g
Bentonite surface	562 m^2/g	493 m^2/g
Cation exchange capacity	76 meq/100g	62 meq/100g
Exchangeable ions	86% Na^+	61% Ca^{2+} 36% Mg^{2+}
Interlayer charge per $O_{10}(OH)_2$-unit	0.30	0.28
Density of bentonite	2.755 g/cm^3	2.847 g/cm^3

3 CLAY/WATER SYSTEMS

3.1 Water composition in contact with bentonite

pH is an important parameter with respect to the corrosion behaviour of the steel canister and the glass waste matrix. In the bentonite backfill, it is not determined by the pH of the formation water alone. Solution equilibria, possible diagenetic reactions and reactions of impurities can all affect the pH.

With a low water flow through the backfill, the water composition is initially modified by the solubility of the bentonite. Both congruent and incongruent dissolution lead to an increase in pH, e.g. according to

$$3\ Na_{0.33}Al_{2.33}Si_{3.67}O_{10}(OH)_2 + 12^1/_2\ H_2O \longrightarrow$$

$$3^1/_2\ Al_2Si_2O_5(OH)_4 + 4\ H_4SiO_4 + Na^+ + OH^-$$

(Na-smectite $\longrightarrow$ kaolinite).

If literature values for montmorillonite solubility /161, 164/ are included in the model calculations, the water composition can be determined in principle. There are, however, difficulties with regard to data selection.

Montmorillonite affects water composition not only through its solubility but also by ion-exchange. Wanner /176/ took this effect into account in model calculations for a bentonite and, with a given groundwater composition, found pH increases of 2 to 3 units.

Snellman's experiments /150/ with a model water show an increase in the alkalinity of the water and in pH to about 10 in the presence of bentonite. Other authors have measured pH values of 9.8 (in 0.01 M NaCl) and 8.8 (1.0 M NaCl) in the aqueous phase in contact with bentonite /104/. According to Lanza and Ronsecco /89/, the pH of water/clay mixes is dependent on the solid fraction (Figure 10). As pH measurement in clay suspensions can be difficult due to the Pallmann effect /122, p.211/ and because the experimental conditions are not described in detail, the literature data are not easy to interpret. It can tentatively be deduced that the pH in bentonite pore-water lies in the range of 8 to 10.

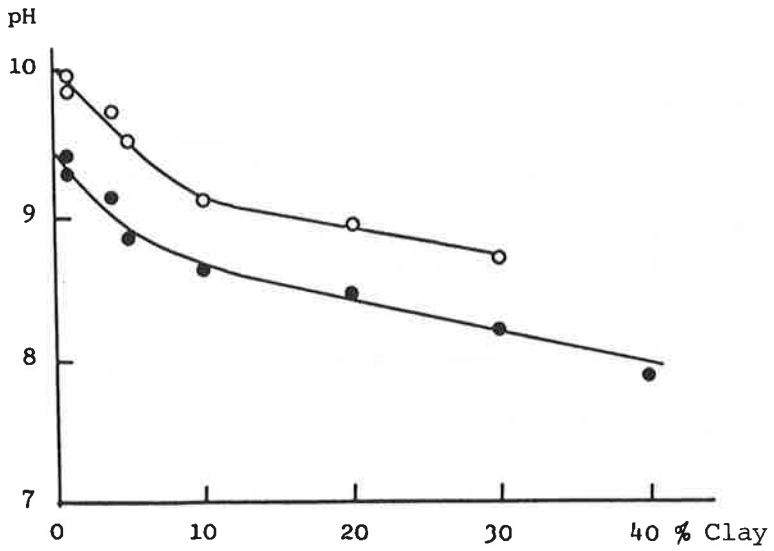

Fig. 10: Dependence of pH on the clay fraction in clay/water mixes.
o: bentonite ●: montmorillonite /89/.

Hydrothermal alteration of montmorillonite in the temperature range 150 to 275°C showed a drop in pH from 8-9 to 3-6 /78/. This acidification was linked with emplacement of aluminium hydroxy complexes in the interlayers. As discussed in section 6.5, such chloritisation of the montmorillonite can result in a drop in pH. Increasing the layer charge also leads to acidification if the cations required to compensate the additional layer charge originate from an outside source:

$$8\ Na_{0.33}Al_{2.33}Si_{3.67}O_{10}(OH)_2 + 2\ Na^+ + 12\ H_2O \longrightarrow$$

$$7\ Na_{0.66}Al_{2.66}Si_{3.33}O_{10}(OH)_2 + 6\ H_4SiO_4 + 2\ H^+$$

The significance of such reactions for the repository situation should not be overestimated. As they proceed very slowly - if at all (sections 6.4 and 6.5) - the residual bentonite can absorb the acid produced by way of dissolution reactions or ion-exchange. Recent information /177/ indicates that the drop in pH was observed only with a particular Ca-bentonite. Investigations of four other bentonites did not reveal this phenomenon.

Bentonites often contain organic and sulphidic impurities. Oxidation of these in the initial disposal phase produces the acidic reaction products CO_2 and SO_2, or SO_3. Heating of a natural clay with 1% pyrite and 0.2 to 1 % organic impurities resulted in the formation of acidic condensates /32, 36/. Laboratory tests gave pH values of 4.1 (50°C), 2.3(100°C) and 1.4 (150°C) for the condensates. In "in-situ" experiments, however, the pH of the condensed moisture was found to be 5 to 6 in the same temperature range. The pH in freshly exposed clay was found to be 10.1 to 10.5. Comparison between laboratory and field experiments suggests that, in the large-scale test, the clay mass functions as a buffer.

3.2 Water uptake and swelling of clay minerals

3.2.1 Swelling of montmorillonite

Smectites and vermiculites can absorb water into the interlayers and thus swell. As A. Weiss /181/ pointed out in his classic work, the main parameters affecting this process are

- the surface density of the charge (or the equivalent surface)
- the charge and solvation behaviour of the interlayer ions
- the electrolyte concentration or the water activity.

Figure 11 shows the behaviour of some three-layer silicates in electrolyte solutions. The lowly charged smectites can disperse completely with monovalent interlayer ions (Figure 12) while the swelling of the Ca-smectites is restricted. It can be seen from Figure 11 that swelling with the introduction of water layers is a stepwise process. The structural aspects are presented in /154, 155/. Emplacement of the first water layer with low water activities leads to a layer widening of 0.25 nm (Figure 13). The cations are partly coordinated by the oxygen of the siloxane surface. With two water layers (Figure 14), the interlayer ions are coordinated octahedrally. With further water uptake, the coordination octahedron alters its orientation (Figure 15). In Ca-montmorillonite the maximum layer widening is around 1 nm.

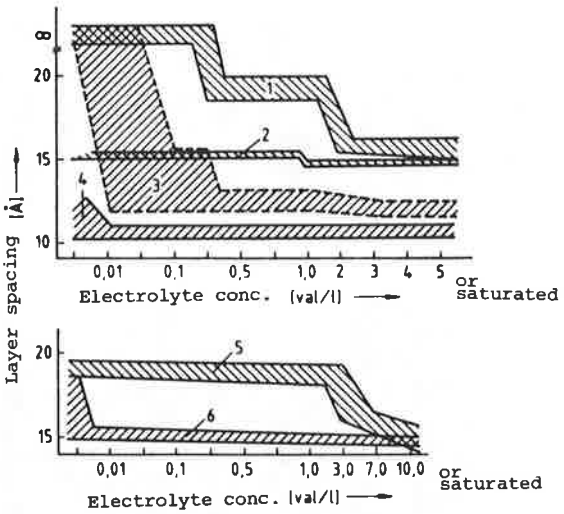

Fig. 11: Dependence of layer spacing of three-layer silicates in aqueous electrolyte solutions on the layer charge, the interlayer cation and the electrolyte concentration /85/.

1. Na-smectites under NaCl solution
2. Na-vermiculites under NaCl solution
3. K-smectites under KCl solution
4. K-vermiculites under KCl solution
5. Ca-smectites under $CaCl_2$ solution
6. Ca-vermiculites under $CaCl_2$ solution

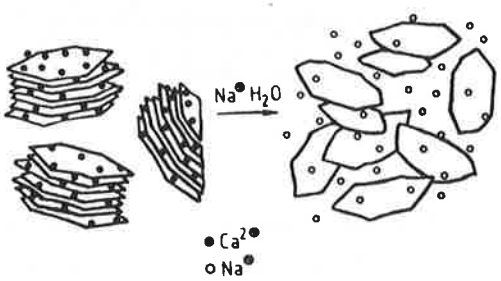

Fig. 12: The formation of colloidal dispersions of sodium smectites. Calcium smectites have only a limited swelling capability /85/.

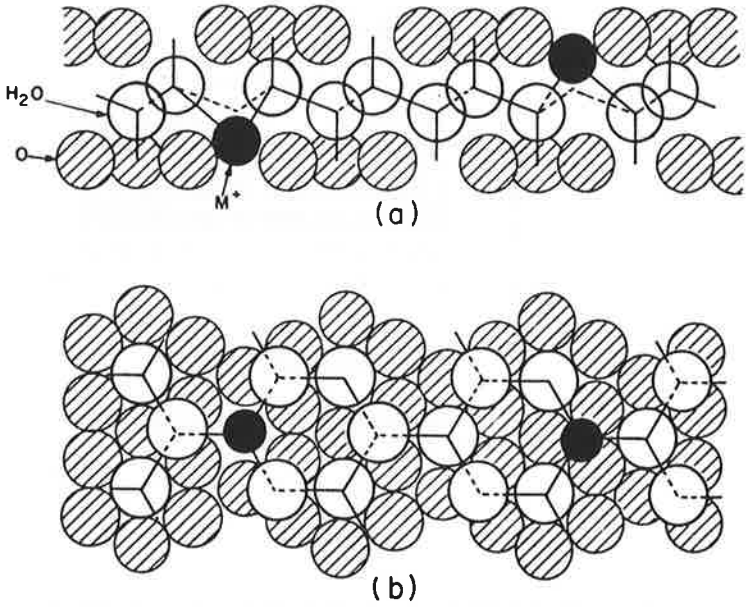

Fig. 13: The water structure in an M^+-montmorillonite with one water layer. The oxygen atoms of the tetrahedral layer are shaded. a) parallel, b) vertical to the c-axis /155/.

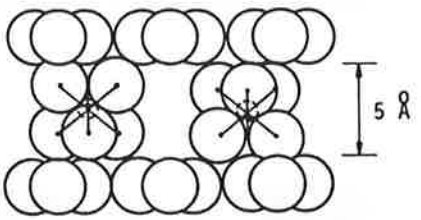

Fig. 14: First and second water layer with octahedral arrangement of six water molecules around every cation. Widening of the layer spacing to around 5 Å. The cations lie in the central plane between the layers /27/.

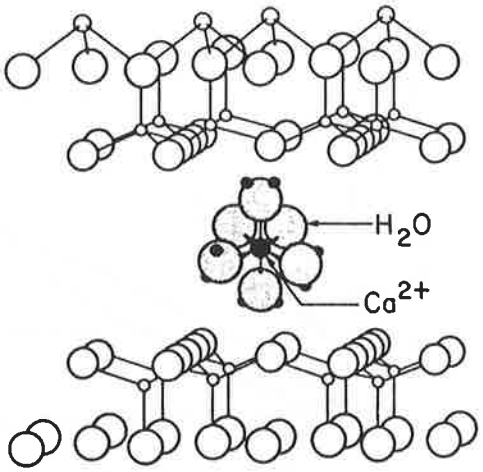

Fig. 15: Exploded diagram of calcium montmorillonite with three water layers /155/.

The emplacement of a maximum of four water layers is termed innercrystalline swelling and is determined to a large extent by the layer charge and the hydration properties of the interlayer ions. More extensive swelling can occur due to a difference in the osmotic pressures in the interlayer space and in the outer solution (osmotic swelling). Because the interlayer ions are fixed for electrostatic reasons, water is taken up into the interlayer spaces to balance concentration, provided there was originally a higher concentration in the interlayer spaces. Osmotic swelling depends to a large extent on the electrolyte concentration and the valency of the dissolved ions. Innercrystalline swelling, on the other hand, depends only slightly on these factors.

The work of Keren and Shainberg /82/ gives a good insight into water uptake by Na- and Ca-montmorillonite because, in each case, the water vapour adsorption isotherms, the crystallographic c-spacing and the heats of immersion were determined for the same clay.

It follows from the sorption isotherms (Figure 16) that the montmorillonite/water interactions are stronger for the Ca-variant than for the Na-modification. The isotherms intersect only at $p/p_o \approx 0.85$ which - in contrast with Na-montmorillonite - can be explained by the limited swelling capability of the Ca-variant.

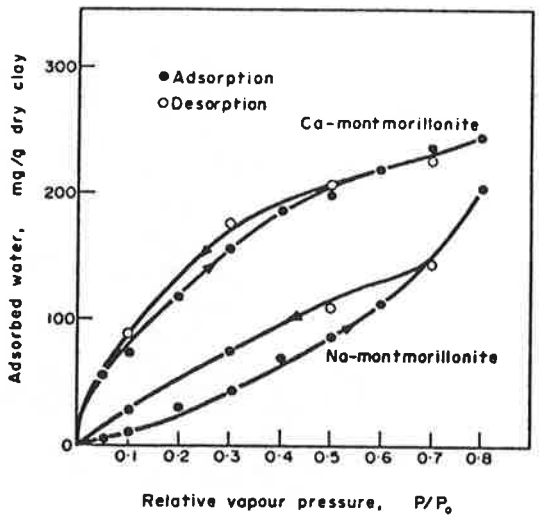

Fig. 16: Water vapour adsorption and desorption isotherms for Na- and Ca-montmorillonite /82/.

While water uptake is continuous with increasing water vapour pressure, this is not true for the alteration of the crystallographic c-axis *) (Figure 17). For Ca-montmorillonite, the layer spacing is already 1.5 nm (corresponding to two water layers) with low water activities, although insufficient water has been incorporated to fill these two layers. This would require 230 mg of water per g clay. In the case of Na-montmorillonite, the layer spacing initially increases continually up to $p/p_o \approx 0.2$ and there reaches a value of 1.26 nm (corresponding to one water layer). Up to $p/p_o \approx 0.6$, this layer is successively filled (114 mg H_2O/g clay). In contrast with the Ca variation, the second water layer is introduced only after filling of the first one (p/p_o 0.6 to 0.9). With p/p_o = 0.9, the layer spacing for the two variants is approximately 1.5 nm although the amount of water absorbed corresponds to more than two monolayers, i.e. some of the water condenses on the outer surfaces of the clay particles.

*) Water uptake in the case of vermiculites is also stepwise /121/.

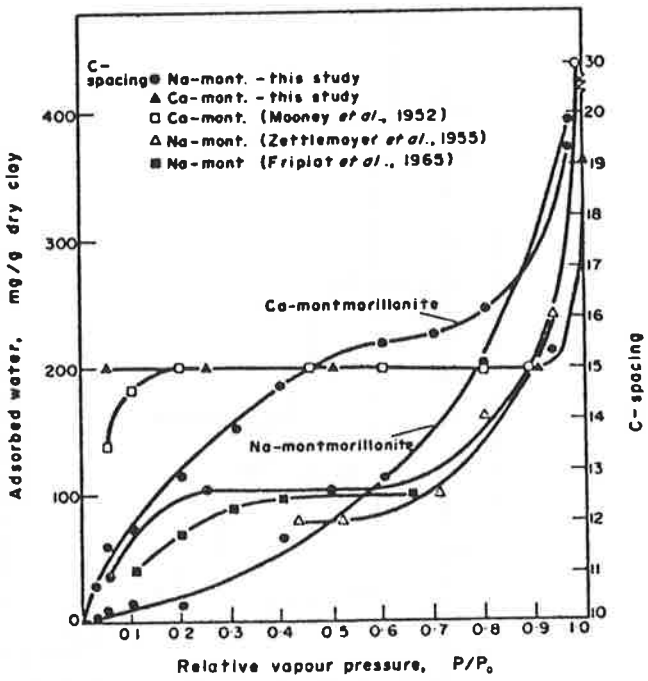

Fig. 17: Adsorption isotherms (●) and c-spacings for Na- and Ca-montmorillonite /82/.

Systematic differences between Na- and Ca-montmorillonite can also be seen in the heats of immersion (Figure 18) and are particularly clear if the values are related to the water and not to the clay fraction (Figure 19).

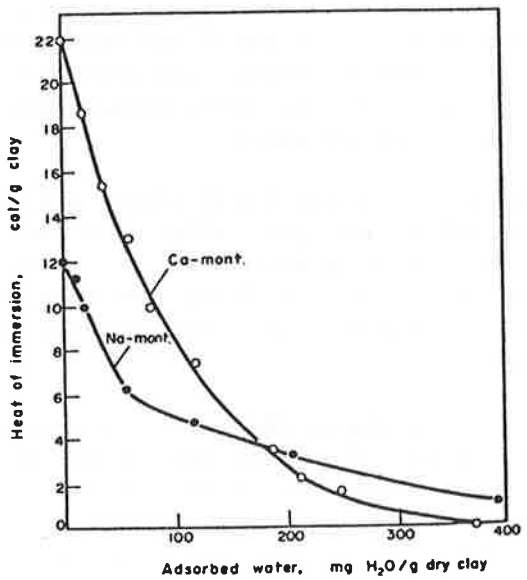

Fig. 18: Heats of immersion for Na- and Ca-montmorillonite after pre-equilibration to specific water contents /82/.

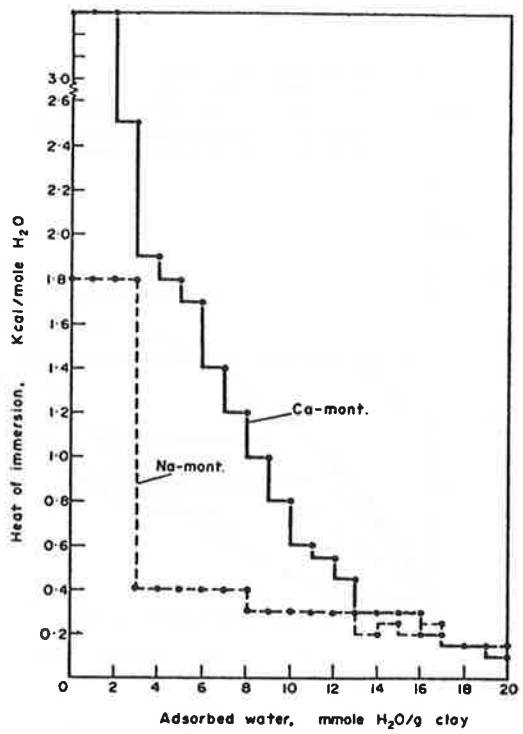

Fig. 19: Heat released per millimole of adsorbed water for Na- and Ca-montmorillonite /82/.

For Ca-montmorillonite, the heat of immersion per mole of water is quite high for the first two adsorbed millimoles with 3.3 kcal and then drops to 2.5 kcal/mole for the third millimole. After these adsorption steps, the calcium is coordinated with 6 to 8 water molecules which is in keeping with the measured layer spacing. Complete filling of the first two water layers occurs with continuously decreasing heat of immersion per mole of water.

For the Na variant, the first three millimoles of water are almost equivalent energetically. The amount corresponds to formation of 2/3 of a monolayer or 3.3 H_2O per sodium ion. Filling of the first and development of the second water layer occurs at a significantly lower level with low energy differences.

As Keren and Shainberg /82/ also include many earlier works in their discussion, it is not necessary to summarise these here. Reference should however be made to Kijne /83/ who has investigated, inter alia, the effect of the interlayer cation (Li^+, Na^+, NH_4^+, Rb^+, Cs^+, Ca^{2+}) on the heat of immersion. The publication by Zettlemoyer et al. /191/ is also of interest as it measured stepwise development of the heat of immersion as a function of the pre-adsorbed water for a Wyoming bentonite.

If a smectite swells within a restricted volume, a swelling pressure builds up which, depending on the density of the material used, can reach several hundred bars. It can thus reach the order of magnitude of the lithostatic pressure in the repository (Figure 20) /27, 131/. Under these conditions, the water content of the bentonite is below 30%. This corresponds to around three interstitial water layers in the montmorillonite structure.

Innercrystalline swelling is therefore of prime importance under repository conditions and osmotic swelling is less significant. This means that the salinity of a groundwater does not influence swelling pressure because only osmotic swelling depends to any extent on ionic concentration. This was confirmed by Swedish investigations (Figure 21): with swelling pressures over ca. 100 bars, the effects of the solution composition disappear.

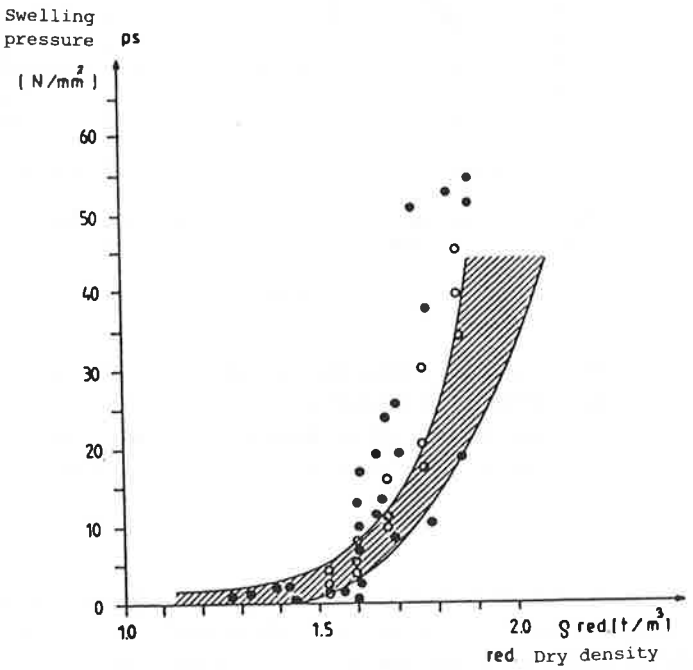

Fig. 20: Swelling pressure of MX-80 and Montigel bentonites as a function of reduced dry density at saturation.
Shaded: range of measured values according to /27/.
Points: results of Swedish investigations.

Where $\rho_{red} = \frac{M_s}{V_o + \Delta V}$

M_s: mass of the bentonite

V_o: original bentonite volume

ΔV: volume increase through swelling

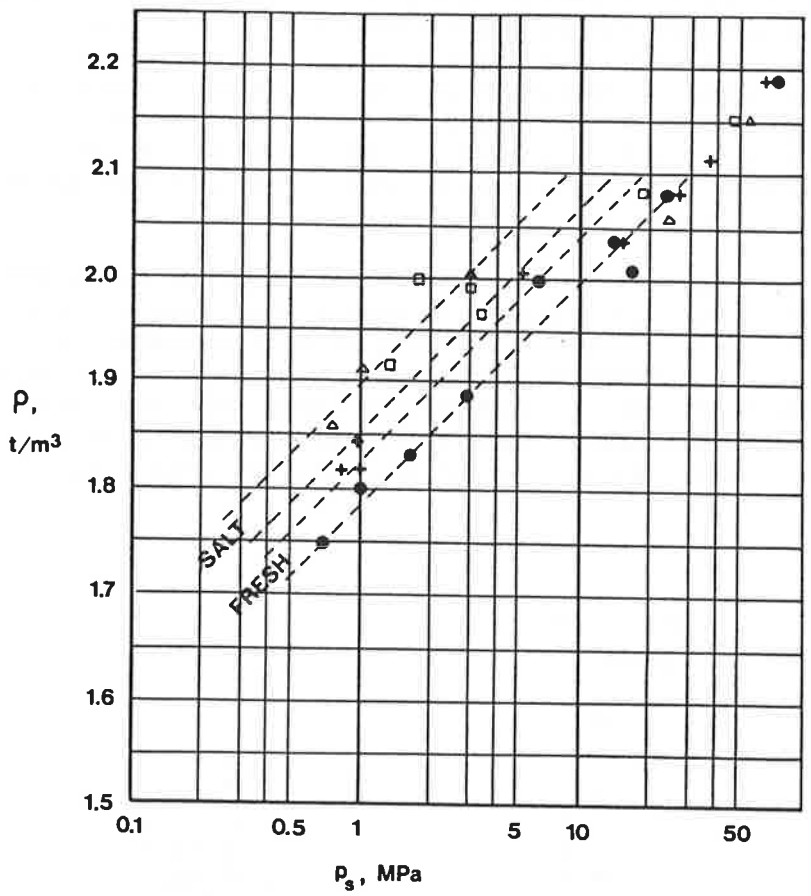

Fig. 21: Swelling pressures of MX-80 bentonite at 20°C with different solutions.
+: synthetic groundwater. ●: distilled water.
Δ: 0.6 M NaCl solution □:0.3 M $CaCl_2$ solution /131/.

With regard to the possible temporal alteration of montmorillonite (Chapter 6), it should be noted that illites or products with illite/smectite interstratifications show a certain swelling tendency. Examples of this are given in Figure 22 /27/. In the case of non-expanding layer silicates it is to be expected that the swelling behaviour will depend on particle size because only the outer surfaces of the clay aggregates are involved in the swelling process.

The swelling of clay minerals is summarised in various books /50, 63, 122/, the main emphasis being on free swelling.

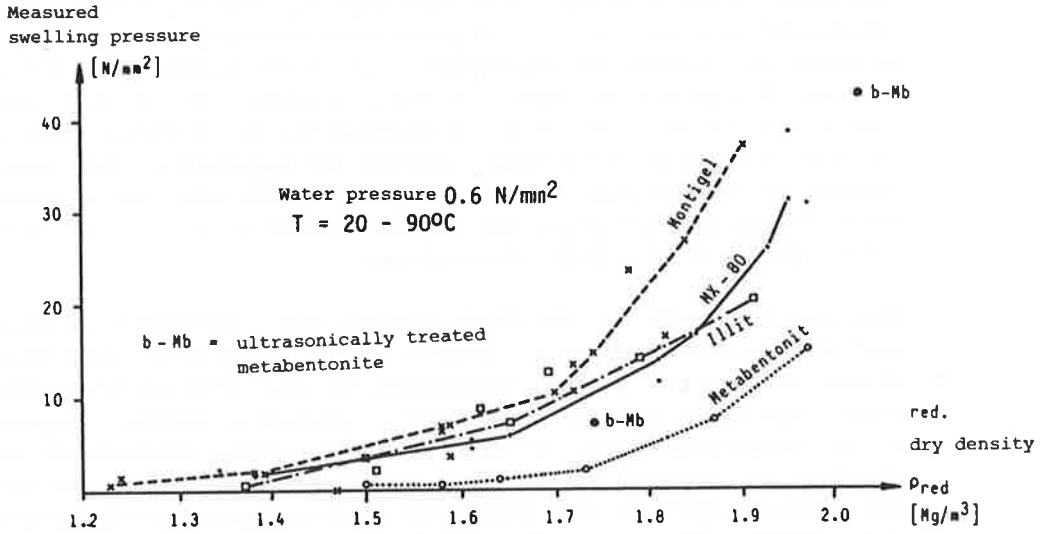

Fig. 22: Comparison of the swelling pressures of different materials /27/.

3.2.2 Interparticular forces and calculation of swelling pressure

There are various methods for predicting swelling pressure on a theoretical basis. When assessing and applying such models it must be noted that the interlamellar spacings of the montmorillonite under repository conditions are 2 nm or less. The understanding of forces operating over such small distances is still incomplete /113/ and caution or even scepticism is in order when continuum models are applied to the molecular scale ("2 Å $\neq \infty$" /113/).

The structure and properties of adsorbed water differ from those of the fluid phase. The lessons to be learned from the story of polywater /51/ serve as a warning to proceed with caution and to resist speculation.

The literature on these two subjects is extensive and only a small part has been taken into consideration here. There is no guarantee that the selection is accurate as Franks /51/ claims "... that many of the publications on the subject of bonded water are of only average quality; this was true in 1960 and still holds today".

3.2.2.1 The DLVO model

The DLVO model (names after Derjaguin, Landau, Vervey and Overbeck) describes the interactions between charged surfaces in aqueous solutions as superposition of an electrostatic repulsion and an attraction by van der Waals forces. The model has proved its worth in general colloid chemistry. As further considerations show that this model cannot be applied to the swelling of compacted bentonite, the basic principles are not presented here. Detailed derivations can be found in /70, 122/ and Sposito /155/ gives a critical discussion.

The basic tenets of the DLVO theory are contained in Figures 23 and 24. In contrast with double layer repulsion, the van der Waals attraction is not dependent on the electrolyte concentration. The DLVO theory therefore predicts a surface repulsion which decreases with increasing electrolyte concentrations and becomes an attraction at high ionic strengths (Figure 24. κ^{-1} is the "thickness" of the electric double layer which increases with decreasing ionic strength). For very small interparticular distances in the atomic range, the model predicts - contrary to experience - an attraction for all ionic strengths. This deviation cannot be explained by inherent defects in the double-layer theory alone (cf. /155/), but other forces which are not taken into account in the DLVO theory become operative. The applicability of the model is therefore restricted to interparticular distances of more than approximately 5 nm /113, 115/.

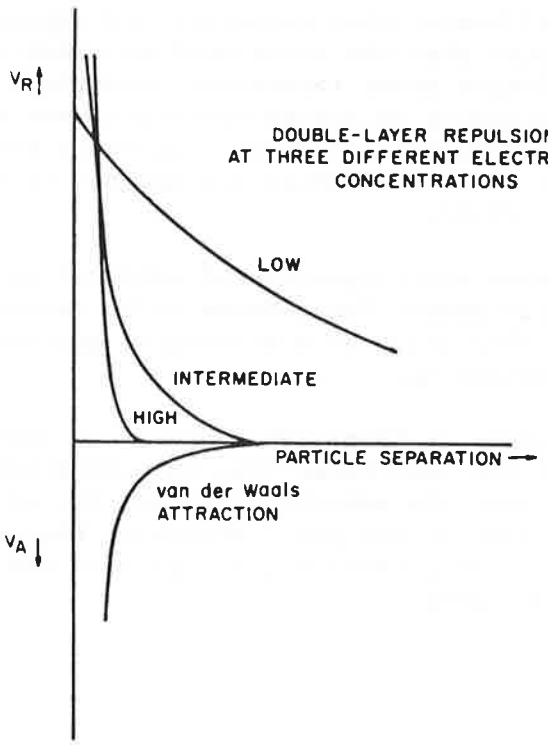

Fig. 23: The DLVO theory: repulsion of the electrolytic double layers with different electrolyte concentrations and van der Waals attraction as a function of particle separation.

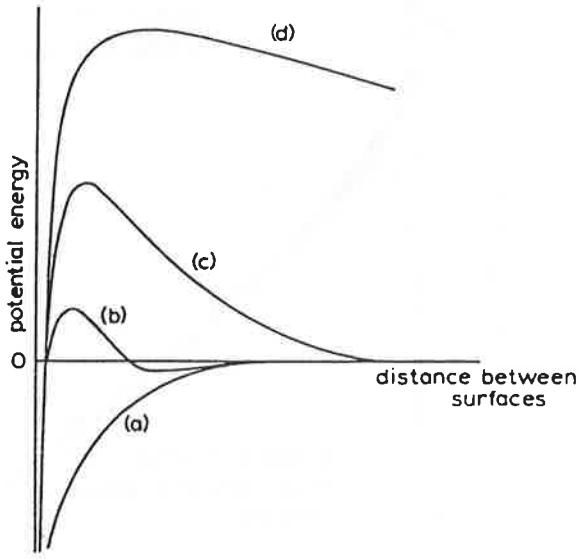

Fig. 24: Effect of electrolyte concentration on total interaction energy of two spherical particles with a radius of 100 nm. a) $\kappa^{-1} = 10^{-7}$cm b) $\kappa^{-1} = 10^{-6}$cm c) $\kappa^{-1} = 10^{-5}$cm d) $\kappa^{-1} = 10^{-4}$cm. κ^{-1} (the "thickness" of the double layer) increases with increasing dilution /124/.

The repulsion force which prevails below distances of 5 nm is considered as a solvation force. It is applied to dehydrate the interlayer cations or the clay surface. Barclay and Ottewill /12/ postulated the solvation force on the basis of compression experiments with clay/water systems (cf. also /119/). Development of a measuring technique for determining forces between mica platelets in the range 0 to 100 nm /76/ has led to a better experimental understanding of solvation force. Figure 25 shows the results of such measurements. The difference between measurement and the DLVO model can be expressed by the relationship

$$\Psi_{solv}(d) = \frac{\alpha}{2\P} \exp\left(-\frac{d}{\delta}\right)$$

(d: variable spacing, $\alpha \approx 0.03$ to 0.05 N·m^{-1}, $\delta \approx 0.3$ to 1 nm). In the temperature range 20 to 65°C, the values of α and δ do not change; on the other hand, the numerical value of α depends on the type of cation and its concentration (/155, p.216/). This agrees qualitatively with the low temperature dependence of the swelling pressure. It is therefore clear from Figure 25 that the DLVO model cannot be applied to the intercrystalline swelling of montmorillonite.

For the sake of completeness, reference should be made to the report /120/ which links deviations from DLVO behaviour of montmorillonite with the geometric arrangement of the clay platelets (cross-linking).

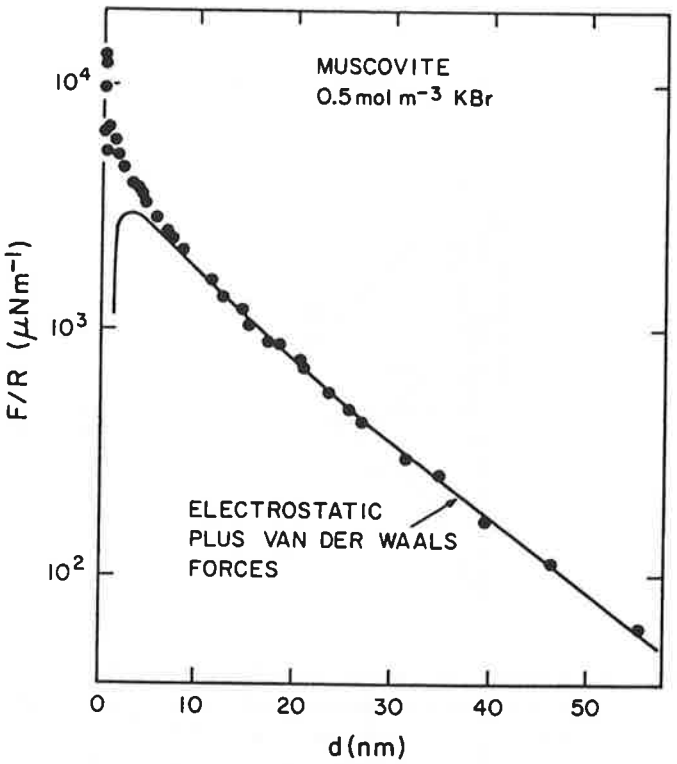

Fig. 25: Force per unit length (energy per unit surface) between muscovite surfaces in aqueous KBr solution at pH 6.2. The curve gives the sum of electrostatic and van der Waals forces /125, 155/.

As already indicated, the DLVO model suffers from the weaknesses of the double-layer theory. Not only are there several double-layer models available, but there are also difficulties involved in their mathematical treatment and, finally, in the selection of numerical values to be used. Values between 2 and 50 are available for the relative dielectric constant of water on phyllosilicates (/155, p.70/). The problem is usually avoided in practice by using the value for pure water ($D \approx 80$).

A recent critique of application of double-layer models to the swelling of montmorillonite can be found in Low /97/. Proceeding from the experimental finding that less than 2% of the exchangeable cations are dissociated, he concludes that double-layer repulsion can only make a small contribution to swelling pressure (Figure 26). Low's critique of earlier works which, given sufficiently large layer distances, found an agreement between the DLVO theory and measurement (e.g./178/), relates to the surface charge density on which the double-layer calculations are based. If the correct value determined from the zeta potential is used in place of the effective surface charge density, model calculation and measurement no longer agree. This line of argument is pursued in a later report /174/.

Models which interpret swelling pressure as osmotic pressure of the interlayer solution and use a double-layer model to determine interlayer concentration /145, 190/ also appear questionable on the basis of the above considerations.

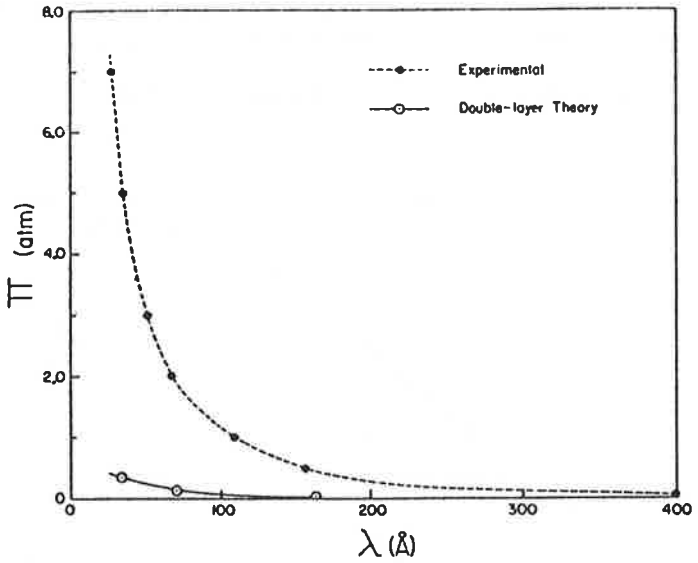

Fig. 26: The relationship between swelling pressure ¶ and the interlayer spacing λ. Comparison of experimental results with the predictions of the double layer theory /97/.

3.2.2.2 Low's semi-empirical model

Low and Margheim /95/ found the following empirical relationship for the swelling pressure P_Q of different Na-montmorillonites

$$(P_Q + 1) = \exp(\alpha \frac{m_s}{m_w})$$

(m_s: g of solid, m_w: g of water). The parameter α could be described (also empirically) as a function of the specific surface S (cm^2/g) and the cation exchange capacity z (meq/g):

$$\alpha = 3.609 \ 10^{-7} S + 1{,}332 \ z - 0{,}678$$

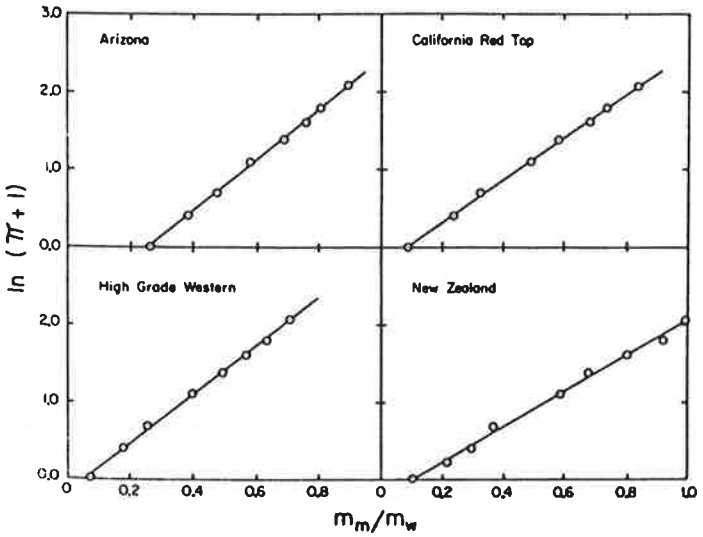

Fig. 27: The relationship between swelling pressure ¶ and the montmorillonite/water ratio m_m/m_w for different montmorillonites /96/.

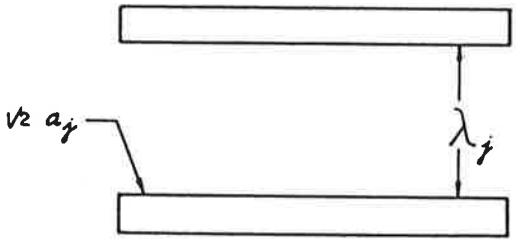

Fig. 28: The significance of a and λ in Low's model of swelling pressure /96/.

A further report /96/ checked this model for numerous other montmorillonites in the range $P_Q \leq 7$ bars and developed it further. The swelling behaviour shown in Figure 27 is described by

$$(P_Q + 1) = \exp \alpha\left[\frac{m_s}{m_w} - \left(\frac{m_s}{m_w}\right)_o\right] \qquad (1)$$

$(m_s/m_w)_o$ is the clay/water ratio at zero swelling pressure. The m_s/m_w ratio is now expressed with interlayer spacing λ (Figure 28). The mass of the interlayer water is $\frac{1}{2}\Sigma a_j \lambda_j \cdot \rho$ (ρ : density of water). The mass of the montmorillonite is $m_s = \Sigma m_j$. As the proportion of crystal edges over the total surface is small, a good approximation of the specific surface is given by

$$S = \Sigma a_j / \Sigma m_j$$

There then results for the proportion of interlayer water

$$\left(\frac{m_w}{m_s}\right)_{intra} = \frac{1}{2} \lambda \rho S$$

It is argued further that the intercrystalline water content (pore-water, water between the clay aggregates) is proportional to the total water content:

$$\left(\frac{m_w}{m_s}\right)_{inter} = r \frac{m_w}{m_s}$$

and thus

$$\frac{m_w}{m_s} = \frac{\lambda \cdot \rho \cdot S}{2(1 - r)}$$

1 - r is the proportion of water in the interlayers. Equation (1) can now be formulated as

$$(P_Q + 1) = \exp\left[\alpha \frac{(2\ (1 - r)}{\rho} \left(\frac{1}{\lambda} - \frac{1}{\lambda_o}\right)\right] \qquad (2)$$

If the semi-empirical expression

$$\alpha = a \cdot S + b \cdot z$$

(a, b: constants) is combined with the surface charge density $\sigma = \frac{z}{S}$, then

$$\alpha = S(a + b \cdot \sigma).$$

Using this term and assuming that $\frac{1 - r}{\rho} = 1$ then

$$(P_Q + 1) = \exp\left[(2a + 2b \cdot \sigma)\left(\frac{1}{\lambda} - \frac{1}{\lambda_o}\right)\right] \qquad (3)$$

finally results from equation (2). $2a = 7.5 \times 10^{-7}$, $2b = 2.3$ (σ in meq/cm^2)/96/.

Initially, this model is persuasive because of its simplicity. It states that the swelling behaviour of a montmorillonite can be estimated from the surface charge density, i.e. from the experimentally easily accessible parameters of specific surface and cation exchange capacity. However, most of the montmorillonites investigated do not show the simple connection between swelling pressure and water content shown in Figure 27. As can be seen from Figure 29, two different values must be used for m_s/m_w and λ_o when describing the swelling properties of these clays. λ_o can also have negative values (Figure 30) which puts the physical significance of this parameter into question.

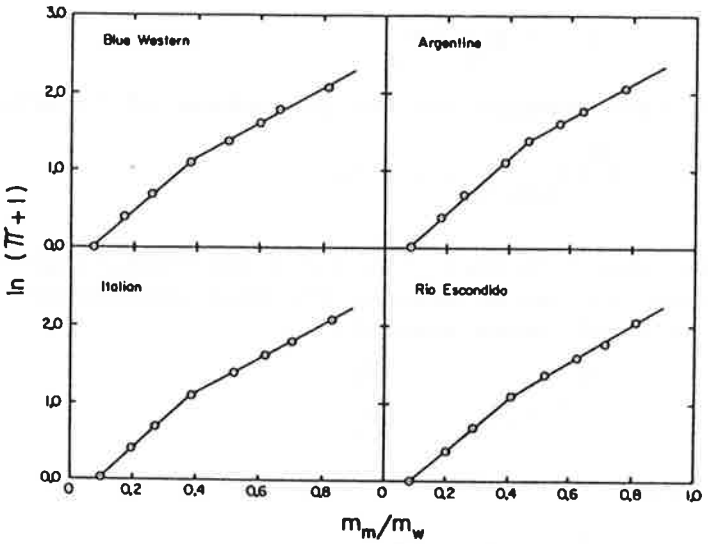

Fig. 29: The relationship between swelling pressure and the montmorillonite/water ratio for a group of montmorillonites (cf. Figure 27) /96/.

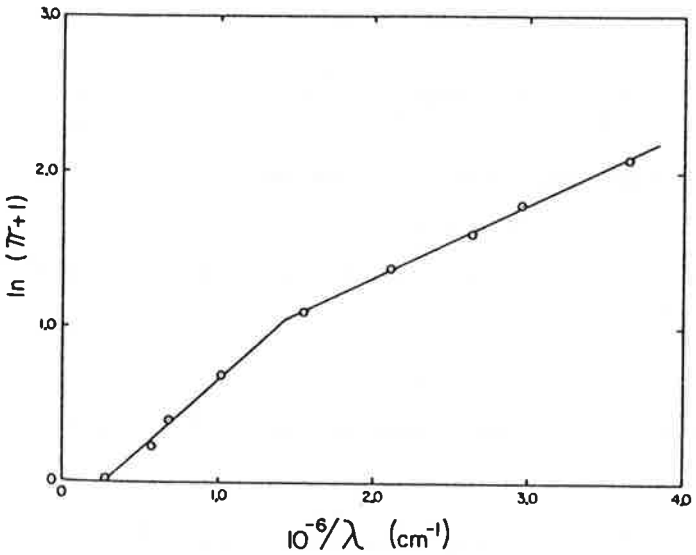

Fig. 30: The relationship between swelling pressure and $1/\lambda$, assuming that the layer spacing λ is independent of the nature of the montmorillonite /96/.

3.2.2.3 Thermodynamic models

Classical thermodynamics describes the properties of macroscopic systems. It is not possible to draw any direct unequivocal conclusions on the swelling mechanism and the structure of adsorbed water from this concept. Introduction of microscopic parameters leads to unnecessary confusion /152/.

It should also be recalled that thermodynamic properties of mixtures (e.g. a clay/water system) can be distributed only formally over the properties of the components /154/. The thermodynamic functions are well-defined parameters if the clay phase is not inert, but in this case the changes should not - as often happens (e.g. /122, p.152) - be attributed solely to the aqueous phase. What follows is to be understood under this reservation.

Reference should be made to Sposito /153/ for an introduction to the thermodynamics of soil waters.

Sposito /152/ and, indirectly, Low and Anderson /94/ have derived the connection between swelling pressure P_Q and relative partial free energy on the basis of equilibrium thermodynamics

$$\bar{g}_w - g_w^o = - \bar{v}_w \cdot P_Q \qquad (1)$$

Given the general relationship

$$\bar{g}_w - g_w^o = (\bar{h}_w - h_w^o) - T(\bar{s}_w - s_w^o) \qquad (2)$$

there results

$$P_Q = - \frac{\bar{h}_w - h_w^o}{\bar{v}_w} + T \frac{\bar{s}_w - s_w^o}{\bar{v}_w} \qquad (3)$$

Since

$$\bar{G}_w - G_w^o = M(\bar{g}_w - g_w^o) = RT \ln a_{H_2O} = RT \ln p/p_o \qquad (4)$$

with equation (1) there results

$$P_Q = - \frac{RT}{M \cdot \bar{v}_w} \ln p/p_o \qquad (5)$$

where:

$\bar{G}_w - G_w^o$: relative partial molar free energy of water in the clay/water system ($J \cdot mol^{-1}$)

$\bar{g}_w - g_w^o$: relative partial specific free energy of water in the clay/water system ($J \cdot g^{-1}$)
The corresponding relative partial parameters enthalpy (H,h) and entropy (S,s) are similarly defined.

$\bar{v}_w$: partial specific volume of the water. With low water contents, the density of the adsorbed water is lower than in the fluid phase /5/ so that $\bar{v}_w > 1\ cm^3 \cdot g^{-1}$. Oliphant and Low /117/ use the empirical correction $\bar{v}_w = 1.002 \exp(0.036 \frac{m_w}{m_s})$.

p, p_o : vapour pressure of adsorbed and pure water

M : molecular weight of the water

a_{H_2O} : activity of the water

Equation (5) implies that the swelling pressure can, in principle, be derived from water adsorption isotherms. The equation can be applied to salt-containing solutions /152/.

The relative partial enthalpy can be determined from the heat of immersion ΔQ since

$$\frac{\Delta Q}{m_s} = \int_{w_o}^{\infty} (\bar{h}_w - h_w^o)\, dw$$

The swelling pressure can only be determined from the heat of immersion if the entropy term in equation (3) is known or is negligible in comparison with the enthalpy term.

Oliphant and Low /117/ determined the relative partial entropies for water in montmorillonite-water mixtures from measurements of heat of immersion and swelling pressure. The data in Table 5 which are based on equation (3) show that the entropy term should not be ignored. With a water/clay ratio of 0.25 - more or less representative for a repository backfill - both terms have the same order of magnitude.

The entropy difference between adsorbed and free water depends on the interlayer cations /83/ and is larger for Ca-montmorillonite than for Na-montmorillonite. Further values for relative partial entropy as a function of water content for various monoionic montmorillonites can be found in /13, 83, 123/.

A thermodynamic discussion of water vapour adsorption isotherms is avoided here as a detailed report on this subject is in preparation /81/.

Table 5: Entropy and enthalpy contributions to swelling pressure P_Q for montmorillonite/water mixtures. m_w/m_m: mass ratio water/montmorillonite /117/.

m_w/m_m (g/g)	P_Q (atm)	$-(\bar{h}_w - h^o_w)v_w$ (atm)	$T(\bar{s}_w - s^o_w)v_w$ (atm)
0.25	131.78	475.29	-343.50
0.30	89.40	142.15	- 52.75
0.35	58.53	72.31	- 13.77
1.50	7.30	1.11	6.19
2.00	3.77	0.604	3.17
3.00	1.88	0.292	1.59
4.00	1.07	0.182	0.888
5.00	0.64	0.123	0.517
6.00	0.42	0.088	0.332
7.00	0.30	0.074	0.226
8.00	0.25	0.057	0.193
10.90	0.0048	0.0869	- 0.0821

4 THE SORPTION BEHAVIOUR OF CLAY MINERALS

At present, there is no comprehensive textbook on ion adsorption from aqueous solutions on mineral interfaces. There are some monographs with contributions from different authors /10, 166/ and books on clay minerals deal with the subject in special chapters /63/. Cation adsorption is often described as simple linear equilibrium distribution (K_d concept) or it is attempted to force experimental results into the form of Freundlich or Langmuir isotherms. Although these isotherms can be derived from thermodynamics, as a rule they are normally used only as an empirical concept. This then leads to the situation where the adsorption in a specific system can be described but its chemistry cannot be understood. (Reference should be made to /101/ for a more detailed discussion of adsorption isotherms.)

Cation adsorption on clay minerals can be satisfactorily described as an exchange reaction of the interlayer ions. In addition, cations can also be bound to surface OH groups. A surface coordination model has been developed for this type of reaction and has led to an improved understanding of the sorption properties of oxidic surfaces. Anion adsorption, which is in general less well understood, can also be integrated into this model.

For a repository situation, special attention must be paid to the sorption behaviour of caesium and strontium and, most importantly, of the actinides. The sorption of iron ions from the canister corrosion products is of further interest. In this case it is not yet known whether adsorption or an irreversible phase alteration takes place. Possible silicic acid adsorption also has to be taken into account because its concentration is an important parameter in glass corrosion /61/.

4.1 Clay minerals as sorbents

The sorption behaviour of clay minerals is closely linked with their structure. Besides exchange of interlayer ions, reactions with surface OH groups are possible. Cation adsorption therefore occurs according to two different mechanisms. The concepts developed by A. Weiss in his classic works /183, 184/ are still valid but can now be expanded with more recent ideas on the formation of surface complexes (Figures 31 and 32). According to these, surface OH groups not only participate in anion exchange reactions but also react with cations. These reaction have recently been investigated for kaolinite in the light of the new aspects /92/.

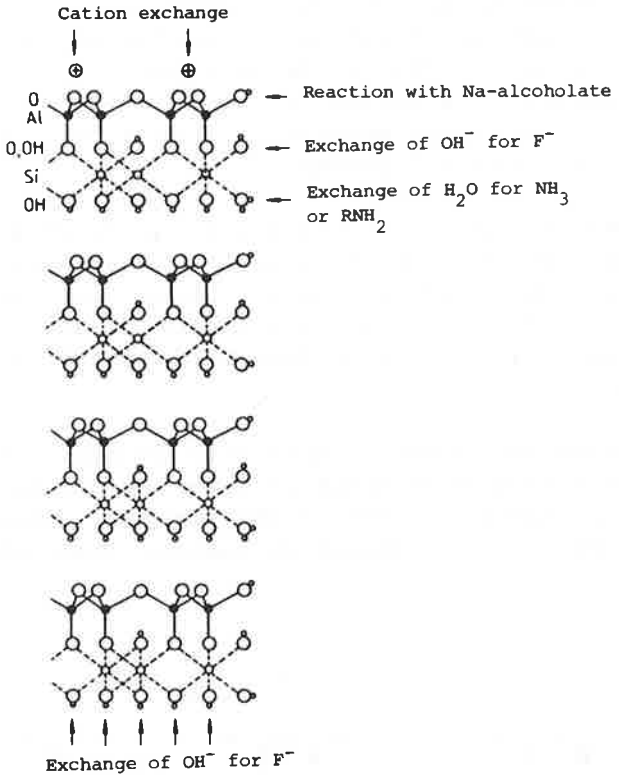

Fig. 31: Ion exchange reactions on kaolinite /184/.

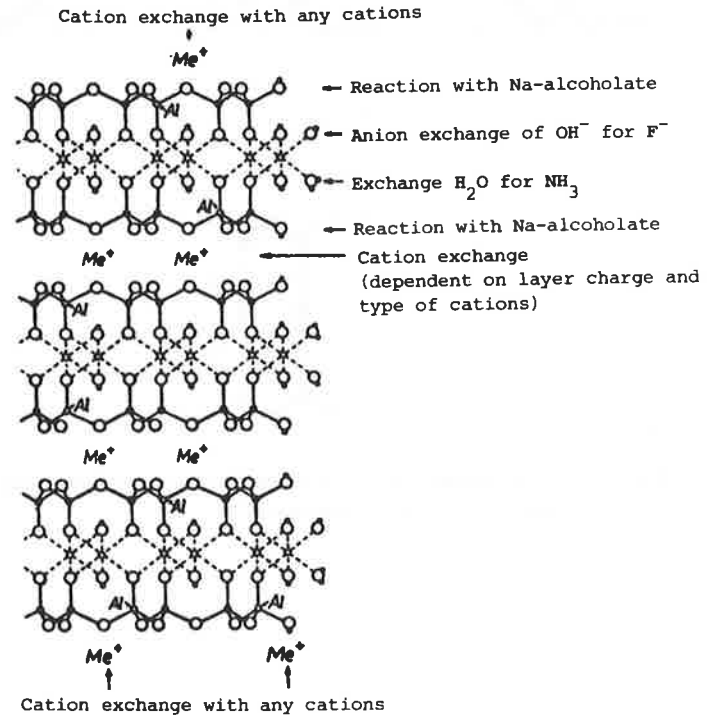

Fig. 32: Schematic representation of ion-exchange reactions on micaceous layer silicates /183/.

In clay mineralogy literature, the sorption sites at the crystal edges are often termed "broken bonds". In the case of smectites, their participation in cation adsorption amounts to around 20%, while the remaining 80% can be attributed to cation exchange in the interlayers /63, p.193; 103/. The marginal groups are involved in protolysis reactions (Figure 33). Their sorption behaviour is therefore pH-dependent.

In the case of micaceous (non-swelling) layer silicates, the interlayer ions are not exchangeable. That such minerals have a relatively high cation exchange capacity is based partly on the fact that the crystal edges are weathered and therefore susceptible to ion-exchange (adsorption on "frayed edges", Figure 34).

Clay minerals are often covered with extremely finely grained iron or aluminium hydroxides or with SiO_2 (e.g. /132/). Such precipitates naturally modify the sorption behaviour; exchange of interlayer ions decreases as against reactions with surface OH groups.

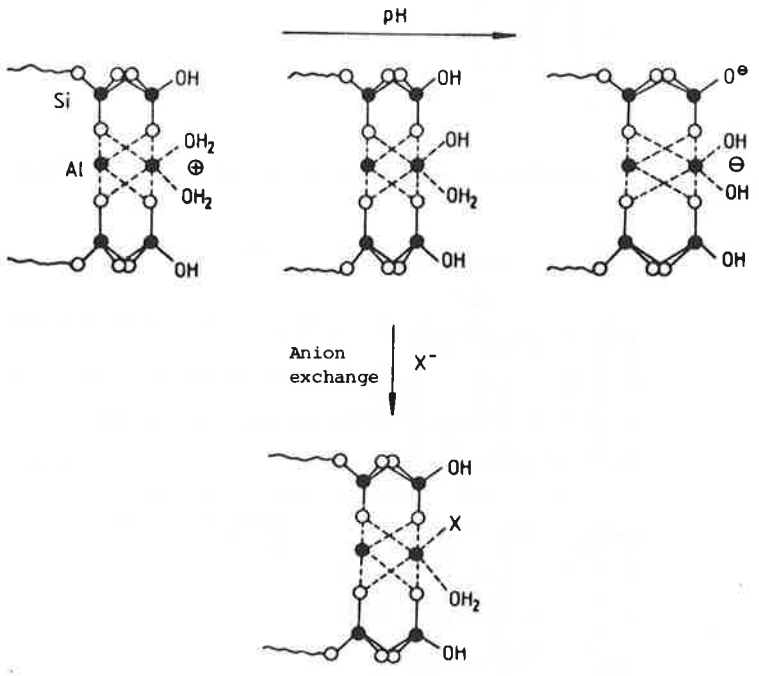

Fig. 33: The pH-dependent formation of edge charges on three-layer silicates /85/.

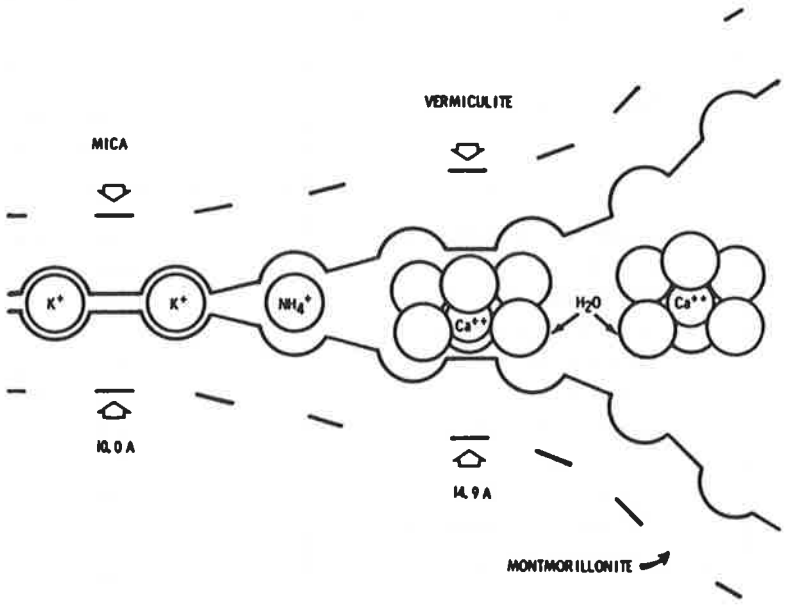

Fig. 34: The conditions at the crystal edge of a weathered mica particle. In contrast with the cations in the unaltered mica structure, the ions in the frayed edges are exchangeable /84/.

4.2 Concepts and models

4.2.1 Cation exchange capacity

The cation exchange capacity of a solid, usually given in milli-equivalents (meq) per 100 g, is a parameter which is influenced by the measuring process. It is usually determined at pH 7 with ammonium acetate /107/. Weiss /182/ gives a comparison of the different methods. Because of surface protolysis processes and because the hydrogen ion itself can be exchanged, the cation exchange capacity is pH-dependent /16, 182/. As an operationally determined parameter, the cation exchange capacity gives no information on the sorption mechanism. This is to be taken into account if the concept is applied to different types of material such as layer silicates, finely grained oxides or humic materials.

Table 6 gives a compilation of the cation exchange capacities of different silicates and some other materials. For illustration purposes, Table 7 shows the exchange capacities compared to specific surface. The differences between swelling and non-swelling minerals are surprisingly low. Finally, Table 8 summarises the exchange capacities determined within the scope of the Nagra research programme.

Table 6: Cation exchange capacities of natural materials according to /91/.

Material	Cation exchange capacity (meq/100g)
Organic material	350 - 130
Zeolites	300 - 100
Vermiculite	150 - 100
Montmorillonite	100 - 70
Chlorite	47 - 4
Illite	40 - 10
Palygorskite	30 - 20
Kaolinite	15 - 3
Pyrophyllite	4
Feldspar, quartz	1

Table 7: Surface-related cation exchange capacities of clay minerals.

	Surface (m^2/g)	Cation exchange capacity (meq/100g)	($\mu eg/m^2$)
Kaolinite	10 - 20	3 - 15	1.5 - 15
Montmorillonite	50 - 120	70 - 100	6 - 20
	700 - 850*		0.8 - 1.4
Illite	65 - 100	10 - 40	1 - 6

* Total surface

Table 8: Cation exchange capacity of various montmorillonites and illites

	Cation exchange capacity (meq/100g)	
MX-80	76.4 (102)*	/107/
Montigel	62.0 (94)*	/107/
Montmorillonite Kinnekulle	41 - 52	/108/
Illite, France	19	/108/
Illite, Sarospatak	33	/108/

* Values calculated for the montmorillonite content

4.2.2 Cation adsorption as ion-exchange

If one takes a sodium-saturated smectite as a cation exchanger, the adsorption of a metal ion M^{z+} can be formulated according to the following reaction equation:

$$z\ Na_s^{z+} + M_l^{z+} \rightleftarrows z\ Na_l^{+} + M_s^{z+}$$

(s: solid, l: liquid). The pertinent mass action constant is

$$K = \frac{a_{M(s)}}{[M^{z+}]} \cdot \frac{[Na^{+}]^z}{a_{Na(s)}^z}$$

Square brackets denote molar concentrations and $a_{M(s)}$ and $a_{Na(s)}$ are the activities of the corresponding ions in the solid phase. Their values cannot be derived theoretically and the activity a_i is usually replaced with the mole fraction x_i.

The distribution coefficient $K_d = x_M/[M^{z+}]$ can be introduced in the above mass action constant. With low loading of the ion-exchanger with M^{z+} ($[M^{z+}]$ at trace levels), x_{Na} is practically constant. The equilibrium constant can now be expressed in a form which allows the ion-exchange model to be checked experimentally:

$$\log K_{d(M)} = \text{const} - z \log[Na^{+}]$$

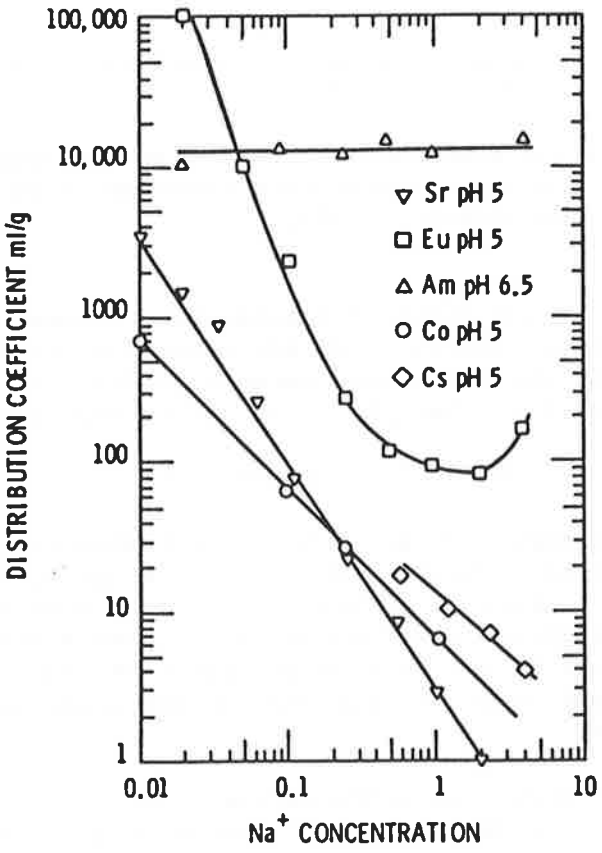

Fig. 35: The distribution coefficients of various ions on Na-montmorillonite as a function of NaCl concentration /144/.

Figure 35 /144/ shows that this relationship is well fulfilled for sorption of Cs^+, Sr^{2+} and Eu^{3+} at pH = 5 (the upward turn in the Eu curve with high chloride contents can be linked with the formation of chloro-complexes). The behaviour of cobalt remains unexplained as it behaves as a monovalent ion.

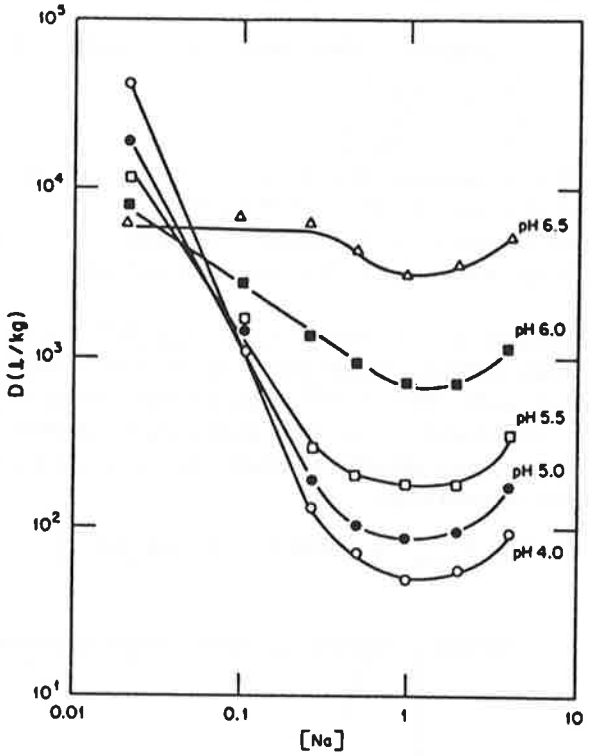

Fig. 36: The distribution coefficient of americium on montmorillonite as a function of pH and NaCl concentration /14/.

Because of the chemical similarities between Am(III) and the lanthanides, similar sorption behaviour would initially be expected. The difference between Eu(III) and Am(III) lies in the cation acidity. The pKa value of the reaction

$$M^{3+} + H_2O \rightleftharpoons MOH^2 + H^+$$

is 6 for americium and 8 to 8.9 for europium /11/. While europium is present as an aquo-ion at pH 5, americium is a hydroxo-complex at pH 6.5. It is known that hydroxo-complexes are more strongly sorbed on clay minerals than the corresponding aquo-ions. As can be seen in Figure 36 /14/, with lower pH values the sorption behaviour of americium approaches that of europium.

Although there are difficulties involved in giving a quantitative description of ion-exchange of clay minerals over wide concentration ranges using mass action constants /48/, there are equilibrium constants for such reactions in the literature (Table 9 /91/). Such exchange constants were also determined for MX-80 /176/.

In the general formulation of an ion-exchange reaction

$$z\ Na_s^+ + M_l^{z+} \leftrightarrows z\ Na_l^+ + M_s^{z+}$$

swelling and shrinking processes of the ion-exchanger are not taken into account. Such effects occur due to the differing hydration of interlayer ions (Figure 37) and are also influenced by the layer charge. These factors play a decisive role for the selectivity and reversibility of the exchange process.

Table 9: Equilibrium constants for ion-exchange reactions on clay minerals at 25°C (e.g. $Na_2X_2 + 2H^+ \leftrightarrows H_2X_2 + 2Na^+$) /91/.

Reaction	Mineral	log K
$Na_2X_2 \rightarrow H_2X_2$	Montmorillonite	6.45
$Na_2X_2 \rightarrow Li_2X_2$	Montmorillonite	- 0.06
	Bentonite	- 0.04
$Na_2X_2 \rightarrow K_2X_2$	Bentonite	0.45
	Beidellite	1.60
$Na_2X_2 \rightarrow RbX_2$	Bentonite	0.93
	Bentonite	3.40
$Na_2X_2 \rightarrow Cs_2X_2$	Montmorillonite	3.16 - 3.34
	Bentonite	1.59
$Na_2X_2 \rightarrow CaX_2$	Vermiculite	0.01
$Na_2X_2 \rightarrow SrX_2$	Montmorillonite	0.24
	Vermiculite	- 0.01
$Na_2X_2 \rightarrow BaX_2$	Montmorillonite	0.04
$CaX_2 \rightarrow K_2X_2$	Montmorillonite	1.06 - 1.82
$CaX_2 \rightarrow SrX_2$	Bentonite	0.11

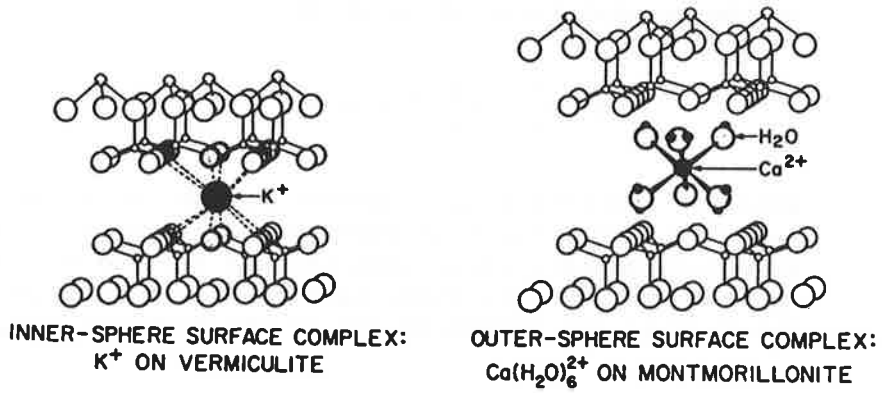

Fig. 37: Inner and outer sphere complexes between metal ions and the hexagonal gaps of the tetrahedral layer of three-layer silicates /155/.

On adsorption of alkali and alkaline earth ions, smectites prefer those which are only slightly hydrated and therefore easily emplaced as an inner sphere complex with the silicate layers. This results in the known selectivity series

$$Cs^+ > Rb^+ > K^+ > Na^+ > Li^+$$

$$Ba^{2+} > Sr^{2+} > Ca^{2+} > Mg^{2+}$$

Sposito /155, p.129/ has interpreted these facts for the alkali ions with the HSAB concept (Hard and Soft Acids and Bases) and was also in a position to explain the difference in behaviour of an octahedrally and an octahedrally as well as tetrahedrally substituted montmorillonite (for other interpretations of the selectivity series see e.g. /55, p.297/).

However, the HSAB concept is not yet in the position to quantify the selectivity of clay minerals on a wide basis. An older overview /140/ and /63, 84/ contain extensive information on sorption selectivity under different experimental conditions. The selectivity of a clay mineral for a particular cation also depends to a large extent on the concentration conditions /31/ so that a comparison of different works is not always possible.

Reference has already been made to the preferred sorption of hydroxo-complexes before the corresponding aquo-ion. This is also true for the adsorption of aluminium /19, 84 p.133/. The hydroxo-complexes polymerise in the interlayers and thus block part of the exchange capacity /9/. This "clogging" can also be caused by emplacement of iron hydroxide or large organic molecules /63, p.211/. Blocking of exchange positions by hydroxides can finally result in products similar to chlorite.

4.2.3 The surface coordination model

In aqueous solutions, water is adsorbed dissociatively on oxidic interfaces. As in the case of hydroxide surfaces, they are covered with surface OH groups. Not only do these groups participate in protolysis reactions but they are also exchangeable against anions and form surface complexes with dissolved metal ions. These reaction possibilities are shown in Figure 38.

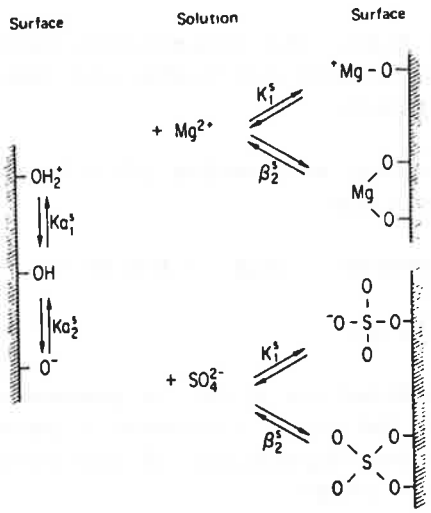

Fig. 38: Possible reactions of surface OH groups of oxides and hydroxides with acids and bases and with cations and anions /161/.

This model was developed and perfected mainly by Stumm /161/ and Schindler /142/. It has proved suitable for finely grained oxides and hydroxides as well as kaolinite /92/.

Cation adsorption is described as complexation with surface OH groups with appropriate mass action constants /141, 159/, (>OH, >MOH signify surface groups):

$$>OH + M^{2+} \rightleftarrows >OM^{+} + H^{+} \qquad {}^{*}K_1^{s}$$

$$2\ >OH + M^{2+} \rightleftarrows (>O)_2M + 2H^{+} \qquad {}^{*}\beta_2^{s}$$

These reactions can be compared with the homogeneous formation of the corresponding hydroxo-complexes:

$$H_2O + M^{2+} \rightleftarrows MOH^{+} + H^{+} \qquad {}^{*}K_1$$

$$2\ H_2O + M^{2+} \rightleftarrows M(OH)_2^{o} + 2H^{+} \qquad {}^{*}\beta_2$$

For a given substrate there is a close correlation between the surface formation constants and the constants of the homogeneous reaction (Figure 39) /141/.

Similarly anion adsorption can be expressed as exchange equilibrium:

$$>MOH + A^- \rightleftarrows >MA + OH^-$$
$$>MOH + HB \rightleftarrows >MB + H_2O$$

A comparison with homogeneous reactions, e.g.

$$MOH^+ + HB \rightleftarrows MB^+ + H_2O$$

is also obvious here. The connections between heterogeneous and homogeneous mass action constants are less good than in the case of cation adsorption.

Besides simple anion and cation adsorbates, mixed surface complexes of the type

$$> M\text{-}A\text{-}M' \quad \text{and} \quad > M\text{-}O\text{-}M'\text{-}A$$

are also known /21/.

The surface coordination model is presented here in a very elementary form. Detailed treatment - particularly of the charge- and loading-dependency of the constants - can be found in the literature cited.

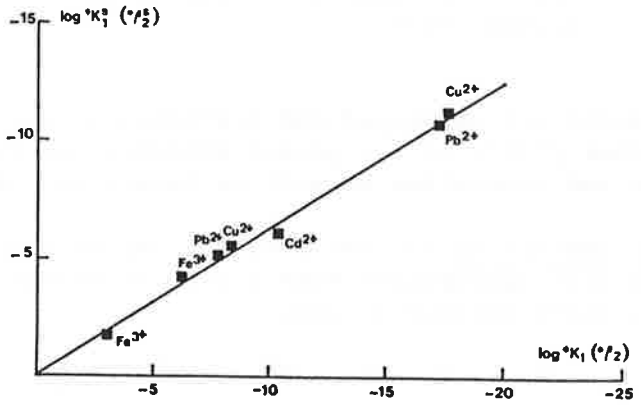

Fig. 39: Comparison of the stability of cationic surface complexes an amorphous SiO_2 ($*K_1^S$, $*\beta_2^S$) with the stability of the corresponding hydroxo-complexes ($*K_1$, $*\beta_2$) /141/.

4.2.4 The effect of ligands on cation adsorption

The effect of ligands on the sorption behaviour of cations cannot generally be predicted because a series of equilibria can be set up in a metal ion/ligand/sorbent system and can be dependent, inter alia, on pH (cf. also /155, p.132/).

If a ligand forms stable dissolved complexes without itself being adsorbed, the sorption equilibria shift to the side of the dissolved metal. Uranium(VI) desorption due to formation of carbonato-complexes at increased pH values is well known (Figure 40). Humic acids can have similar effects (Figure 41).

The complex formed in the solution can also be preferentially adsorbed. This is the case, for example, with adsorption of hydroxo-complexes on smectites.

The ligand adsorbed on a solid surface can bind cations in the form of binary surface complexes. In natural systems, coadsorption of humic acids with metal ions would be expected. Such a system was investigated by Tipping et al. /167/ (Figure 42). At pH values below 6, copper is more strongly adsorbed on goethite in the presence of humic acid. At higher pH values, the concentration of dissolved humic acid increases. It is now available as a dissolved ligand and, correspondingly, less copper is adsorbed in the presence of humic acid (cf. also Figure 4.6 in /155/). Ho and Miller /71/ report similar findings in a haemetite/humic acid/uranium system.

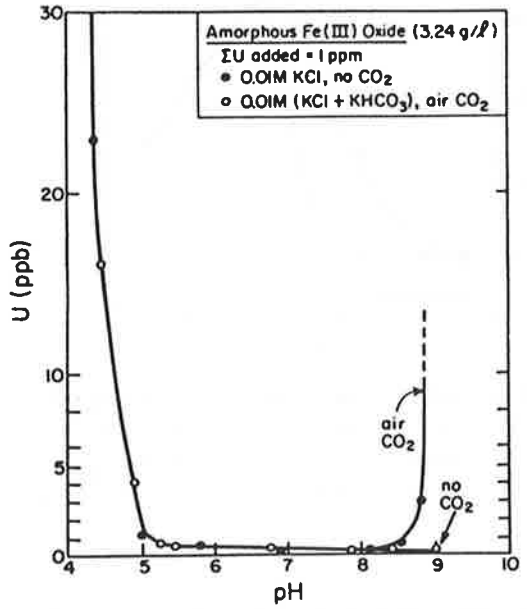

Fig. 40: Adsorption of uranyl ions on amorphous iron(III)-hydroxide with and without carbon dioxide /88/.

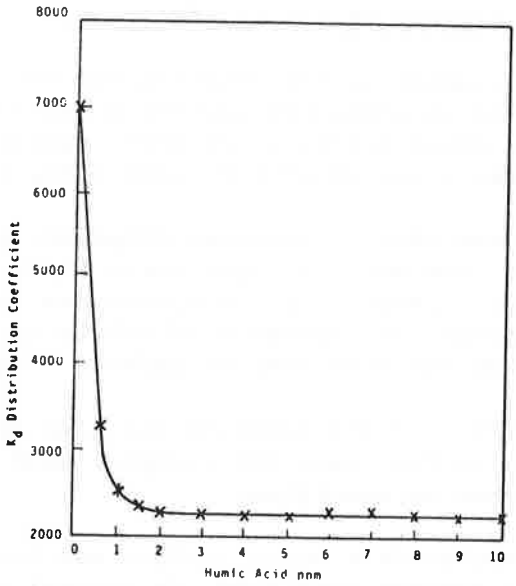

Fig. 41: The effect of humic acid on copper adsorption on iron(III)-hydroxide /66/.

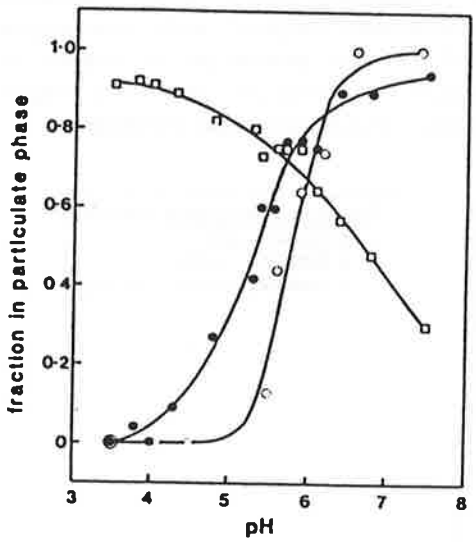

Fig. 42: The adsorption of copper on goethite with (●) and without (o) addition of humic acid.
□ : adsorption of humic acid without copper.
(0.1 g FeOOH/litre, $[Cu^{2+}] = 10^{-5}$M, 10 mg humic acid/litre) /167/.

Benjamin and Bloom /18/ have investigated the effect of various XO_3 and XO_4 ligands on the sorption of zinc, cadmium and cobalt on iron hydroxide and have discovered that arsenate and phosphate increase metal adsorption. In this connection, mention should also be made of investigations of adsorption of EDTA and EDTA-cobalt complexes /75/.

4.3 Experimental results

4.3.1 Cations

McKinley and Hadermann /101/ give realistic and conservative K_d values for bentonite for 28 elements. A further compilation of K_d values for clay minerals is also contained in /103/. Tables 10 and 11 give, by way of illustration, the K_d values of important nuclides for different minerals.

Data for strontium and caesium can be found in /9/ and /8/ contains an overview of literature data on sorption of fission products on geological sorbents. Adsorption of strontium and caesium on natural bentonite, active bentonite and four natural clays was investigated by Brodda and Merz /24/ in distilled water and in various salt solutions. The K_d values are given as a function of nuclide concentration.

Table 10: Distribution coefficients for Sr^{2+}, Cs^{+} and TcO_4^{-} on clay minerals /29/.
CEC = cation exchange capacity.

	Strontium		Caesium		Technetium	
	K_d (ml/g)	Conditions	K_d (ml/g)	Conditions	K_d (ml/g)	Conditions
Kaolinite (CEC = 5.0 meq/100g)	55 257 200 2 100	pH = 7.5 pH = 10 0.0014 N $MgCl_2$, Mg-Kaol. 0.2 N $CaCl_2$, Ca-Kaol. 0.002 N $CaCl_2$, Ca-Kaol.	94 $2.5 \cdot 10^3$ 900	0.1 M NaCl dist. water Mg-Kaol.	< 4	0.51 M NaCl, pH = 7 0.03 N CaCl, pH = 7 0.03 N NaCl, pH = 7 0.03 N $NaHCO_3$
Illite (CEC = 14 meq/100g)	117 200 90 2	pH = 7.5 0.007 N $MgCl_2$, Mg-Ill. 0.002 N $CaCl_2$, Ca-Ill. 0.1 N $CaCl_2$, Ca-Ill.	$2.9 \cdot 10^4$ $2.6 \cdot 10^4$ $2 \cdot 10^3$ 10^5	0.1 M NaCl dist. water K-Illite Na-Illite	4.7 0.5 10.3 0.0	as above
Montmorillonite (CEC = 87 meq/100g)	506 10 700	pH = 7.5 0.1 N $CaCl_2$, Ca-Montm. 0.002 N $CaCl_2$, Ca-Montm.	$2 \cdot 10^4$ $5 \cdot 10^3$	K-Montm. Ca-Montm.	0.2	as above

Table 11: Distribution coefficients for actinides on clay minerals /29/.
CEC = cation exchange capacity.

	Thorium		Neptunium		Plutonium		Americium/Curium	
	K_d (ml/g)	Conditions	K_d (ml/g)	Conditions	K_d (ml/g)	Conditions	K_d (ml/g)	Conditions
Kaolinite (CEC = 5.0 meq/100g)	600 $2 \cdot 10^5$	pH = 3.0 pH = 6.2	4.2 0.5 3.6 122	pH = 7; 0.51 M NaCl pH = 7; 0.03 N $CaCl_2$ pH = 7; 0.03 M NaCl 0.03 M $NaHCO_3$, neutral	352	pH = 6.25	4.3/3.2	pH = 5; 0.25 M NaCl
Illite (CEC = 14 meq/100g)	170 $4 \cdot 10^5$	pH = 3.7 pH = 7.0	42 14 27 295	as above	129	pH = 5.9	-	
Montmorillonite (CEC = 87 meq/100g)	$2 \cdot 10^5$ $2 \cdot 10^4$ $2 \cdot 10^5$	pH = 5.5 pH = 6.5 pH = 7.9	40 17 46 9	as above	630	pH = 9.2	34/37	pH = 5; 0.25 M NaCl

Beall and Allard /16/ have investigated the sorption behaviour of americium and neptunium(V) on various clay minerals. Neptunium is poorly sorbed on montmorillonite (K_d = 0.06 m^3/kg) which points against preferred sorption of lowly-charged ions by ion-exchange. Figure 43 shows the behaviour of americium. A pH effect is noted only with high ionic strength and pH values below 7. At pH 8, the K_d values of americium on non-swelling clay minerals (muscovite, chlorite, kaolinite) are somewhat higher than on montmorillonite.

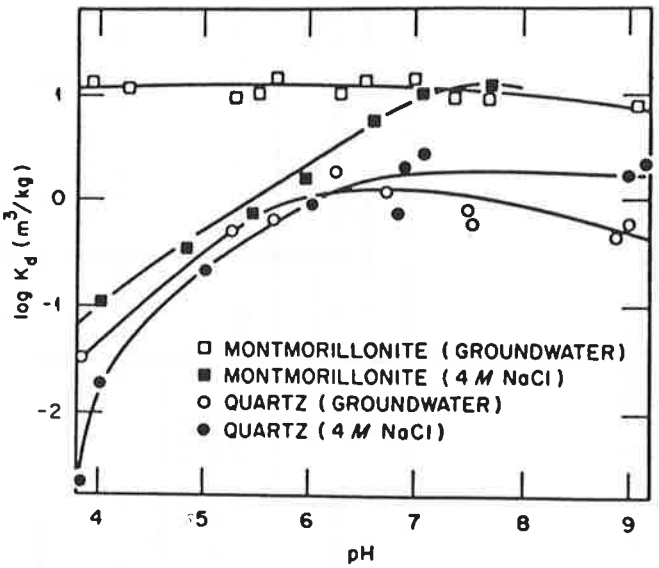

Fig. 43: The adsorption of americium on montmorillonite and quartz in groundwater and in 4 M NaCl solution /16/.

Investigations of uranium(VI) sorption on clay minerals have shown a direct relationship between sorption capacity and ion-exchange capacity /20/. At concentrations below 10^{-4} moles/litre, K_d values were found which rise from 50 to 10^3 for kaolinite, illite and montmorillonite. The work also contains adsorption isotherms on various clays in the range 10^{-5} to 10^{-2} moles U(VI) per litre as well as the effect of some other metal(II) ions on uranyl sorption at pH 6. The effect of ionic strength on the sorption behaviour of actinides and fission products on montmorillonite has been investigated in depth in /15, 146/. Most measurements were carried out at pH = 5. Because hydrolysis drastically alters sorption properties, the results can only be extrapolated to higher pH values if the cation is still present as an aquo-complex.

4.3.2 Anions and weak acids

The surface coordination model of anion adsorption /108, 155, 161/ can basically be applied to clay minerals such as kaolinite and smectites. Account has to be taken of the fact that, in the case of smectites, basically only the border OH groups contribute to anion adsorption. Their anion exchange capacity is therefore dependent on particle size. Given these new aspects,

the systematic work of A. Weiss /180/ on anion exchange is still applicable. The anion exchange capacites in Table 12 are taken from this work.

Table 12: Anion exchange capacity (AEC) of various clay minerals (exchange for fluoride at pH 7.1) as compared with their cation exchange capacity (CEC) /180/.

	CEC (meq/100g)	AEC (meq/100g)
Montmorillonite Geisenheim	91	31
Montmorillonite Wyoming	99	23
Montmorillonite Cyprus	108	23
Beidellite Unterrupsroth	111	21
Kaolinite Milos	7.2	13.3
Kaolinite Schnaitenbach	2.6	6.6

The sorption of phosphate on clay minerals has been extensively investigated in connection with the nutrient content of soils (summary in /63, p.228/). It is to be noted here that, besides sorption, a precipitation reaction can also occur on calcium bentonite.

Other anions were investigated in less depth. There is very little information on silicic acid and humic acid. Anions such as iodide and pertechnate are not sorbed on clays.

The adsorption behaviour of silicic acid on α-FeOOH can be described as surface equilibrium /160/. The low pH-dependence of adsorption is characteristic of this system (Figure 44). It is assumed that the silicic acid in the soil is adsorbed on iron- or aluminium hydroxide /116/. In contrast with the work cited above, there is a clear adsorption maximum at pH 9.

It follows from investigations by Siever and Woodford /147/ that clay minerals, and montmorillonite in particular, adsorb silicic acid and thus, under certain conditions, represent a silicic acid sink (Figures 45 and 46). The possibility of the silicic acid polymerising on the clay surface cannot be ruled out as was the case with iron(III) hydroxide /189/. There are no investigations at higher temperatures which would allow a prediction to be made for the repository.

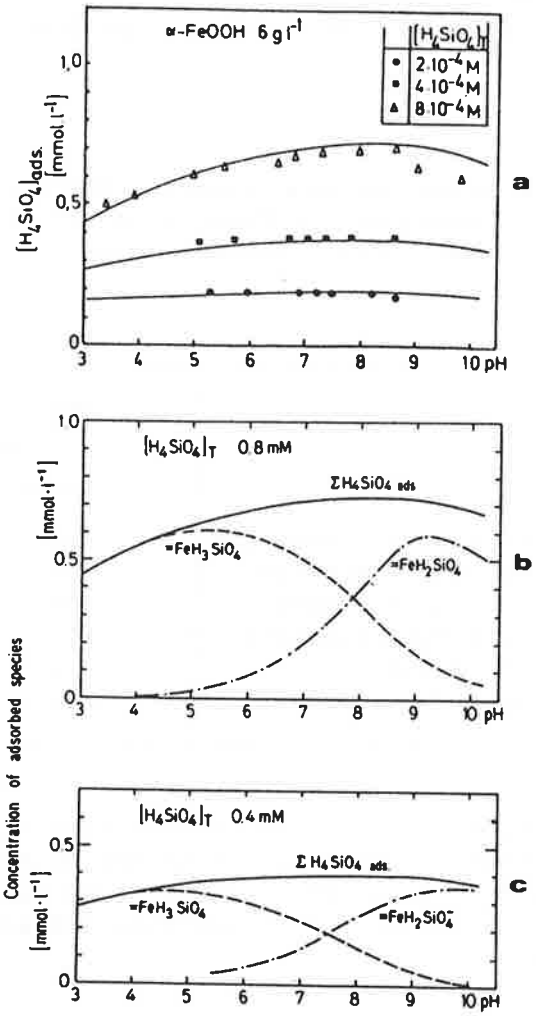

Fig. 44: Adsorption of silicic acid on goethite as a function of pH. The points represent experimental measurements and the lines were calculated with equilibrium constants /160/.

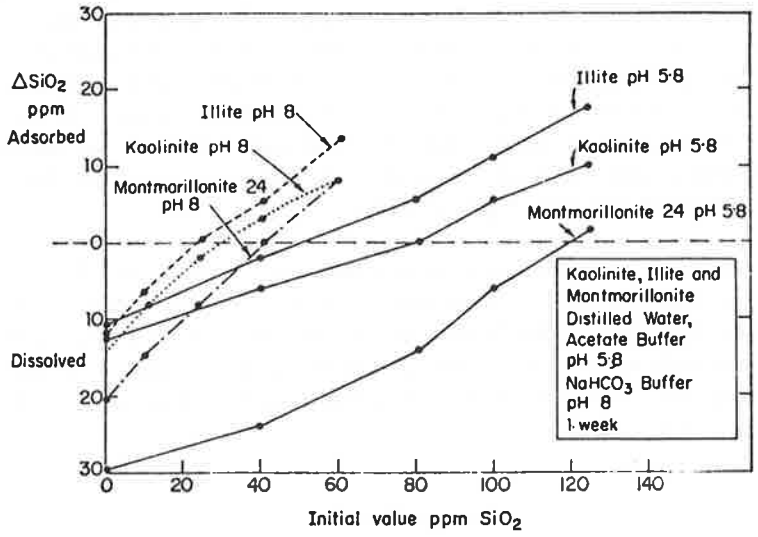

Fig. 45: Dissolution and silicic acid adsorption of clay minerals in distilled water and in buffer solutions /147/.

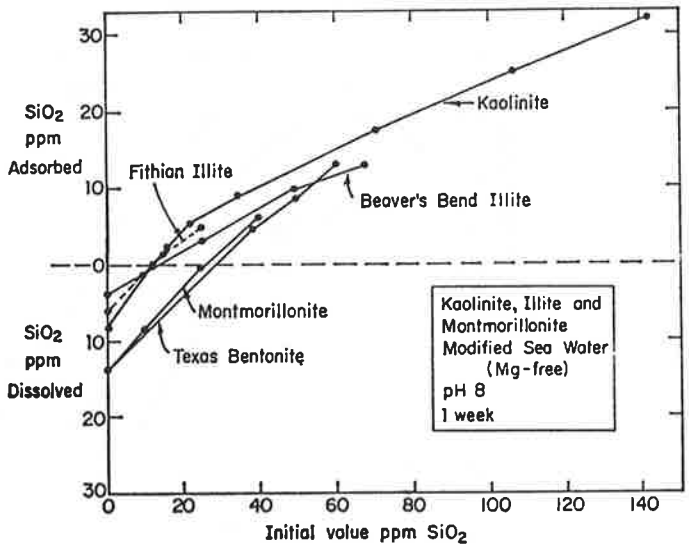

Fig. 46: Dissolution and silicic acid adsorption of clay minerals in magnesium-free sea-water at pH 8 /147/.

When boric acid is adsorbed on sodium and potassium layer silicates /149/, the interlayers are involved in the sorption process. Investigations lead to the conclusion that hydroxide precipitations on the clay and aluminium hydroxides in the interlayers provide the main contribution to sorption capacity: a montmorillonite washed with acid takes up only very small quantities of boric acid. In calcium bentonite, boric acid can be bound by precipitation.

Humic materials are adsorbed on oxidic surfaces (Figure 47 /34/, cf. Figure 42). Bonding of such materials on clay minerals is, according to current concepts /62, 157/, by hydrogen bonds or polyvalent metal ions (Figure 48). Such a "humic acid-clay complex" /63, p.354/ is predestined for adsorption of further cations /187/.

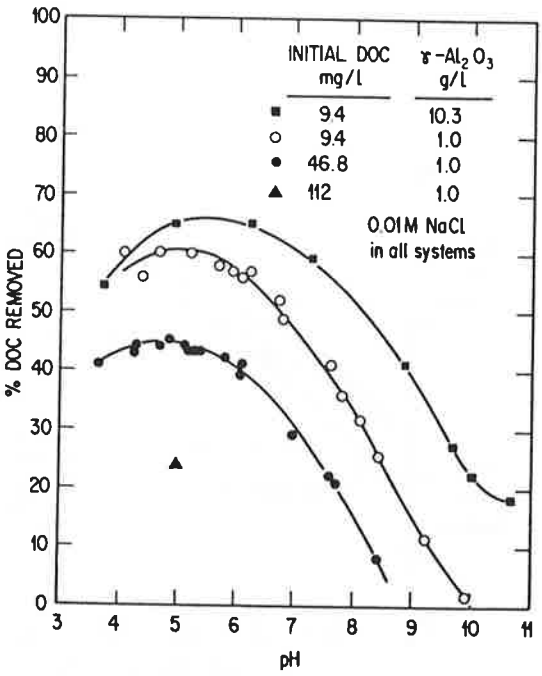

Fig. 47: Adsorption of humic materials from Urnersee sediments on aluminium oxide as a function of pH, DOC (dissolved organic carbon) content and amount of solid material /34/.

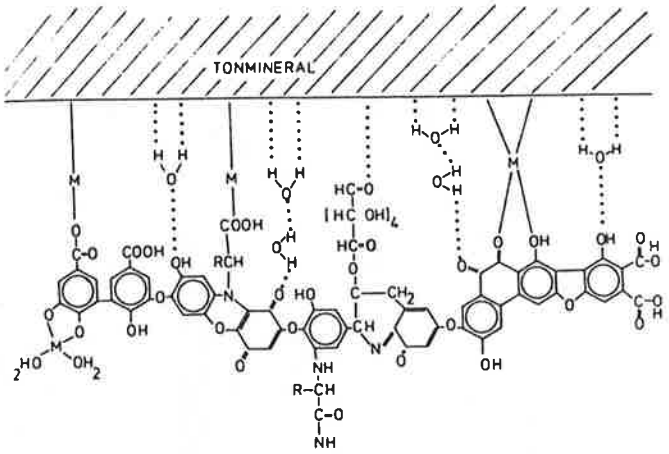

Fig. 48: Concepts of adsorption of humic acid on clay minerals /63, 157/.

Emplacement of macromolecular organic materials in the interlayers reduces the cation exchange capacity of smectites ("clogging"). Fulvic acids appear to be introduced into the interlayers of montmorillonite only with pH values below 4, i.e. under conditions where aluminium is released by partial dissolution of the montmorillonite and incorporated into the interlayers.

4.3.3 Temperature effects

The effect of temperature on the sorption capacity of smectites is summarised in /103/. In a model groundwater, the differences in K_d values of cations at 23 and 60°C are low (Figure 49). In bentonite-sand mixes, the K_d values of most nuclides increase slightly with a temperature increase to 65°C /2/. In a salt solution, the K_d value of europium increases by a factor of around 3 with a change from ambient temperature to 70°C /114/. The K_d values of strontium and caesium on a bentonite alter only insignificantly with increased temperature (100°C) and increased pressure (100 bars) (Figure 50 /24/).

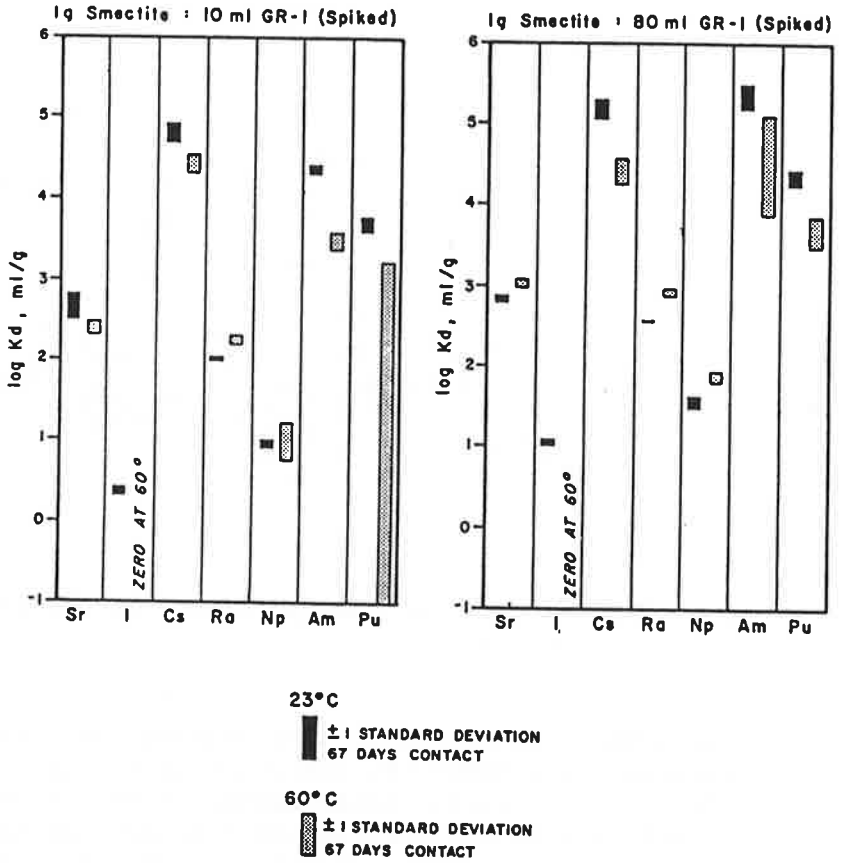

Fig. 49: Effect of temperature and solid/solution ratio on the sorption of radionuclides on clay from fissure infills in Hanford basalt /103/.

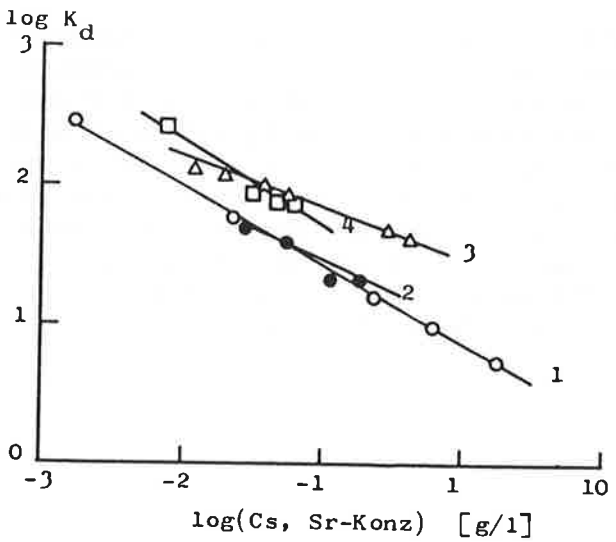

Fig. 50: K_d value as a function of equilibrium concentration of Cs and Sr in aqueous solution at different temperatures and pressures (natural bentonite)/24/. (1: Sr, 1 bar, 25°C; 2: Sr, 100 bars, 100°C; 3: Cs, 1 bar, 25°C; 4: Cs, 100 bars, 100°C).

Sorption of Sr-90 on different clays and chlorite is influenced only slightly by temperature, particularly with high solid/liquid ratios in the range 20 to 60°C /90/. Cs-137 behaves differently on the same solids: the K_d value is significantly lower at 60°C than at 20°C. The difference can be more than an order of magnitude.

Temperature dependence in the range 5 to 65°C has also been investigated in an extensive work on sorption of uranium(VI) and radium at trace levels on clay minerals and various SiO_2 modifications /3/ and of uranium(VI) on minerals of the mica group /4/.

The aqueous phases were 0.01 molar solutions of sodium chloride and sodium hydrogen carbonate. Figures 51 to 57 show some of the results for montmorillonite and illite.

As can be seen from a comparison of Figures 51 and 52, formation of uranium(VI) carbonato-complexes can alter the direction of the temperature effect on illite. The strongest sorption on montmorillonite (Figures 53 and 54) is at 65°C in both solutions. However, as with illite, the formation of carbonato-complexes results in drastically lowered K_d values. Also noticeable are the lower K_d values on montmorillonite as compared with illite.

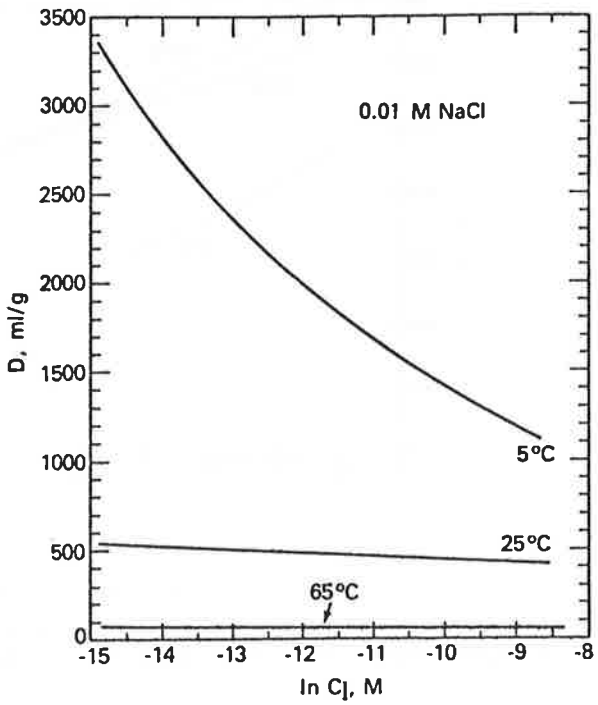

Fig. 51: The distribution coefficient of uranium(VI) on illite in 0.01 M NaCl solution at different temperatures and uranium concentrations /3/.

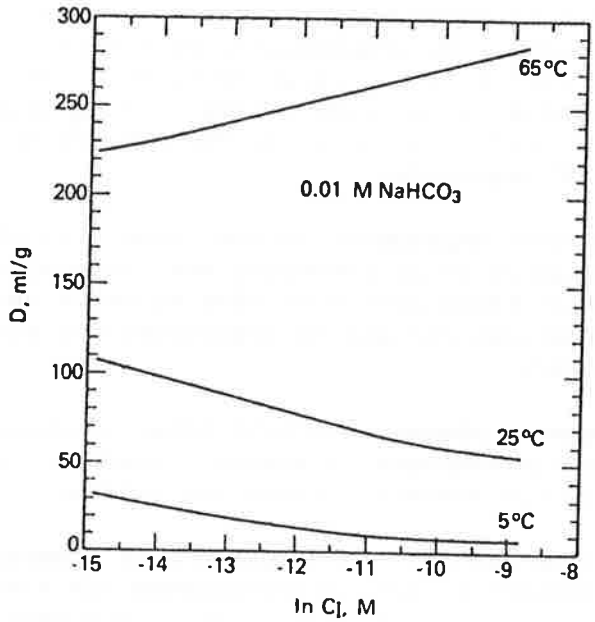

Fig. 52: The distribution coefficient of uranium(VI) on illite in 0.01 M $NaHCO_3$ solution at different temperatures and uranium concentrations /3/.

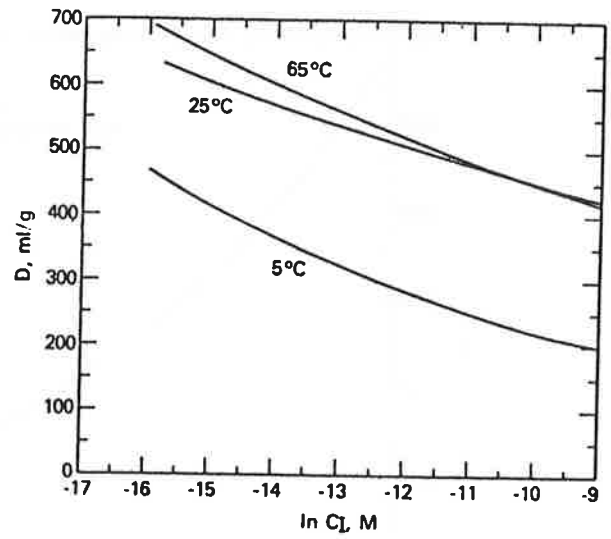

Fig. 53: The distribution coefficient of uranium(VI) on montmorillonite in 0.01 M NaCl solution at different temperatures and uranium concentrations /3/.

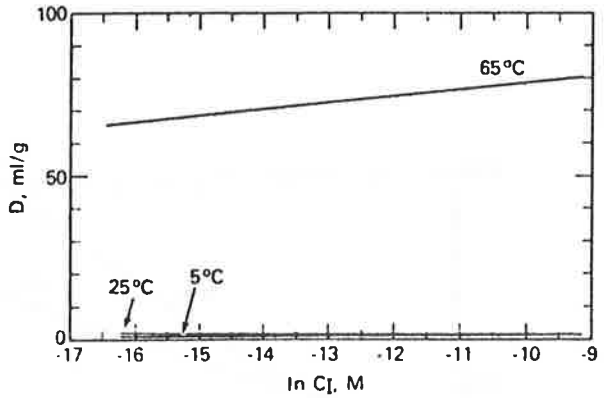

Fig. 54: The distribution coefficient of uranium(VI) on montmorillonite in 0.01 M $NaHCO_3$ solution at different temperatures and uranium concentrations /3/.

Temperature dependence is also reversed in the case of sorption of radium on illite on changing from chloride- to bicarbonate solution (Figure 55). There are considerable differences between the sorption behaviour of illite and montmorillonite (Figures 56 and 57), with illite being the better sorbent under certain conditions.

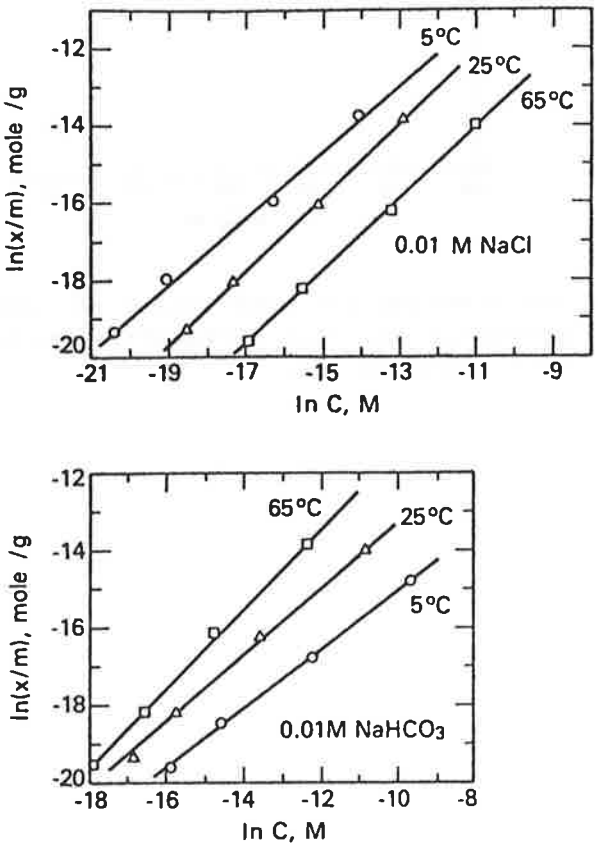

Fig. 55: Linearised Freundlich isotherms of radium adsorption on illite at different temperatures in NaCl and $NaHCO_3$ solution /3/.

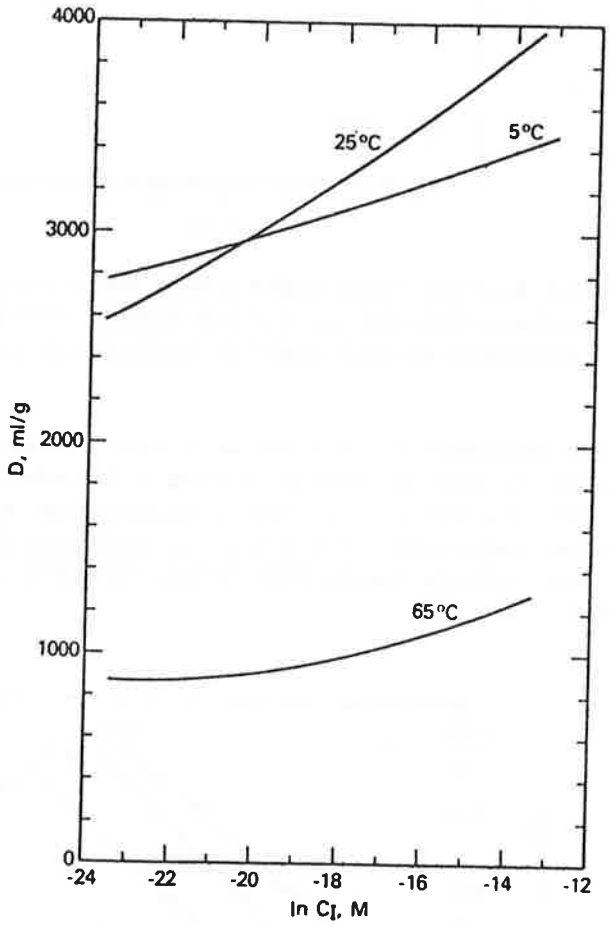

Fig. 56: The distribution coefficient of radium on montmorillonite at different temperatures in 0.01 M NaCl solution /3/.

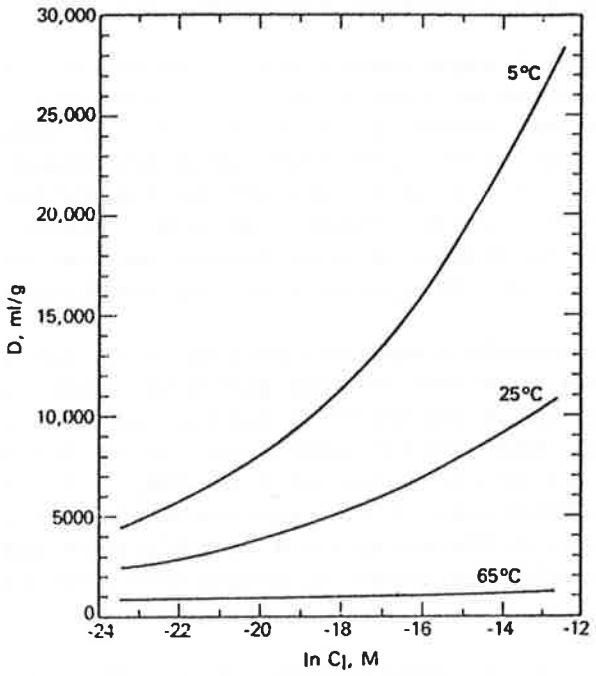

Fig. 57: The distribution coefficient of radium on illite at different temperatures in 0.01 M NaCl solution /3/.

In many cases the temperature effect on sorption behaviour appears to be small. However, as the research discussed in the last pages shows, the effect can become significant. The direction of the temperature course of the K_d values depends not only on the mineral but also on other parameters such as the temperature-dependence of complex equilibria. Experimental investigation in realistic systems would seem to be necessary for critical nuclides.

5 DIFFUSION AND TRANSPORT PROCESSES IN COMPACTED BENTONITE

Most sorption experiments were carried out in aqueous clay suspensions under widely varying conditions (clay/solution ratio, water chemistry) so that a direct comparison of different works is not always possible. Such investigations cannot, therefore, generally be applied to repository conditions where compacted bentonite rather than a suspension exists. The bentonite functions as a diffusion barrier and causes additional retardation of certain nuclides by sorption.

Water-saturated, compacted bentonite is idealised as a membrane with fixed negative charges and mobile cations. In an ideal situation it is therefore a cation conductor. In compacted bentonite, the average layer spacing in the montmorillonite fraction is in the order of 2 nm /44, 130/ and is therefore less than the thickness of the electrical double layer. Such a system will behave differently to a solid/liquid system with pores whose diameter is large in comparison with the electrical double layer:

- anions are excluded because of selective cation conductivity
- instead of volume diffusion in pore-water, surface diffusion can contribute significantly to material transport and can thus lead to unexpected diffusion coefficients.

Neretnieks /110/ has made special reference to the second aspect.

5.1 Diffusion coefficients and experiments

Different diffusion coefficients D should be distinguished when describing diffusion through porous media. D_w describes the diffusion coefficient in the macroscopic aqueous phase.

The pore diffusivity D_p is linked under ideal conditions (no interactions with the pore-wall) with D_w by the relationship

$$D_p = D_w \frac{\delta}{\tau^2}$$

$\frac{\delta}{\tau^2}$ is a geometry factor with
δ : constrictivity
τ : tortuosity

With one-dimensional diffusion through a porous layer, stationary mass flow is

$$\phi = \varepsilon D_p \frac{\delta c}{\delta x} \qquad \text{(Fick's first law)}$$

where ε is the porosity. The effective diffusivity D_e can be determined from steady-state experiments and is defined by

$$D_e = \varepsilon D_p$$

The apparent diffusivity D_a is different from D_p if, in non-stationary experiments, the diffusing particle is retarded by interaction with the pore-wall.

$$D_a = \frac{D_p}{R}$$

is valid. R is the chromatographic retention or retardation factor which is derived from linear distribution of a substance between solution and solid:

$$R = \frac{n_t}{n_l} \quad \frac{n_l + n_s}{n_l} = 1 + \frac{c_s V_s}{c_l V_l}$$

With $V_t = V_s + V_l = V_t(1-\varepsilon) + V_t\varepsilon$ and $\rho K_d = c_s/c_l$

it follows that

$$R = 1 + \rho K_d \frac{1 - \varepsilon}{\varepsilon} \qquad (1)$$

n_s, n_l, n_t: moles of sorbable material. s: on solid, l: in solution, t: total

V_s, V_l, V_t: volume of solid material (s), solution (l) and total volume (t)

c_s, c_l : concentration of sorbable material on solid ($c_s = n_s/V_s$) and in solution ($c_l = n_l/V_l$)

ρ : density of the sorbent (related to V_s). As K_d is normally given in m^3/kg, the ratio is $c_s/c_l = \rho K_d$

ε : porosity

If equation (1) is formulated with the reduced density

$$\rho' = \rho (1 - \varepsilon)$$

this results in

$$R = 1 + \rho' K_d \frac{1}{\varepsilon} \qquad (2)$$

The formulae

$$R \simeq 1 + \rho K \frac{1}{\varepsilon} \qquad (1a) \text{ and}$$

$$R \simeq 1 + \rho K \qquad (1b)$$

result from equation (1) for slightly porous materials ($\varepsilon \ll 1$) and for media with $\varepsilon \simeq 0.5$. It is not clear in some publications whether ρ or ρ' has been used and no difference can then be drawn between equation (2) and the approximation (1a).

With low diffusion rates, it can take months or even years to set up steady-state conditions. For experimental purposes, mostly apparent diffusivities from non-stationary tests are determined. The effective diffusivity is calculated from this using the above formulae.

The usual arrangements for diffusion experiments on compacted water-saturated bentonite are given in Figures 58 and 59 /47/. The formulae required for test evaluation are also given in this work.

Kahr et al. /80/ have investigated ion diffusion on compacted bentonite with defined water contents using a non-stationary method.

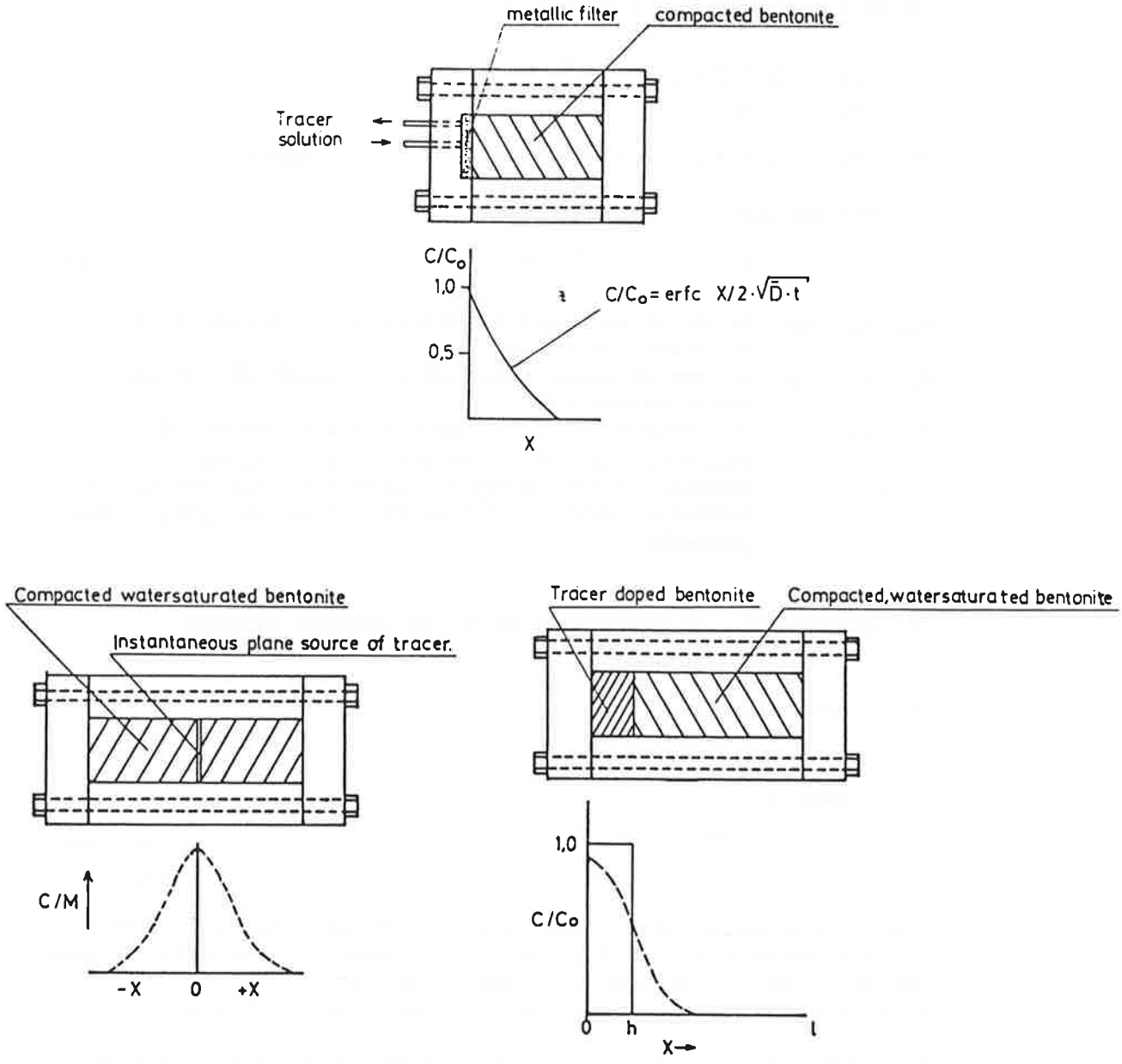

Fig. 58: Arrangements for non-stationary diffusion tests on compacted bentonite with theoretical concentration profiles /47/.

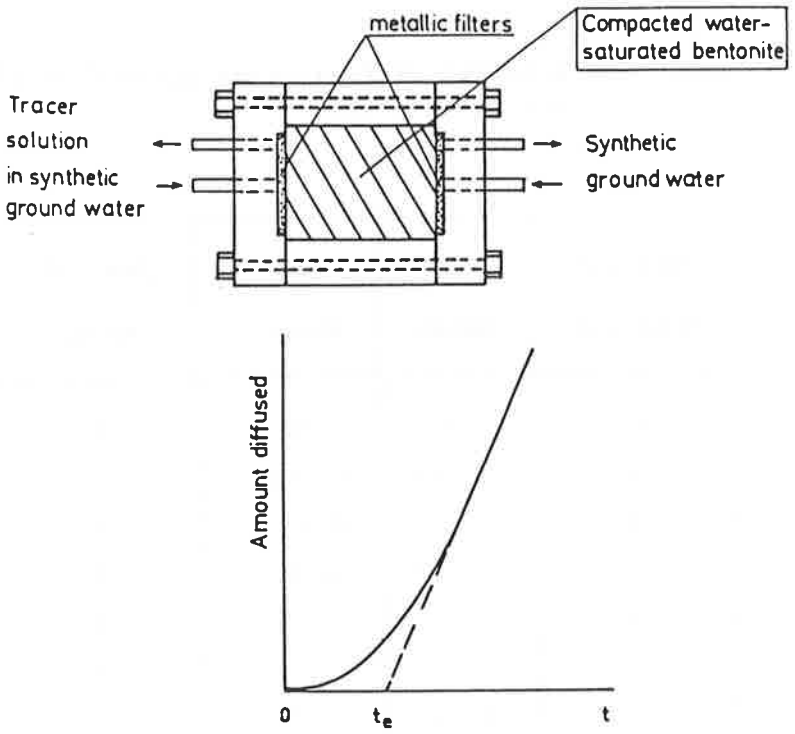

Fig. 59: Arrangement for steady-state diffusion tests on compacted bentonite /47/.

5.2 Experimental results

Results of diffusion measurements on MX-80 and Montigel can be found in /80/. Erbslöh Ca-bentonite as well as MX-80 have been investigated in extensive Swedish studies /44, 45, 168/. Summary discussions can be found in /47, 110/.

As several compilations of diffusivities already exist /80, 110, 158/, the information here is restricted to Tables 13 and 14. The diffusivities of various ions as a function of water content are summarised in Figure 60. Data on diffusion behaviour of water are taken from /80/ (Figure 61). Schreiner et al /43/ report on the diffusion of relevant nuclides in marine sediments and clays. Lai and Mortland /87/ have determined the activation energies of self-diffusion on Na- and Ca-montmorillonite (Table 15); they decrease with decreasing water content. It can also be deduced from this work that a sodium diffusion can be measured in a kiln-dried sample ($D = 7.4 \cdot 10^{-13}$ $m^2 s^{-1}$) while diffusion of sulphate is not measurable.

With relation to transport of colloidal particles (hydrolysis products, pseudo-colloids), diffusion measurements with large molecules are of interest. Sodium ligninsulphonates (molecular weights from 354 to 30,000) eosin and anthrachinosulphonate have all been investigated /46/. The diffusivities observed are in the order of 10^{-15} $m^2 s^{-1}$.

Table 13: Apparent diffusivities $D_a \cdot 10^{12}$ in m^2/s for saturated bentonite /158/.

Reference	/168/	/168/	/44, 45/	/110/
Material	MX-80	MX-80	MX-80	No information
Sr	1.8	12	23	25
Am	0.004	0.014		0.015
Cs	1.4	2.0	7.5	8
I	0.032	0.12	4	9
Cl			6	
HS			9	
Np	0.22	0.37		0.4
Pu	0.003	0.03		0.03
Pa	0.57	0.6		1
Ra				25
Tc	1.4	5.3 (53)		53
Th	0.0046	0.0085		0.01
U	0.58	0.82		1

Table 14: Effective diffusivities $D_e \cdot 10^{12}$ in m^2/s for saturated bentonite /158/.

Reference	/168/	/44, 45/	/110/
Material	MX-80	MX-80	No information
Sr	31'000		10'000 - 67'000
Cs	1'800		1'800 - 9'000
I	0.1	0.21	4
Cl		0.31	6
HS		0.018	9
H_2		3.6	
Np	52		52 - 88
Tc	1.4		
U	19		

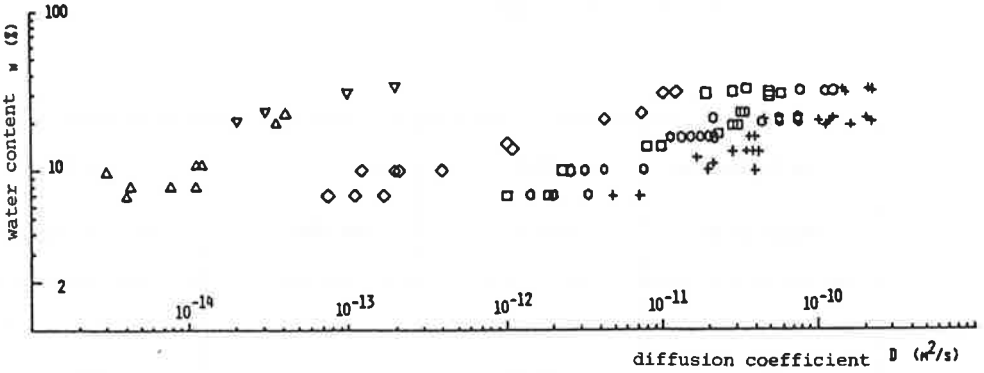

	Ion	Salt
▽	Th^{4+}	$Th(NO_3)_4$
△	UO_2^{2+}	$UO_2(NO_3)_2$
◇	Cs^+	CsCl, CsJ
□	Sr^{2+}	$SrCl_2$, SrJ_2
o	K^+	KCl, KJ
+	Cl^-, J^-	KCl, KJ, CsJ

Fig. 60: Measured apparent diffusivities for unsaturated bentonite at ambient temperature from /80/.

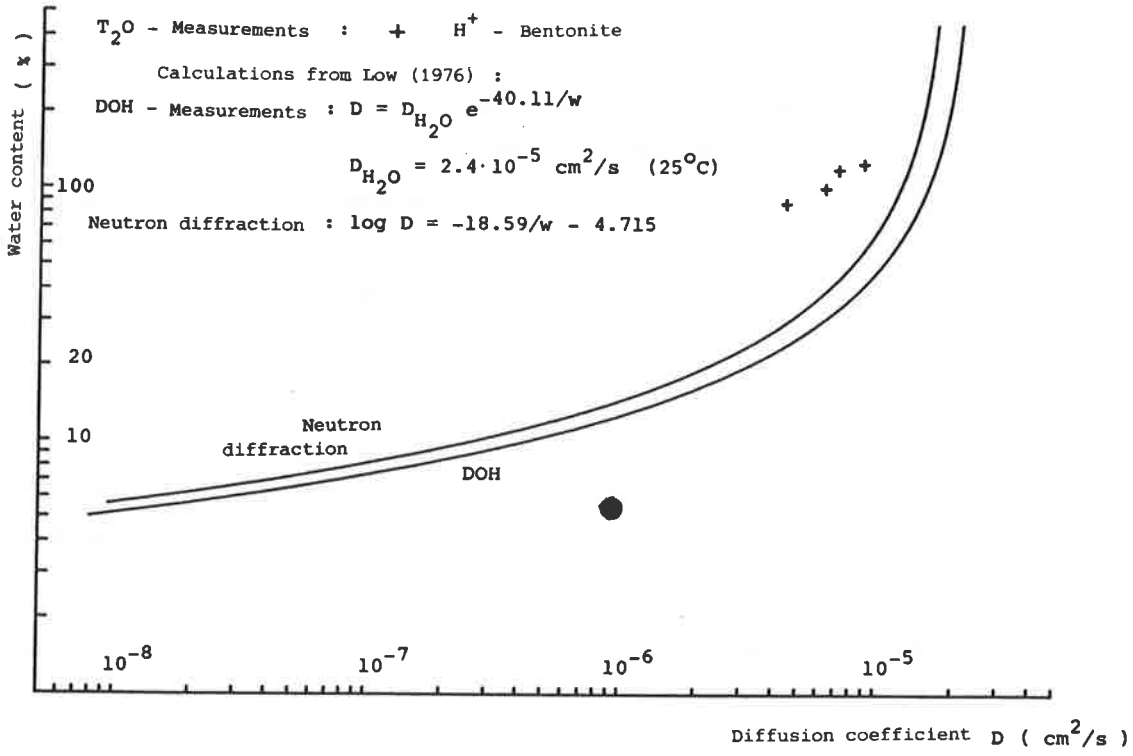

Fig. 61: Diffusion of water in bentonite /80/.
● : value from /186/.

Table 15: Self-diffusion coefficients D and related activation energies E for Na^+ and Ca^{2+} in bentonite/water mixes /87/.

Ion	Bentonite content %	D ($cm^2sec^{-1} \times 10^6$)	E ($cal\ mol^{-1}$)
Na^+	8.9	5.70 ± 0.11	6040 ± 181
	12.9	4.47 ± 0.09	5176 ± 155
	15.2	3.60 ± 0.07	3806 ± 114
Ca^{2+}	17.9	2.36 ± 0.07	10856 ± 326
	23.9	1.95 ± 0.06	9654 ± 290
	28.0	1.75 ± 0.05	8747 ± 262

Different test results and anomalies in diffusion behaviour show that the classic pore model (diffusion in pore-water and sorption on pore-walls, Chapter 5.1) is only of limited application to compacted bentonite /47, 110/. Abnormally high effective diffusivities of caesium, strontium and protactinium imply that surface diffusion dominates /110/.

The diffusion behaviour of the anions also does not agree with the classic model (e.g. /45/). The reason for this could be anion exclusion from the cation-conducting clay membrane. The use of K_d values from batch tests together with equation (1) therefore leads to false diffusivities. The measured anion diffusivities depend strongly on the test conditions: Kahr et al. /80/ have measured significantly higher values than Eriksen and Jacobsson /44, 45/ (cf. also /47/).

5.3 The barrier effect of the backfill material

If the nuclides released from the waste matrix decay within the backfill material, the bentonite functions as a containment barrier. By way of illustration, some examples from a work by Wood /188/ are introduced. Figures 62 and 63 show the relationship between the K_d values and the layer thickness of the backfill required to ensure a certain retention time. The calculations were carried out for the one-dimensional case with $D_w = 10^{-9}\ m^2 s^{-1}$, $\rho' = 2\ kg \cdot l^{-1}$ and $\varepsilon = 0.1$. The two equations

$$c/c_o = \text{erfc}\left[\frac{x}{2}\left(\frac{Dt}{R}\right)^{-\frac{1}{2}}\right]$$

and

$$R = 1 + K_d \frac{\rho'}{\varepsilon}$$

were used as a basis and $c/c_0 = 0.05$ is used as the criterion for the breakthrough (x: diffusion path).

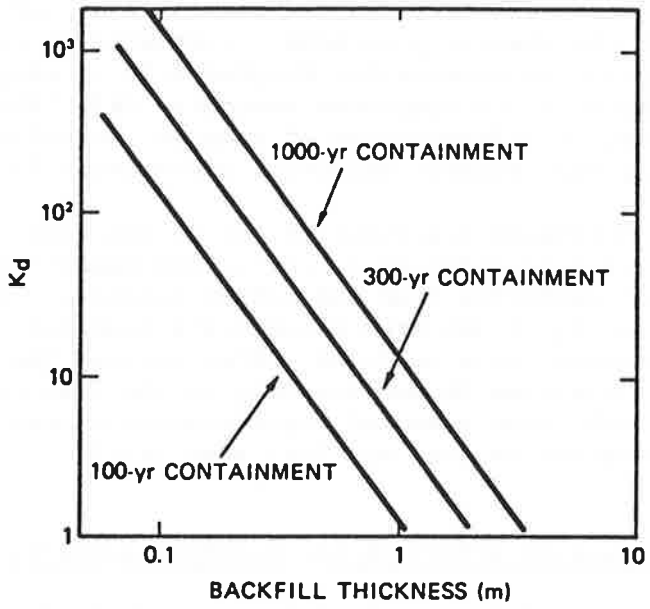

Fig. 62: Values required for the distribution coefficient K_d and the thickness of the backfill material for total retention of nuclides during pre-determined times (K_d in l/kg) /188/.

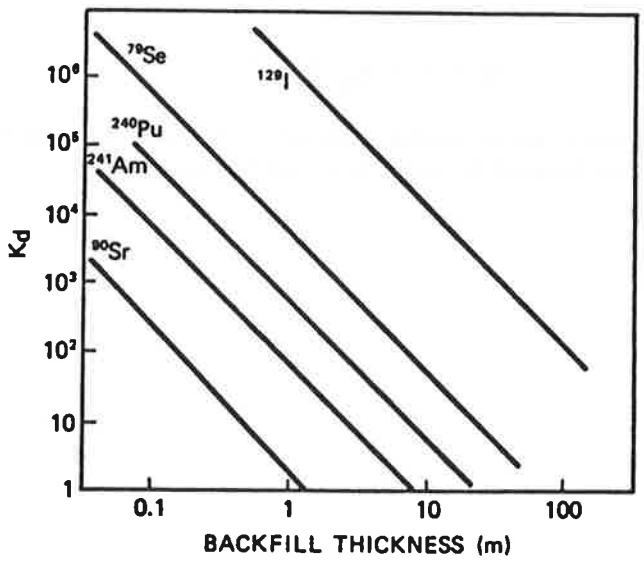

Fig. 63: Values required for K_d and thickness of backfill for nuclide retention during five half-lives /188/.

As Figures 62 and 63 show, it can be assumed that short-lived nuclides such as Sr-99 (K_d = 60 l/kg) and Am-241 decay within the backfill material. The same could also be true for the plutonium isotopes 239 and 240 /110/. On the other hand, it is practically impossible to design a backfill in such a way that e.g. Se-79 or even I-129 decay within its confines. The bentonite layer functions simply as a retardation section for these nuclides /188/.

5.4 The gas permeability of bentonite

The gas permeability of compacted bentonite is important for the Nagra concept because the steel canister will corrode with hydrogen production. With a realistic corrosion rate of 5 to 10 µm per year, 12 to 24 moles of hydrogen per canister and year will have to escape through the bentonite. Opinions have been voiced to the effect that this quantity of gas cannot be removed by way of diffusion, so that a hydrogen pressure which exceeds the lithostatic pressure could be built up in the repository /111/.

Previous values for gas permeability of compacted bentonite /134/ can be interpreted with diffusion processes /135/. Estimates show that 10% of the corrosion hydrogen at most can escape by means of diffusion /111/, cf. also /102/.

In connection with this problem, the pressure-dependence of hydrogen permeation in MX-80 was measured /135/. Above a critical pressure P_c which, depending on the density of the bentonite, is 20 to 90% of the swelling pressure, the gas permeability increases dramatically. At pressures below P_c, hydrogen migration is probably mainly by diffusion of the dissolved gas. With pressures over P_c, paths of higher gas permeability form in the bentonite and can lead away large quantities of hydrogen.

5.5 Electrical conductivity

Electrolyte resistance is an important parameter for corrosion reactions in aqueous solutions. This is particularly true for localised corrosion where anodic and cathodic reactions are separated /60/. With electrolyte resistances over ca. $10^4\,\Omega\,cm$, the risk of formation of corrosion elements at low general corrosion rates is very small. In such cases, cathodic protection of underground steel constructions is not necessary in practice. Measurements on Montigel and MX-80 show that, with a water content of 30%, the conductivity is $10^{-4}\,\Omega^{-1}cm^{-1}$ (Figure 64 /79/); from the point of view of canister corrosion, a poorly conducting electrolyte is present. Comparable conductivities are given by Calvet /28/. Further information can be found in /53, 123/.

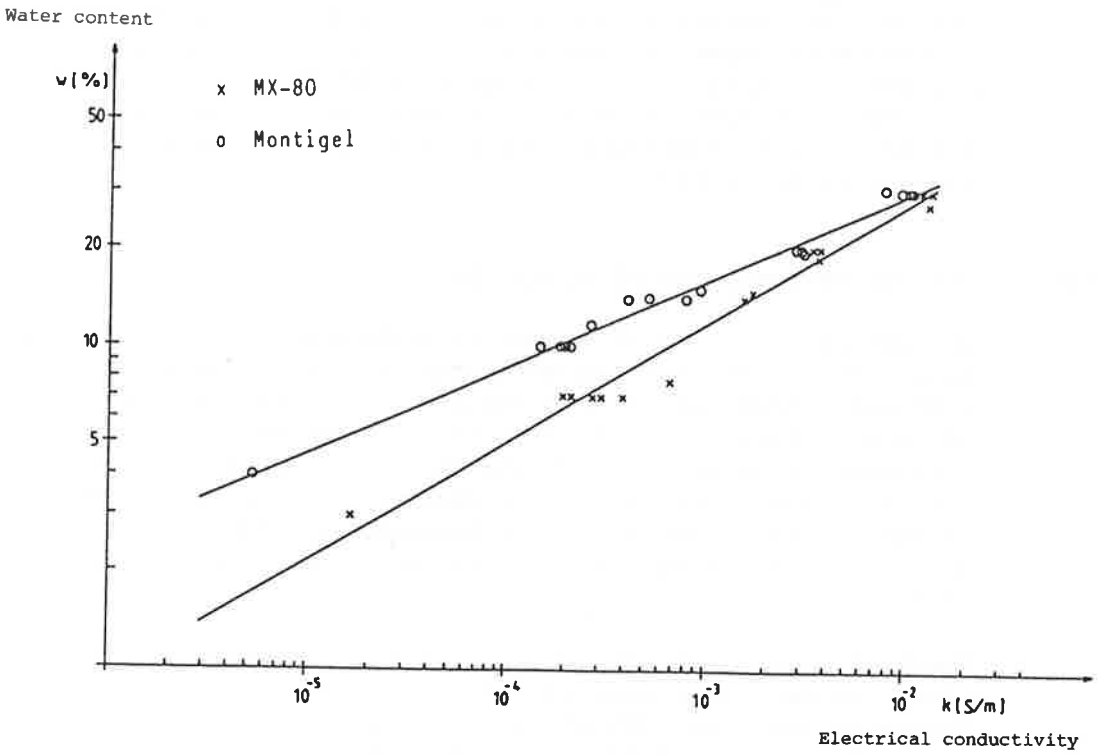

Fig. 64: Electrical conductivity k of bentonite MX-80 and Montigel at ambient temperature as a function of water content w /79/.

6 THE STABILITY OF MONTMORILLONITE

Natural occurrence of old bentonites is an indication of their long-term stability. However, when considering the behaviour of the repository backfill, the possibility of montmorillonite alteration is to be taken into account. Basically, the following possibilities exist:

- irreversible layer collapse with dry heating
- phase alterations with complete breakdown of the smectite structure
- increase in the layer charge due to isomorphic substitution of silicon with aluminium or by redox processes. Illite is formed with simultaneous or subsequent supply of potassium
- emplacement of hydroxide layers in the interlayer spaces of the montmorillonite. This is linked with a decrease in cation exchange capacity and swelling capability.

Besides temperature and pressure, further important parameters to be considered are:

- pH value and the concentrations of alkali- and alkaline earth ions and silicic acid
- the solid to water volume ratio.

In assessing experimental work from the point of view of final disposal, account should be taken of the fact that often strongly diluted clay suspensions were used.

6.1 The thermal stability of dry bentonite

On dry heating, smectites initially give off their interlayer water. At higher temperatures, water is split off from structural OH groups with the result that the structure finally breaks down. According to general information /85/, the corresponding temperatures are 100 to 200°C and 550 to 800°C. Above 800°C the structure becomes unstable. This information agrees with thermogravimetric measurements on MX-80 and Montigel /106/.

According to /63, p.313/, the release of interlayer water depends on the hydration energy of the interlayer ions. The more stable the aquo-complex, the higher the temperature. There is no clearly defined temperature limit for release of water from structural OH ions. It occurs rapidly at temperatures over 500°C but could be occurring slowly at temperatures over 300°C. The activation energies are 225 and 210 kJ/mole for sodium- and calcium-smectite respectively.

Rehydration of bentonite is of particular interest from the point of view of its behaviour under repository conditions. Experiments at 250 to 500°C over a period of one year have shown that all the structural water is released between 370 and 440°C, which is linked with a loss of expandability /7, p.188/.

According to /63/, the release of interlayer water from calcium- and sodium-bentonite is reversible up to temperatures of 300 - 390°C and >390°C respectively. The release of structural water is also partly reversible. If alteration of the cation exchange capacity through heating is taken as the criterion of reversibility, then sodium-montmorillonite is more resistant than calcium-montmorillonite /63, Table 7-6/. Table 16 /172, p.80/ summarises the ranges of thermal stability of different clay minerals. The reversibility of water release was taken as the assessment criterion.

In two cases - which hardly apply to repository conditions - water release is irreversible after heating to 105 to 125°C. If the cation exchange capacity of the montmorillonite is completely saturated by potassium, drying at 110°C leads to irreversible layer collapse /63, p.488/. Dehydration of lithium-montmorillonite is also irreversible after drying at 105 to 215°C /63, p.328/. It is assumed that the small lithium ion passes into octahedral positions in the layer and thus reduces the layer charge. With hydrothermal treatment of lithium-montmorillonite, the lithium remains in the interlayer positions even at 300°C because of its high heat of hydration /40/. An irreversible collapse in the temperature range 200 to 300°C is detected with nickel, zinc, manganese and "H-Al" (Al-hydroxy complexes ?) in the interlayers. For iron(III) this occurs only at 400°C /172, p.59/.

6.2 The thermodynamic stability of clay minerals

Geochemical literature contains many works on the stability ranges of individual solid phases including the clay minerals in the system HCl-SiO_2-Al_2O_3-M_2O-MO-H_2O (M: alkali- or alkaline earth ion). The thermodynamic data for many silicates, mainly the mixed phases, are uncertain and predictions of stability limits are correspondingly unreliable. The data of Helgeson et al. /22, 69/ and Robie et al. /139/ are usually used as a basis for calculations. Tardy and Garrels /165/ give a method for estimating the free energy for layer silicates from data on their components. /68/ contains a comprehensive collection of equilibrium diagrams. Reference should be made to Drever's work /37/ for an elementary understanding of such diagrams and their construction. Giggenbach /58/ gives a more detailed discussion.

In graphic representations, silicic acid concentrations are often used as variables besides $[M^+]/[H^+]$ or $[M^{2+}]/[H^+]^2$ (Figures 65 and 66). They show that at 60°C - which corresponds to the repository temperature after several hundreds of years - montmorillonites are unstable in a quartz-saturated solution. Their stability field is widened with higher silicic acid concentrations. As can be seen from Figure 67, a temperature increase also leads to widening of the montmorillonite ranges.

Figures 69 to 72 give information on the stability conditions in the presence of alkaline earth ions. Magnesium was included because of the possibility of chlorite formation. For the sake of brevity, the system components $HCl-H_2O-Al_2O_3-SiO_2$ are not given in the legends to Figures 65 to 72.

Table 16: The thermal stability of three-layer silicates /172/.

Type	Elements in the 2:1 - layer	Temperature limit (°C) at 1 - 2 kbar
	completely expandable phases	
K dioct	(AlSi)	230
K dioct	(MgAlSi)	400
Na dioct	(AlSi)	350 - 450
Ca dioct	(AlSi)	300 - 500
Mg trioct	(MgSi)	<250
Mg trioct	(MgAlSi)	430
Na trioct Beidellite	(MgAlSi)	550
Na trioct Hectorite	(MgAlSiNa)	800
	phases with interstratifications	
K dioct	(AlSi)	400
K dioct	(AlSiMg)	430
Na trioct Beidellite	(MgAlSi)	780
Na trioct Hectorite	(MgAlSiNa)	800

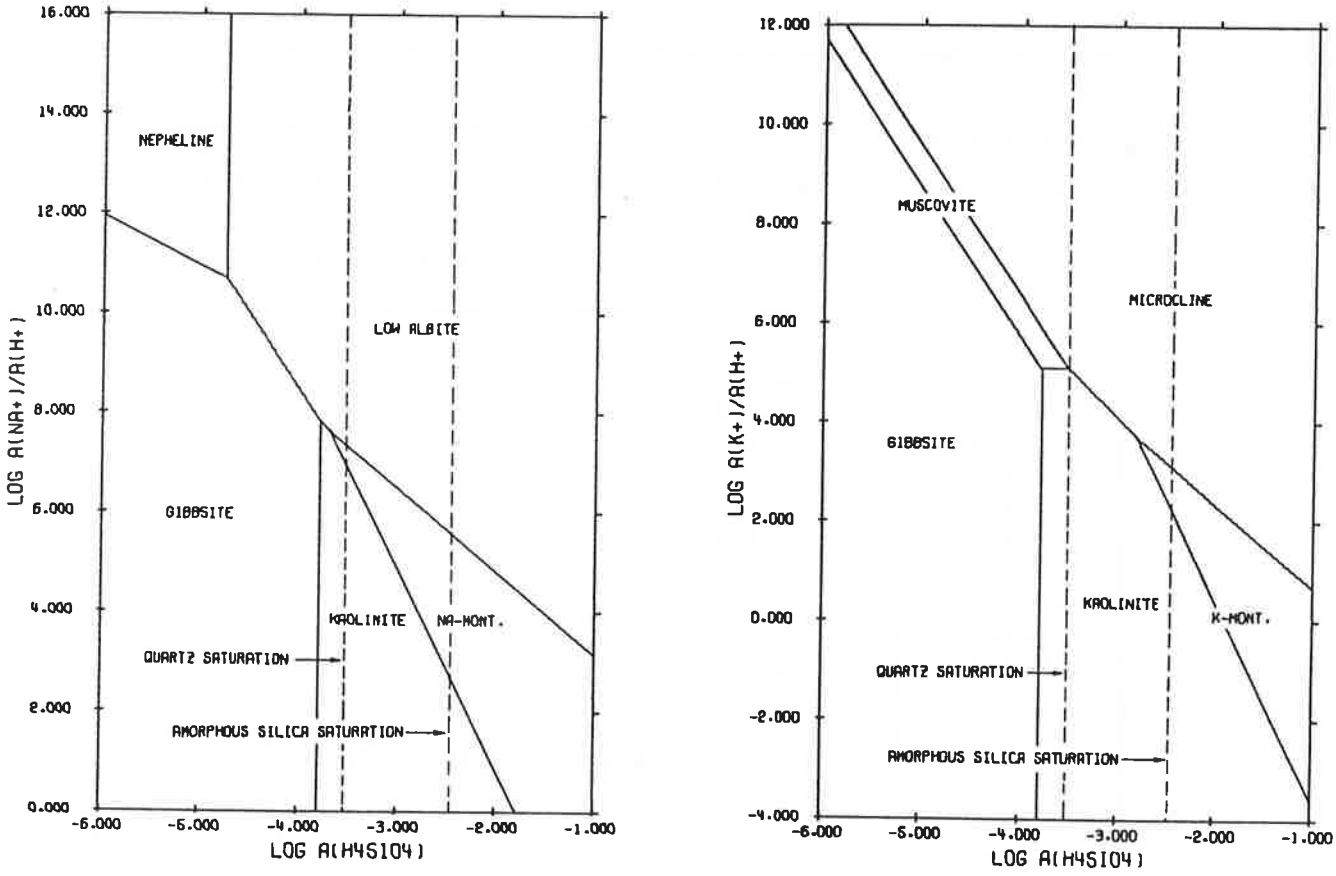

Fig. 65: Equilibria with the partial components NaO_2 (left) and K_2O (right) at 60°C /68/.

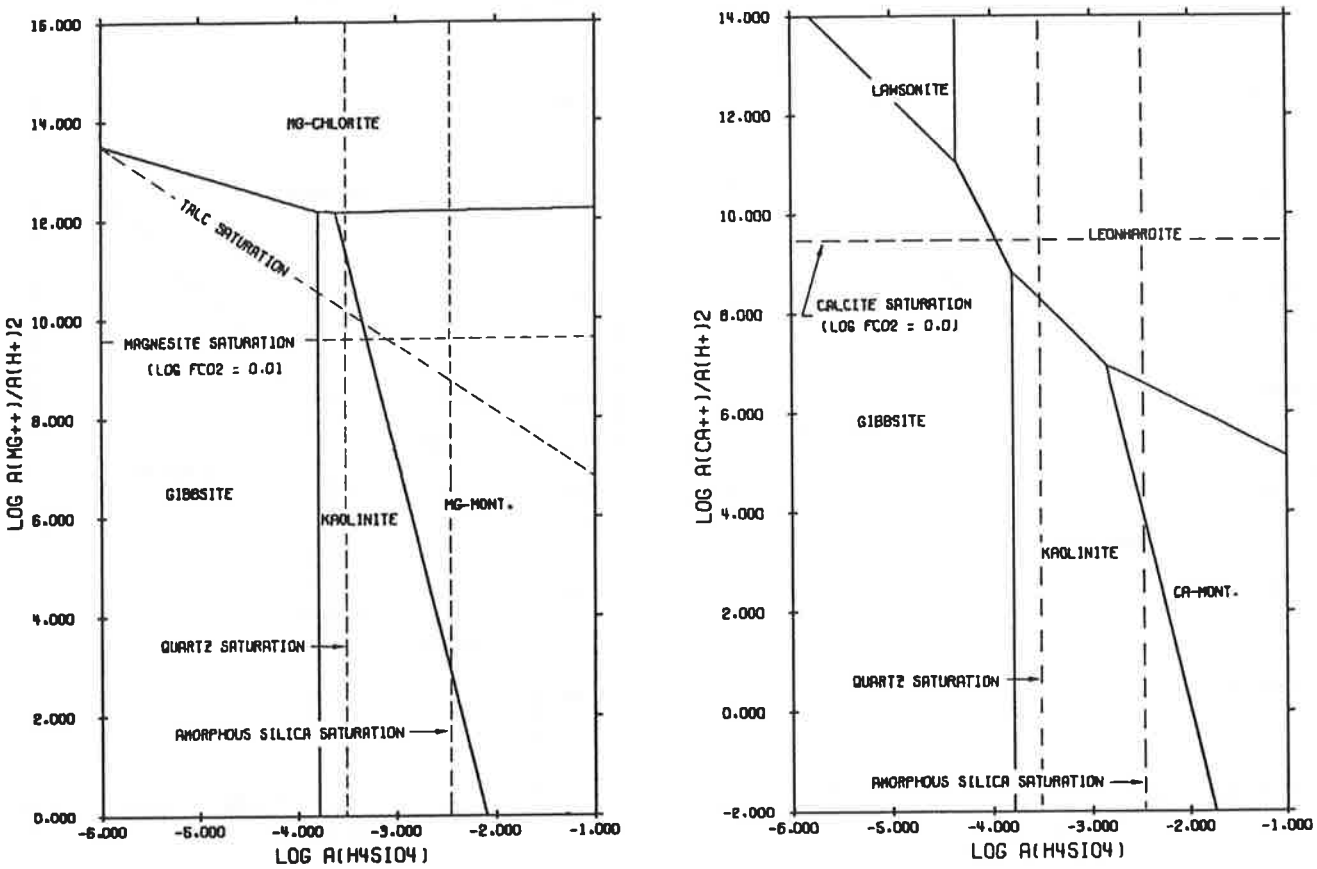

Fig. 66: Equilibria with the partial components CO_2-MgO (left) and CO_2-CaO (right) at 60°C /68/.

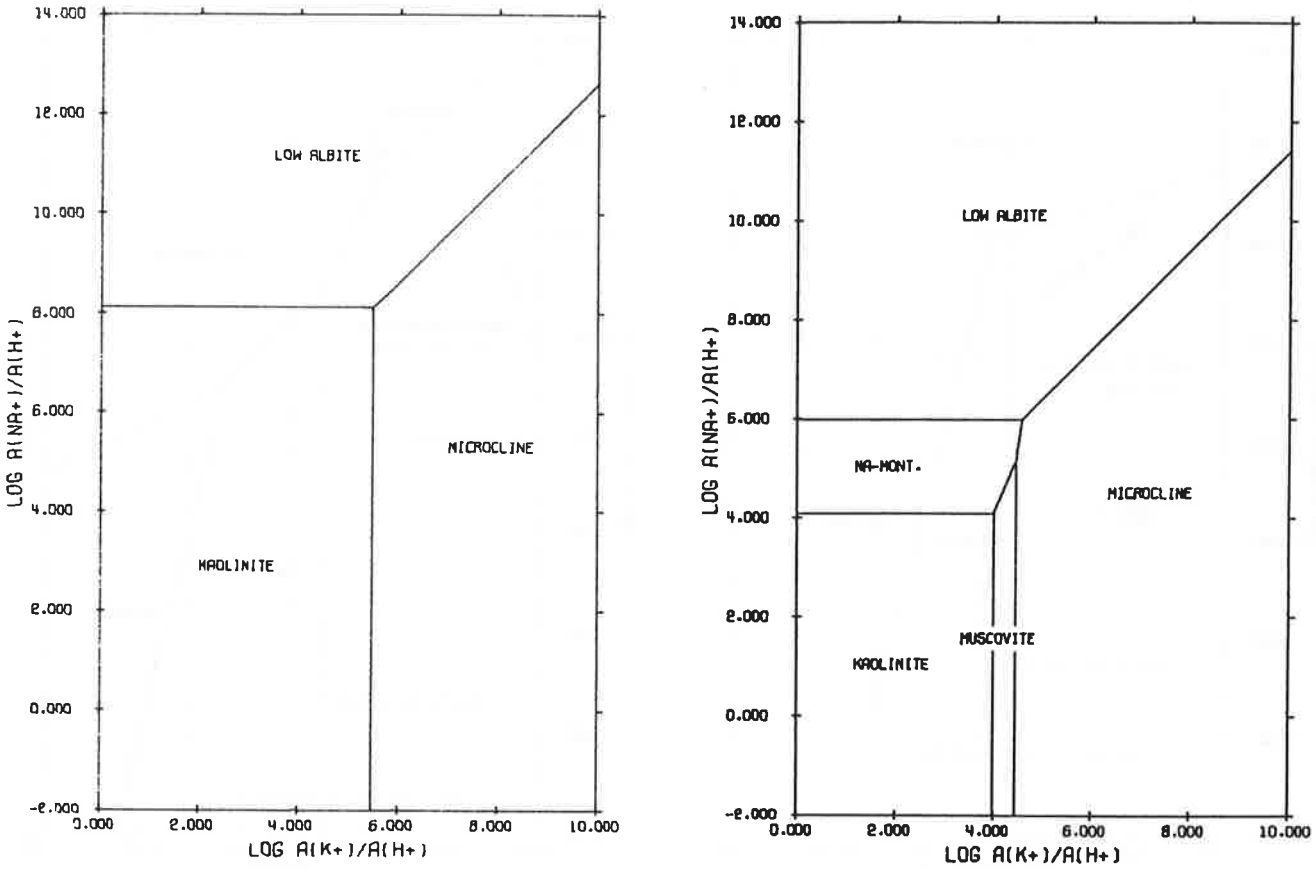

Fig. 67: Equilibria with the partial components K_2O-Na_2O at 25 (left) and 150°C (right) in quartz-saturated solutions (25°C: log a(H_4SiO_4) = -4.00. 150°C: log a(H_4SiO_4) = -2.67) /68/.

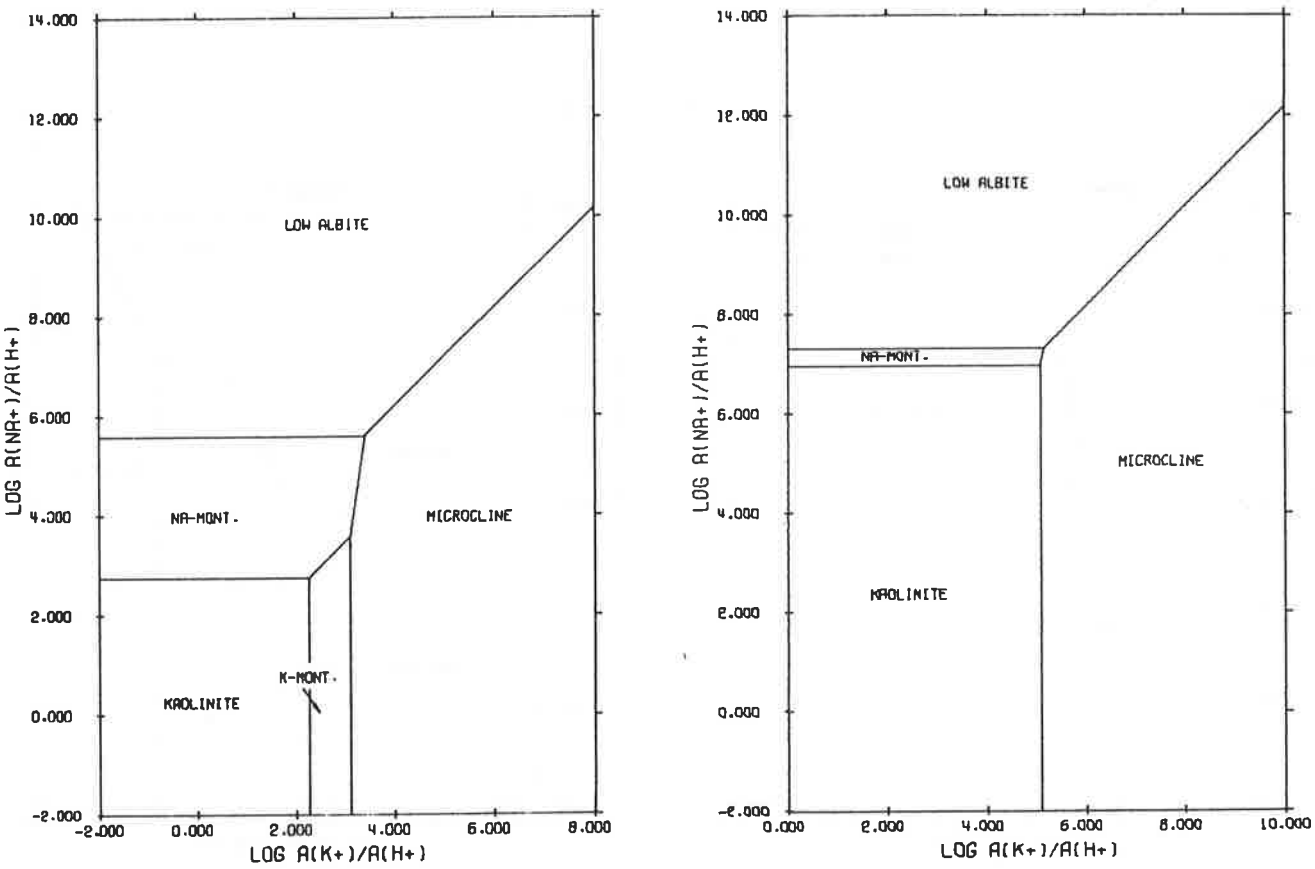

Fig. 68: Equilibria with the partial components K_2O-Na_2O at 60°C and quartz-saturation (right, log $a(H_4SiO_4)$ = 3.52) and saturation with amorphous silica (left, log $a(H_4SiO_4)$ = -2.47) /68/.

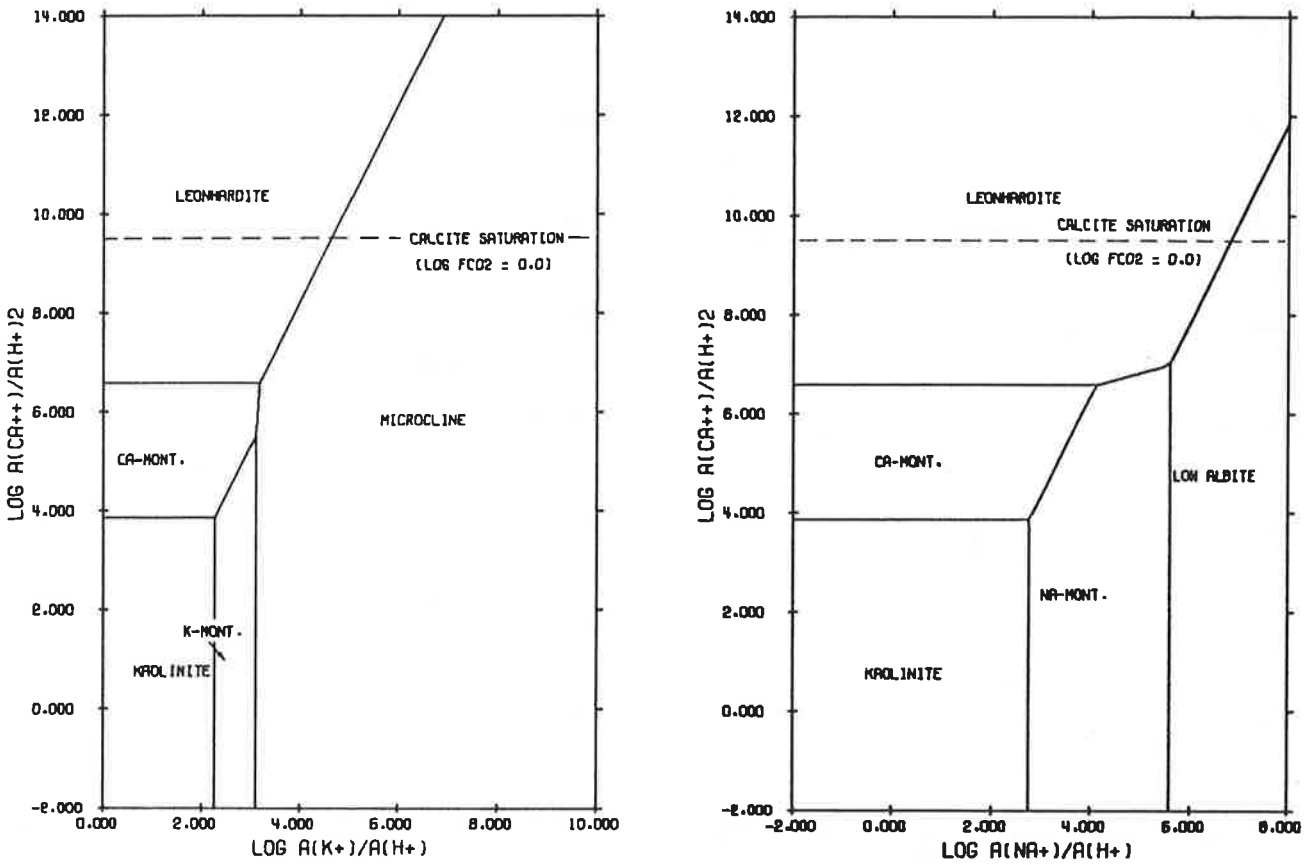

Fig. 69: Equilibria with the partial components CO_2-CaO-K_2O (left) and CO_2-CaO-Na_2O (right) at 60°C and saturation with amorphous silica (log a(H_4SiO_4) = -2.47) /68/.

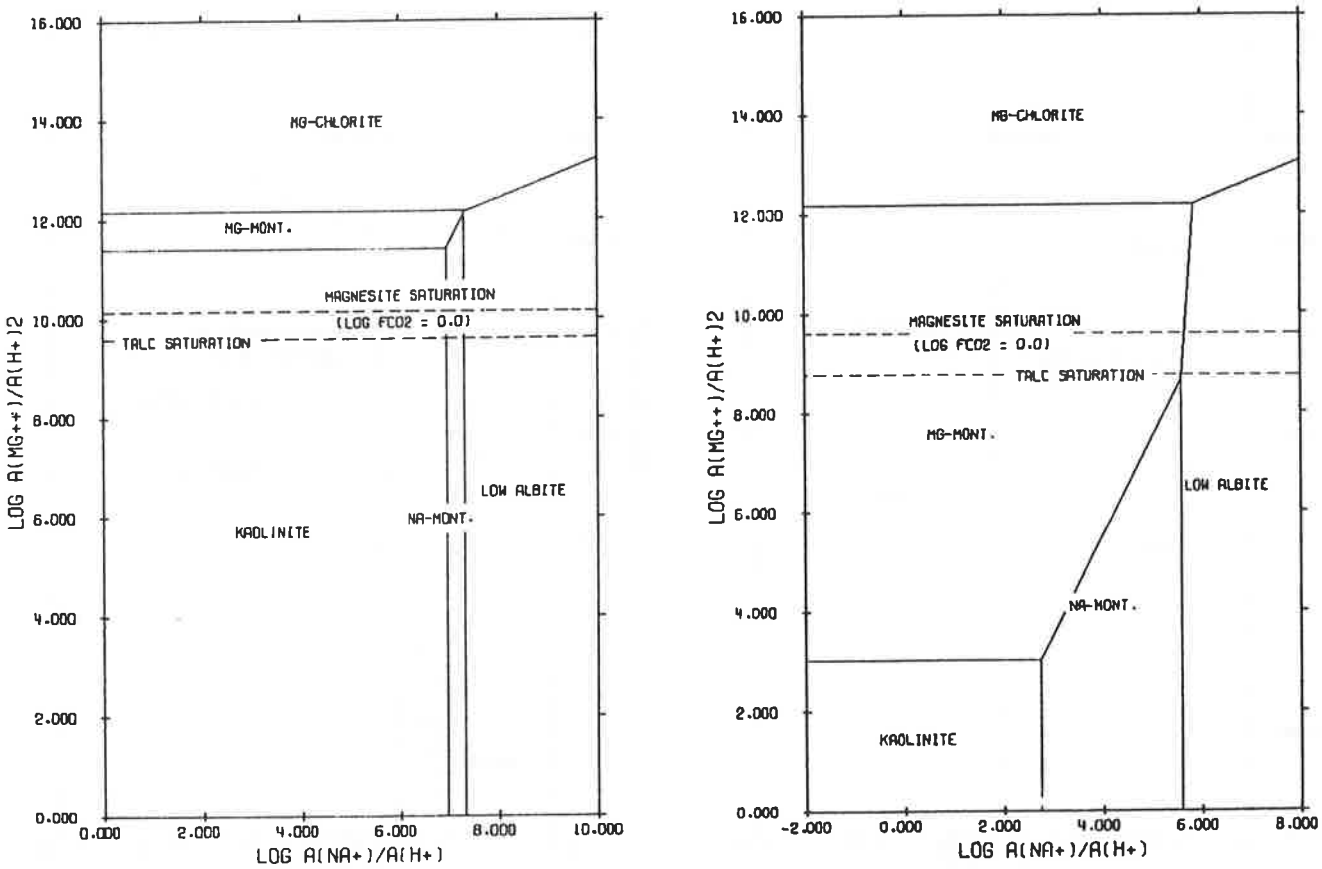

Fig. 70: Equilibria with the partial components CO_2-MgO-Na_2O at 60°C with quartz saturation (left, log a(H_4SiO_4) = -3.52) and saturation with amorphous silica (right, log a(H_4SiO_4) = -2.47) /68/.

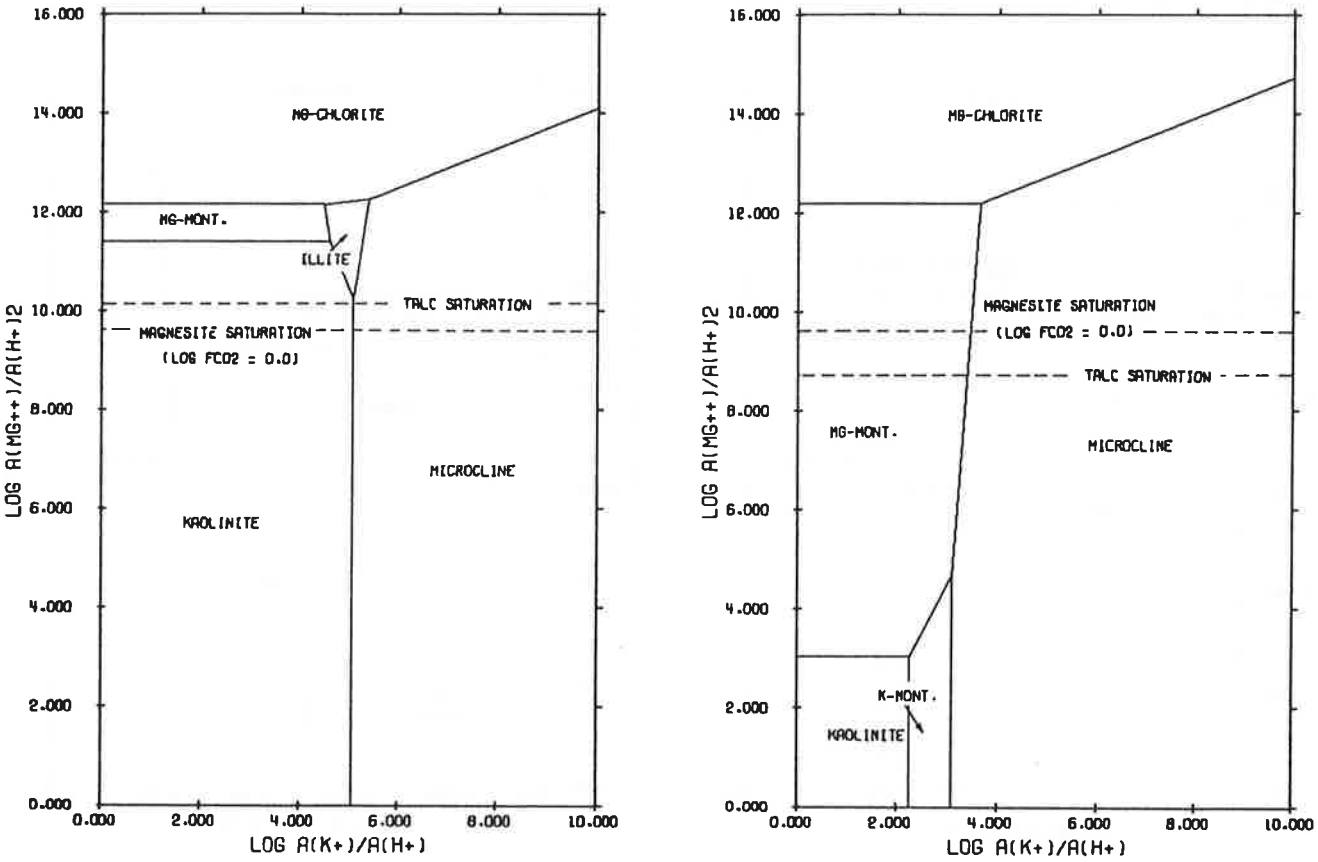

Fig. 71: Equilibria with the partial components CO_2-MgO-K_2O at 60°C with quartz saturation (left) and saturation with amorphous silica (right) /68/.

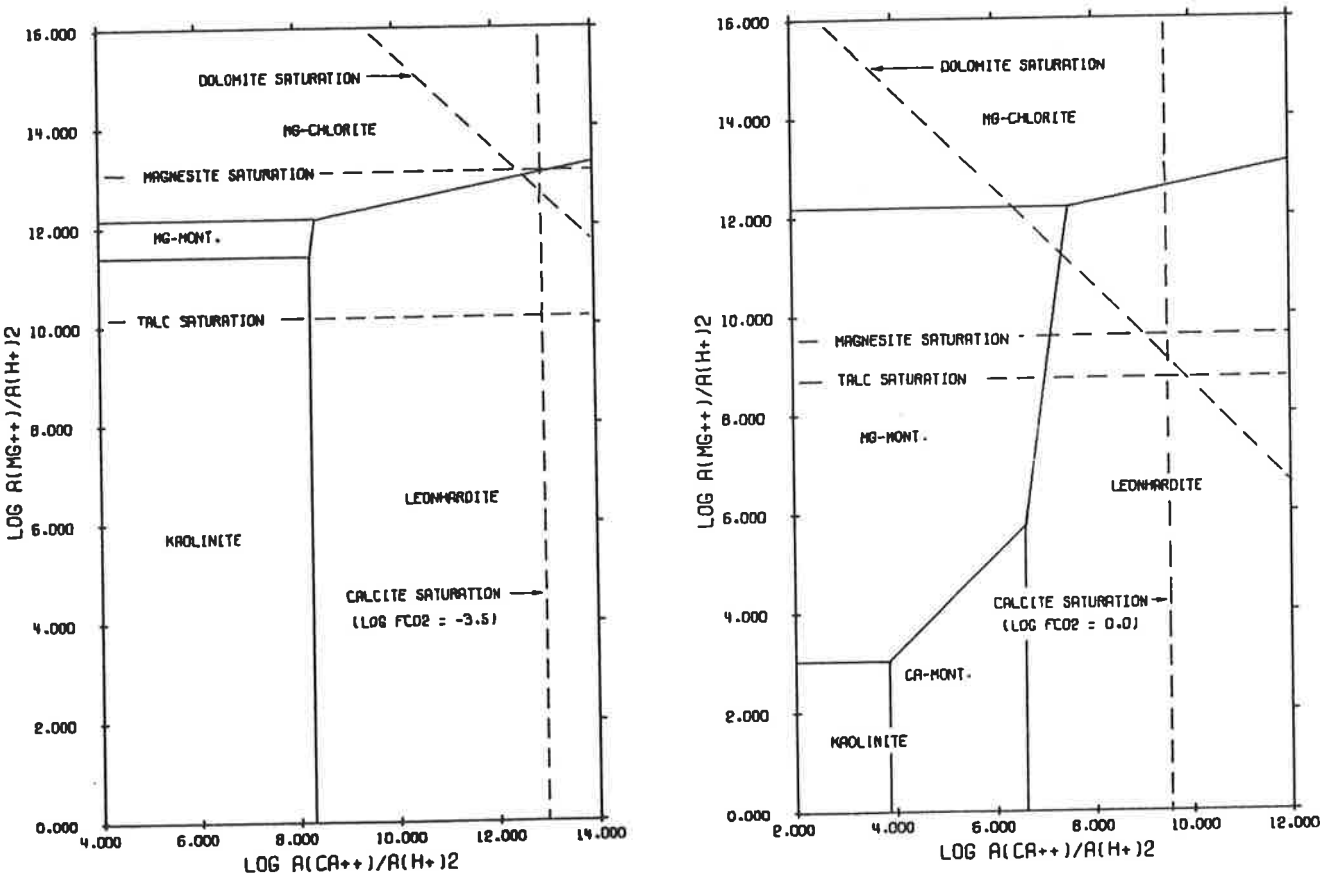

Fig. 72: Equilibria with the partial components CO_2-MgO-CaO at 60°C with quartz saturation (left) and saturation with amorphous silica (right) /68/.

Figure 73 shows that the composition of granitic waters often lies outwith, or on the limit of, smectite stability /112/. Only the illite field is well covered. From the point of view of repository conditions, it is to be noted that the water composition under the practically stagnant conditions is determined mainly by the bentonite itself. Under the assumption that montmorillonites form a reversible solubility equilibrium, phase alterations would not occur. This assumption probably only applies as an approximation: montmorillonites react to form products with higher layer charge with formation of SiO_2 (and possibly kaolinite) /138/.

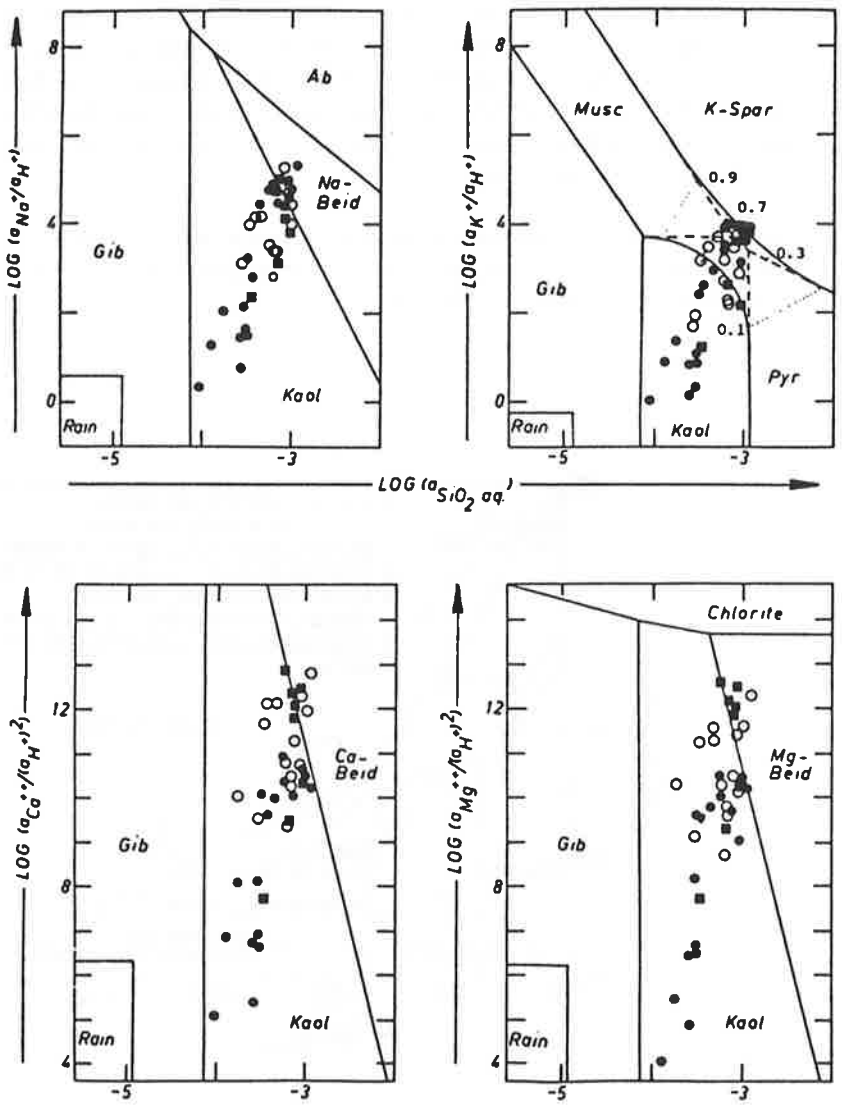

Fig. 73: The thermodynamic stability ranges of clay minerals and the composition of weathering solutions. The dotted lines delineate the stability field of illite for different layer charges. Metastable range extensions for kaolinite and feldspar are dashed.
o: granitic and rhyolitic waters.
●: waters from granite and weathered granites.
■ : waters from basalt and gabbro.
/112/.

The illite/montmorillonite stability limit cannot be determined exactly because of the inaccuracy of thermodynamic data. As I/S interstratifications also occur besides endmembers, they can also be seen as a single phase of variable composition. Figures 74 and 75 /1, 56/ give the relevant stability diagrams. Water compositions as found in contact with clay minerals cling to the montmorillonite/kaolinite or montmorillonite/illite equilibrium lines in Figure 75.

High pH values as well as high potassium contents favour the formation of illite or the illite fraction in I/S interstratifications (Figure 76 /98/).

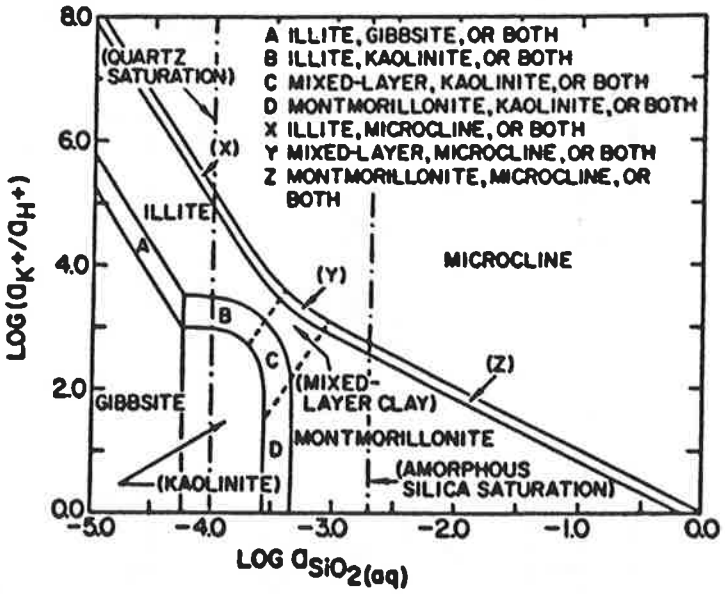

Fig. 74: The stability ranges of the clay minerals at 25°C, taking account of montmorillonite/illite interstratifications /1/.

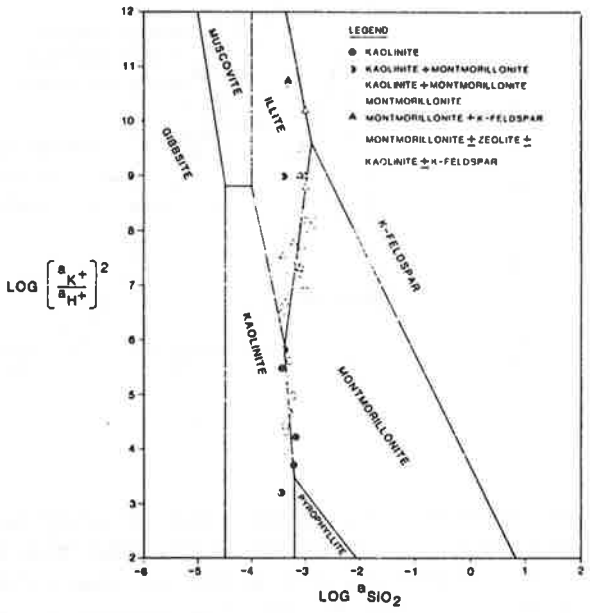

Fig. 75: The thermodynamic stability ranges of clay minerals with analyses of waters in contact with clays /56/.

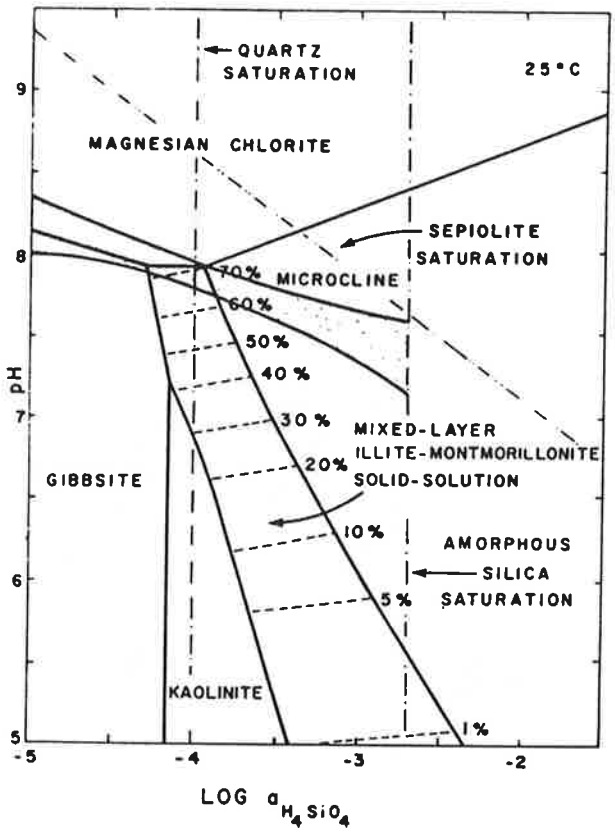

Fig. 76: The thermodynamic stability of clay minerals in idealised sea-water at 25°C. The fractions of the illite component are given in the illite-montmorillonite field. The dotted area comprises the approximate sea-water composition. The activities of Na^+, K^+, Ca^{2+} and Mg^{2+} are 0.316, $6.17 \cdot 10^{-3}$, $2.29 \cdot 10^{-3}$ and $1.62 \cdot 10^{-2}$ /98/.

6.3 Reaction series on alteration of dioctahedral smectites

The hydrothermal alteration of smectites was investigated systematically by Eberl /41/. Figure 77 is taken from this work and gives an overview of possible reactions; it also helps in understanding the following sections.

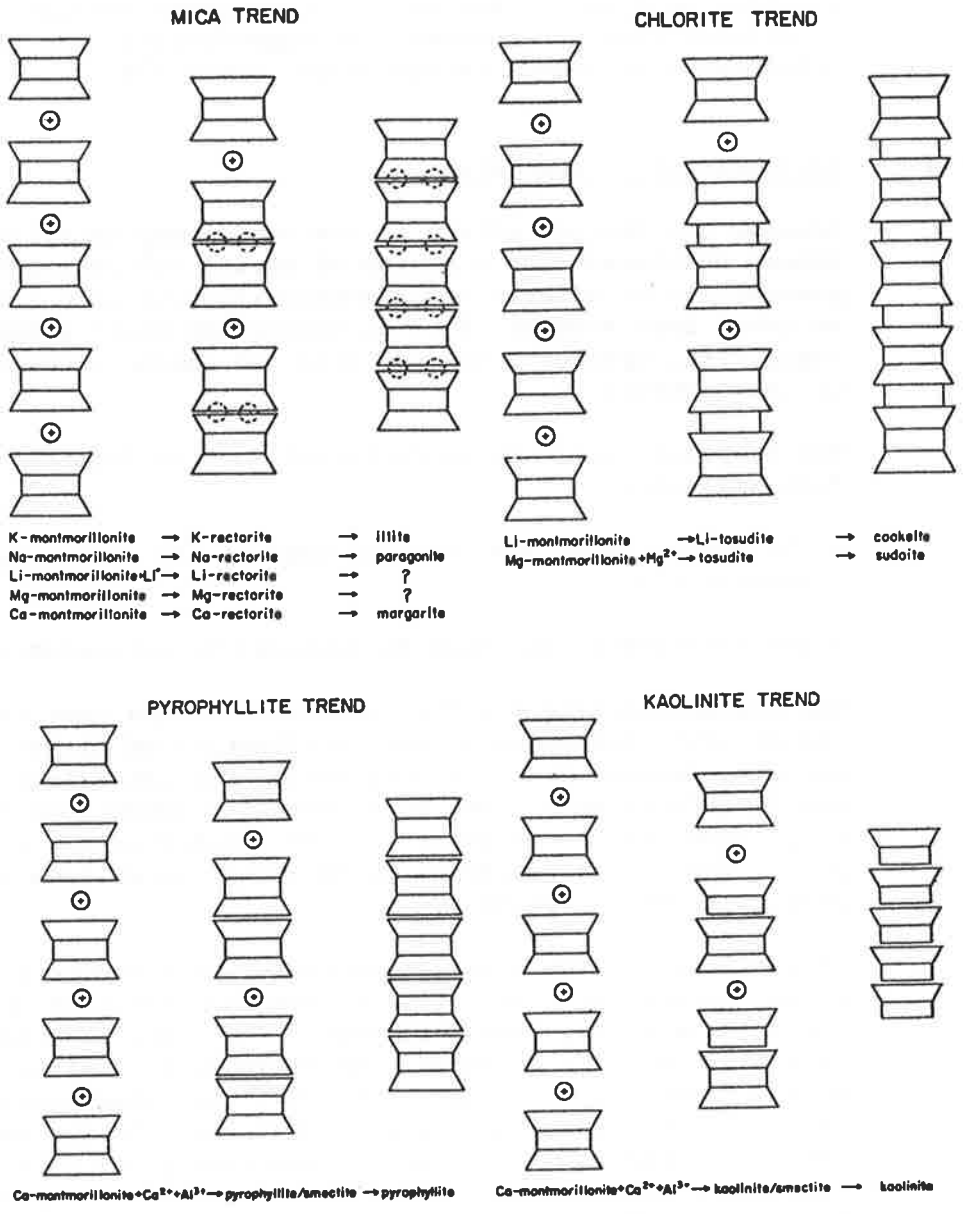

Fig. 77: Possible diagenetic reactions of montmorillonites to form products with interstratifications and new minerals /41/.

The investigations were carried out with a clay:water ratio of 1 in the temperature range 300 to 500°C. The results cannot simply be applied to lower temperatures. The stability field of rectorite widens at higher temperatures. For example, natural calcium rectorite is unknown and smectite/pyrophyllite interstratifications do not appear to occur naturally.

With increased pH, smectites react to form feldspars /41, 78/ or, at temperatures below 150°C, to form zeolites /78/. In a slightly acid milieu the smectite structure remains intact even in diluted clay suspensions. The expandability can be reduced by emplacement of aluminium hydroxide layers /78/.

6.4 Illitisation of smectites

Because the barrier effect of the repository backfill has to remain unaltered over a period of around 10^6 years, the possibility of alteration of montmorillonite into illite has to be taken into account. Such an alteration would affect swelling capability, hydraulic conductivity and cation exchange capacity of the backfill.

Two prerequisites must be fulfilled for the formation of illite from smectites:

- the layer charge must be increased to around 0.6 by isomorphic substitution
- the interlayer ions must be replaced by potassium ions.

The montmorillonite → illite transition occurs over intermediate stages with increasing interstratification of illite layers with smectite layers. With low diagenesis, the interstratifications are disordered and, under more intensive conditions (T, p, t), they transform increasingly into an ordered series /136, 172, p.91/. There will therefore be no abrupt alteration in the properties of the backfill.

If the layer charge alone is increased, the smectite properties remain intact /6, p.26/. (It follows, however, from investigations by Marmy and Gaultier, that a K-montmorillonite suffers irreversible layer collapse with alternating wetting and drying at 80°C /99/. In this case, the cation exchange capacity decreased by a third of the initial value.) In the case where entry of potassium ions into the repository controls illite formation, the reaction can be estimated from the potassium supply from the groundwater, the repository dimensions and the cation exchange capacity. With an assumed water inflow of 0.7 l per canister and year and a potassium concentration in the water of 1.15 moles/m^3, complete alteration of the montmorillonite to illite would take around $7.5 \cdot 10^7$ years /109/. Slightly different assumptions still result in a time of $3 \cdot 10^6$ years /108/.

If reactions are being discussed, then the conditions which lead to an increase in the layer charge are less easy to understand. In addition to experimental evidence, which is open to contradiction, natural analogues can be used to handle this problem area. Uncertainties arise from the fact that it is still not certain whether smectite-illite alteration should be described with kinetic or equilibrium models /6/.

Two meetings have been held on the subject of smectite alteration /6, 7/ and their results are taken into account in the following. Reference should also be made to a Canadian literature overview /77/ and a work on natural analogues /30/.

6.4.1 Investigation of natural smectites

According to an assessment by Velde /72, p.91/, naturally occurring montmorillonite is stable up to 80 to 100°C at a depth of 100 m. An upper temperature limit of 150°C is quoted for calcium montmorillonite at a greater depth. Up to 200°C and at depths up to 1500 m, I/S interstratifications are found, the illite fraction increasing with temperature. Illite is found over 200°C, mostly together with chlorite.

Figure 78 gives a summary of the findings of various authors /72, p.94/. In the following, some further works on the behaviour of natural clay minerals are summarised.

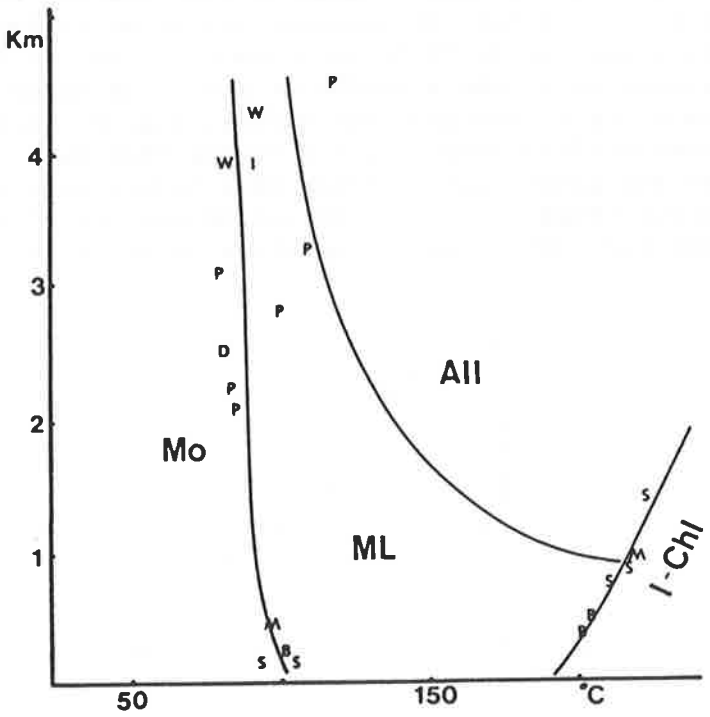

Fig. 78: Stability fields of natural clay minerals in a temperature/depth diagram. Mo: completely expandable phases. ML: ordered and disordered interstratifications (30 - 80%). All: Allevardite. I-Chl: Illite-chlorite paragenesis. Tertiary and more recent sediments were considered. The letters indicate the observations of different authors /72/.

The metabentonite from Kinnekulle (Sweden) has been investigated in some detail. It is some 450 Ma old and was heated to at least 100°C for several hundred years by a basalt intrusion some 280 Ma ago /108, 132, 173/. Under these conditions, the penetration of potassium into the original bentonite resulted in a product with I/S interstratifications rather than illite. The average layer charge per formula unit on the outer side of the bentonite layer was 0.4 and 0.37 in the centre. The corresponding potassium content of the interlayers is 72 and 54% respectively of the cation exchange capacity.

A French illite produced from a montmorillonite laid down in the Oligocene (23 to 52 Ma ago) was also investigated /108/; its cation exchange capacity is 19 meq/100 g. The corresponding value for a representative metabentonite sample is 48.4 meq/100 g. In both cases, the exchangeable cations were mainly calcium and magnesium. Up to a reduced dry density of 1.9 Mg/m^3, the swelling pressure of this illite lies in the same range as MX-80 (Figure 22) and is significantly higher than the swelling pressure of the Kinnekulle metabentonite /27/. The hydraulic conductivity of the illite was determined at $K = 10^{-12}$ $m \cdot s^{-1}$ /27/; this is a factor of 20 higher than the conductivity of MX-80.

Investigations of clay minerals from oil wells in the Gulf of Mexico are of particular interest with respect to a repository /38, 126/. The minerals range in age from the Pleistocene to the Eocene (2 - 56 Ma). At borehole depths up to 5500 m, temperatures up to 170°C were reached. For the aspects of relevance here, the significant result of these investigations is that, up to the greatest depths, clay minerals with I/S interstratifications occurred rather than pure illite. Figure 79 shows the proportion of expandable layers as a function of borehole temperature. The potassium content of the clay fraction of the expandable layer proportion is given in Figure 80.

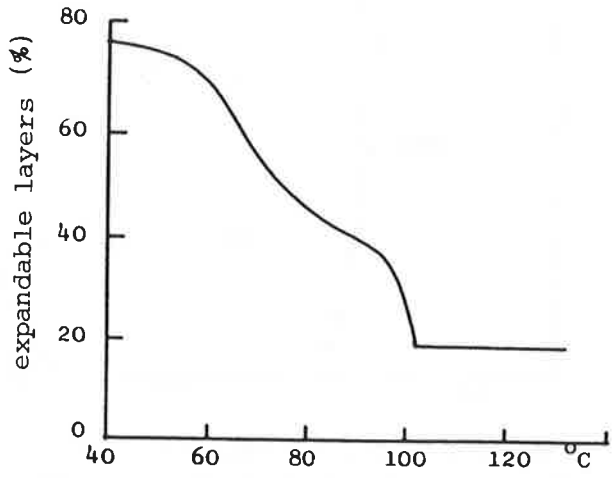

Fig. 79: The connection between the proportion of expandable layers in illite/smectite interstratifications and the temperature in Well E /38/.

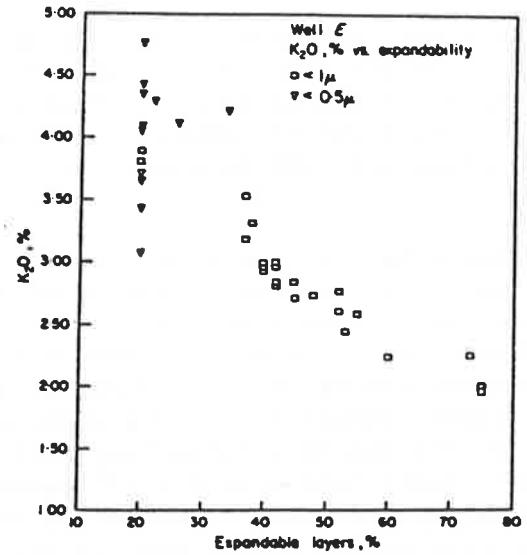

Fig. 80: The connection between potassium content of the clay fraction and the proportion of expandable layers in interstratifications in Well E /126/.

It can be concluded from Figure 79 that, with a repository temperature of around 60°C and a sufficient supply of potassium, a decrease in the expandable layer proportion by around 30% but no complete illitisation is to be expected. Pollastro /127/ shows an increasing proportion of I/S interstratifications with increasing depth in Tertiary sediments. Below the Tertiary/ Cretaceous boundary (65 Ma), increasing proportions of illite are found, formed from the I/S clays ("selective cannibalisation of smectite layers").

Investigations by Środoń /156/ on clay sediments lead to the conclusion that the salinity of the water does not affect the extent of illitisation. Excluded from this are solutions with high potassium and magnesium contents.

6.4.2 Laboratory investigations of illitisation

Looking through the literature occasionally gives the impression that there is a "magic temperature" of 100°C which is the limit for illitisation through isomorphic substitution of Si(IV) by Al(III). If the reaction is thermally activated, fixing such a limit is dangerous when extrapolation is over very long time periods.

Based on hydrothermal reactions of glasses, Eberl and Hower /38/ have determined an activation energy of 82 ± 14.6 kJ/mole for the alteration of synthetic beidellite into a product with I/S interstratifications. This value agrees with the results of other authors for the breaking of chemical bonds in the tetrahedral layer. According to this work, alteration of smectite to an I/S interstratification with 20% expandable layers at 55°C would take around $6 \cdot 10^5$ years (Figure 81). This alteration time appears very conservative in comparison with the findings for clay minerals from the oil wells.

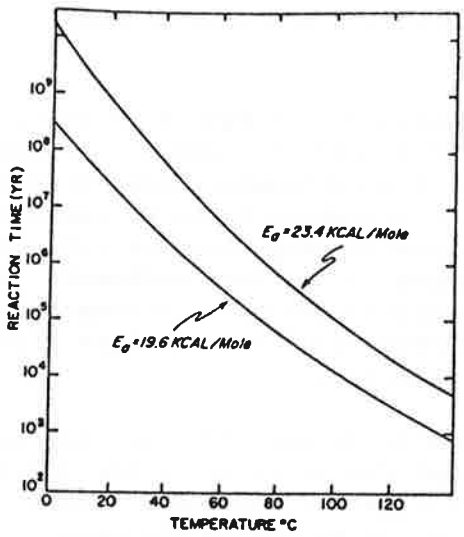

Fig. 81: Calculated alteration times of a fully expandable smectite into an illite-smectite mineral with 20% expandable layers as a function of temperature for two activation energies /38/.

Investigations by the same authors in the temperature range 260 to 490°C /39/ show that interstratifications are also formed under these reaction conditions (cf. also /41/). A product with paragonite/smectite interstratifications forms from sodium-saturated Wyoming bentonite while I/S interstratifications form from potassium-containing bentonite. It is noteworthy that, with a high clay:water ratio (1:1), final pH values of 4.4 to 5.4 result.

Eberl /40/ has investigated the effect of interlayer cations in Wyoming bentonite on the formation of interstratifications at 300 and 400°C. For alkali ions, there is a correlation between the free hydration enthalpy and the formation of I/S interstratifi- cations (Figure 82). The sodium bentonite had still not reacted after 30 days at 300°C.

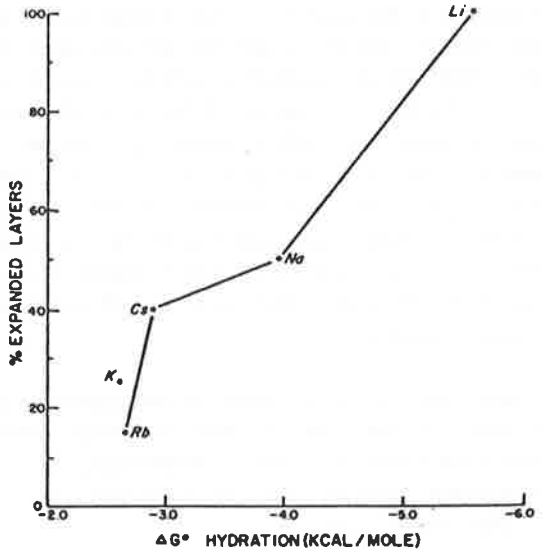

Fig. 82: Proportion of expandable layers of alkali bentonites remaining after 7 days of hydrothermal treatment at 400°C. There is a relationship between degree of alteration and the hydration energy of the cation /40/.

At 400°C a product similar to rectorite with 50% expandable layers was produced after the same length of time. Initial products with alkaline earth ions reacted directly under these conditions to form a phase similar to rectorite. In contrast with the case of alkali ions, the reaction rate here is proportional to the hydration energy. Calcium montmorillonite shows no interstratification after 30 days at 300°C. After the same time period at 400°C, mainly rectorite with 50% expandability was present.

Hower and Roy's study /73/ of the hydrothermal reactions of sodium-saturated Wyoming bentonite showed that the layers charge increased after 180 days at 250°C. After saturation of the reaction products with potassium, the proportion of expandable layers was still 60% (20 mg smectite in 0.5 ml basalt water). This shows on the one hand that potassium ions are not necessary for increasing the layer charge and, on the other hand (as mentioned in the introduction), that an increased layer charge does not necessarily lead to layer collapse in the absence of potassium. After longer test times (120 days) at 250°C in potassium-free preparations, a decrease in the cation exchange capacity from 80 to 40 to 50 meq/100 g was detected. This effect

is interpreted as emplacement of aluminium hydroxo-complexes. While the solubility of montmorillonite was almost congruent at 150°C, at 250°C proportionally more silicon than aluminium was released into the solution. With such incongruent dissolution, it can be assumed that some of the aluminium was emplaced in the interlayers.

Addition of calcium to the solution (0.8 mmoles/litre) slowed down the reaction slightly. The reaction rates measured were higher than those determined by Eberl and Hower /38/ at higher temperatures but were significantly lower than the data in /138/. The activation energy determined from only two temperature values is astonishingly low at 12.5 to 13.5 kJ/mole and contrasts with the values of 82 /38/ and 125 kJ/mole /138/. This contradiction is discussed in detail in /73/. One of the possible reasons for the discrepancy is the differing clay:water ratio. Reference has already been made /59, 61/ to the problems involved in determining and using activation energies of heterogeneous reactions.

There are various indications from investigation of natural clays that mainly magnesium and calcium impede alteration to I/S interstratifications /7, 38/. Roberson and Lahann /138/ carried out a laboratory investigation (10 mg clay in 1 ml water) at 270 and 350°C. The reaction

$$\text{Smectite} + K^{+} \longrightarrow \text{I/S interstratification} + SiO_2$$

was inhibited by Na^{+}, Ca^{2+} and Mg^{2+} in the approximate ratio 1:10:30 (concentration conditions on equivalent basis) (Figures 83 and 84). The high activation energy of 125 kJ/mole is connected with the fact that the smectite→I/S reaction occurs as a solid state reaction ("solid state reorganization") under these conditions. It is assumed that, after an initial selective removal of silicic acid by dissolution, aluminium changes from octahedral to tetrahedral positions. The activation energy of 82 kJ/mole given by other authors is attributed to a dissolution-precipitation mechanism which was blocked in the current investigations by the buffered solution.

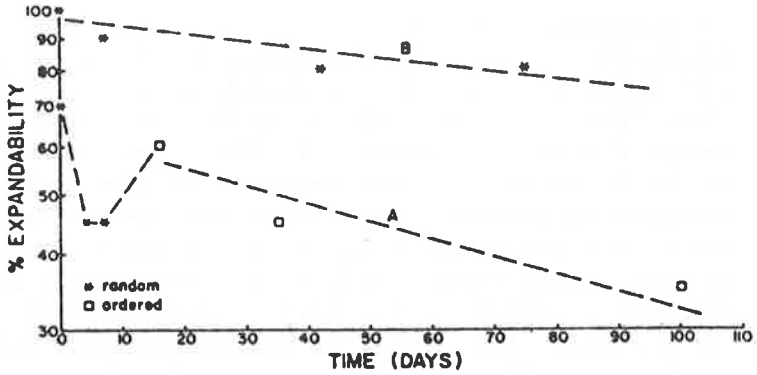

Fig. 83: Expandability of the reaction products of Polkville montmorillonite as a function of reaction time at 270°C in water with 400 ppm K^+.
A: Na-montmorillonite. B: Ca-montmorillonite /138/.

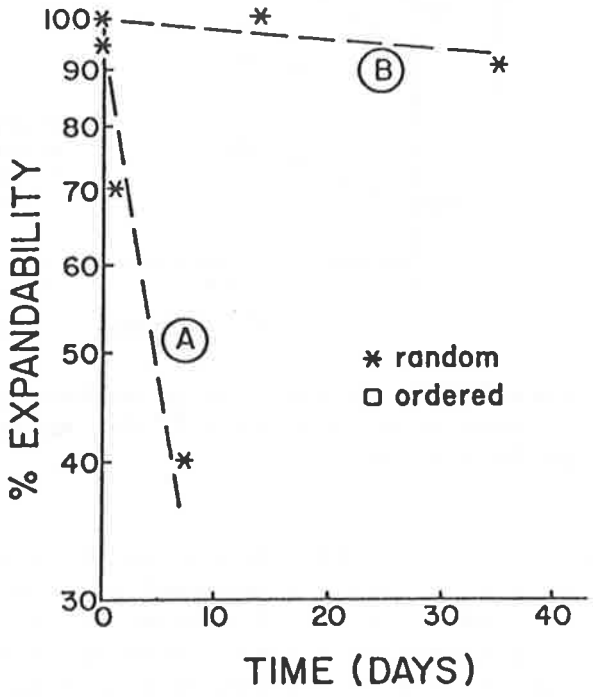

Fig. 84: Expandability of the reaction products of Ca-montmorillonite (Polkville) as a function of time at 270°C in two different starting solutions.
A: 800 ppm K^+. B: 800 ppm K^+ + 100 ppm Mg^{2+} /138/.

6.4.3 Illitisation of iron-containing smectites

In principle, the negative layer charge of a clay mineral can be produced not only by isomorphic substitution but also by the reduction of octahedrally coordinated iron(III). According to /38, 126/ this illitisation mechanism could be operative at low temperatures, for example in the ocean. Stucki et al. /162/ have shown by experiment the increase in the layer charge on iron-containing sodium montmorillonites due to reduction of the iron with dithionite ($Na_2S_2O_4$) in a citrate-hydrogen carbonate buffer. Under these conditions, there is no simple correlation between increase in the layer charge and the iron(III) content of the clay. The change in cation exchange capacity as dependent on the iron(III) content is given for four initial products in Figure 85.

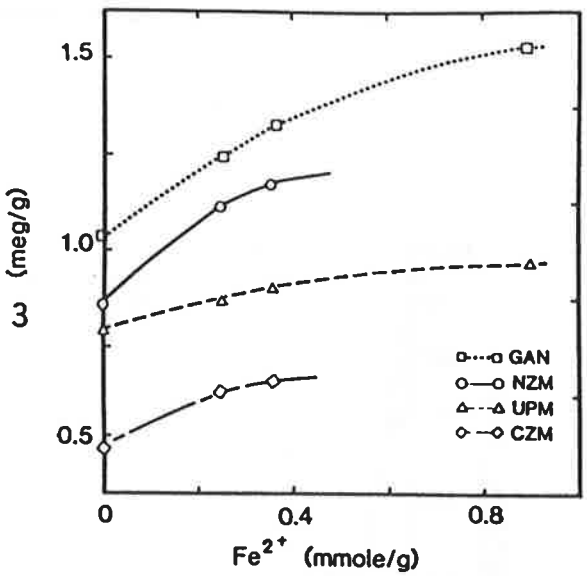

Fig. 85: Correlation between cation exchange capacity ω and the content of octahedral Fe^{2+} for different clays (cf. Table 17) /163/.

The reduction of iron(III) should result in a decrease in the swelling capacity. This was observed in naturally occurring oxidised and reduced forms of a bentonite and was also verified in laboratory experiments /163/. Because of the measurement process selected, it is not possible to draw conclusions on the swelling pressure of compacted bentonite.

An iron-rich smectite was formed on hydrothermal alteration of a basalt/bentonite mixture /7, p.189/. Further information on iron-containing smectites can be found in /57/.

Table 17: Cations per $O_{20}(OH)_4$-unit, cation exchange capacity (CEC) and iron content of the smectites from Figure 85 /162/.

Material	Formula of the unit cell tetrahedr. octahedr.	CEC (meq/g)	Fe^{2+} (mmol/g)	Fe_{tot} (mmol/g)
UPM	$Na_{0,70}Si_{7,97}Al_{0,03}Al_{2,99}Mg_{0,52}Fe^{3+}_{0,42}Fe_{0,012}$	0.876	0.015	0.539
CZM	$Na_{0,44}Si_{7,04}Al_{0,96}Al_{2,69}Mg_{0,47}Fe^{3+}_{1,10}Fe_{0,004}$	0.496	0.004	1.257
NZM	$Na_{0,70}Si_{7,37}Al_{0,63}Al_{2,29}Mg_{0,51}Fe^{3+}_{1,31}Fe_{0,006}$	0.799	0.007	1.502
GAN	$Na_{0,93}Si_{7,12}Al_{0,88}Al_{0,19}Mg_{0,11}Fe^{3+}_{3,72}Fe_{0,008}$	1.046	0.009	4.201

UPM: Upton montmorillonite, Wyoming
CZM: Czechoslovakian montmorillonite
NZM: New Zealand montmorillonite
GAN: Nontronite, Garfield, Washington

6.5 Chloritisation of smectites

In this context, chloritisation generally means the emplacement of non-stoichiometric charged hydroxide layers into the smectite interlayers (chlorite structure, see Figure 9). Such a process can reduce the cation exchange capacity and the expandability of the smectites. Besides magnesium hydroxide (emplaced in the case of chlorite), other hydroxides of di- and trivalent metals can be emplaced.

In contrast with illitisation, this process has received little attention when considering a repository, although the phenomenon of chloritisation is well known in the literature and has been treated in detail.

When montmorillonite is altered to chlorite in oceanic sediments because of the high magnesium content of the sea-water ($2.7 \cdot 10^{-3}$ moles/litre, $\log \frac{[Mg^{2+}]}{[H^+]2} = 13.4$) /172, p.68/, the hydroxide interlayers in the soil material contain mostly aluminium. Rich /144/ has published a comprehensive overview with 144 literature citations. Johnston and Miller's work /78/ contains a summary of recent literature.

In rarer cases, the interlayers of clay minerals in soils contain iron(III) as well as aluminium. Their formation can occur through weathering of non-stoichiometric chlorite layers according to /137/:

$$[Mg_4Al_2(OH)_{12}]^{2+} \rightarrow [Mg_3Al_2(OH)_{10}(H_2O)_2]^{2+} \rightarrow [Al_2(OH)_4(H_2O)_8]^{2+}$$

Another possible formation process consists of emplacement of hydroxo-complexes of slightly hydrolysable cations (e.g. Al(III)) with subsequent condensation. Since the smectites prefer ions with low hydration energy on ion exchange, emplacement of the hydroxo-complex is favoured over the corresponding aquo-ion (e.g. /19/).

If it is assumed that the formation of polymeric hydrolysis products is favoured on clay surfaces (e.g. /19, 137/), it can be seen that the formation of interlayers leads to a drop in pH:

$$(2Na^+)_{Sm} + (AlOH^{2+})_{aq} \rightarrow (2Na^+)_{aq} + (AlOH^{2+})_{Sm}$$

$$(3AlOH^{2+})_{Sm} + Na^+_{aq} + H_2O \rightarrow (Al_3(OH)_4^{5+})_{Sm} + (Na^+)_{Sm} + H^+_{aq}$$

(aq: particle in the aqueous phase. Sm: particle in smectite). It is possible that the drop in pH of a calcium montmorillonite suspension at 30°C from 8.7 to around 4 in the course of 30 days can be explained by such effects /57/. The partly dissolved montmorillonite could be considered as an aluminium source. The authors do, however, admit that the drop in pH could be explained by the special method of preparing the montmorillonite. On the other hand, drops in pH to between 3 and 6 on hydrothermal alteration of bentonites in the range 175 to 275°C could obviously be correlated with the formation of aluminium hydroxide interlayers /78/, cf. also /162/.

Numerous works deal with the synthesis of hydroxide interlayers /137/. These investigations give important indications of possible formation conditions. The prerequisite for formation of Al-OH layers is availability of aluminium, which assumes a low pH. pH values below 6 are necessary for the formation of such layers, with an optimum of pH $\simeq$ 4.5. These formation conditions are explained by the solubility minimum of the aluminium hydroxide at pH $\simeq$ 6-7 and by the hydrolysis behaviour of the aluminium (Figure 86, /11/).

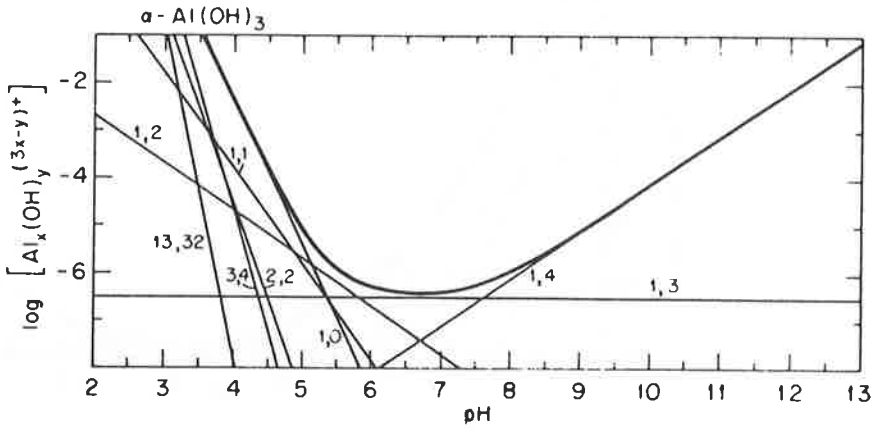

Fig. 86: Distribution of the aluminium hydroxo-complexes in equilibrium with gibbsite (α-$Al(OH)_3$) as a function of pH at 25°C. Polynuclear species form only at pH values below 5 /11/.

The information on loss of expandability and reduction of cation exchange capacity is extensive (e.g. /35, 73, 137/). Of interest is the observation that the exchange capacity returns to its original value after several months with high aluminium content and gibbsite is formed /170/. The instability of the hydroxide interlayers with a high aluminium loading and a high [OH]/[Al] ratio is well-known /137/. This phenomenon should occur only rarely in nature because only incomplete aluminium hydroxide interlayers form in the clay minerals in the ground and exist in an insular form or at the edges of the smectite crystals.

It is to be expected in the repository that, besides chloritisation of the montmorillonite by aluminium, a similar reaction could occur through interaction with the canister corrosion products. Interlayers of iron(III)-hydroxides are rarely found in clay minerals from soils because of the low availability of iron in comparison with aluminium (Figure 87); these products can however be readily synthesised /137/. They appear to be less stable than the aluminium analogues.

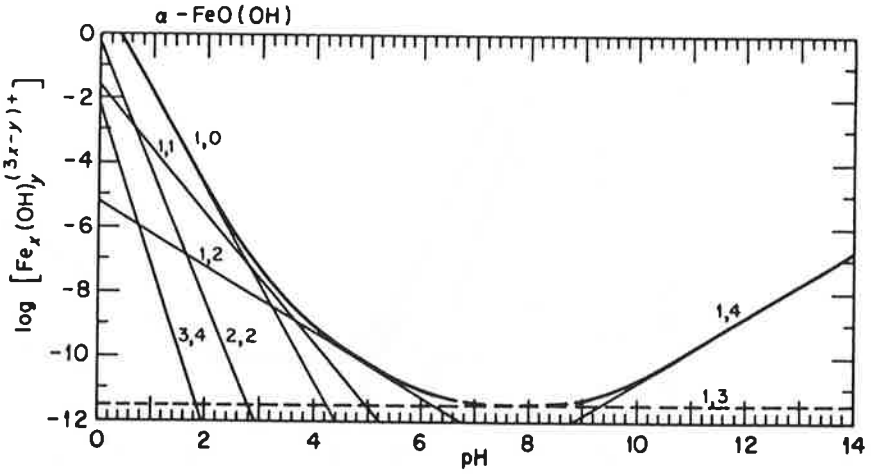

Fig. 87: Distribution of iron(III)-hydroxo complexes in equilibrium with goethite (α-FeOOH) as a function of pH at 25°C. Polynuclear species form only at pH values below 3 /11/.

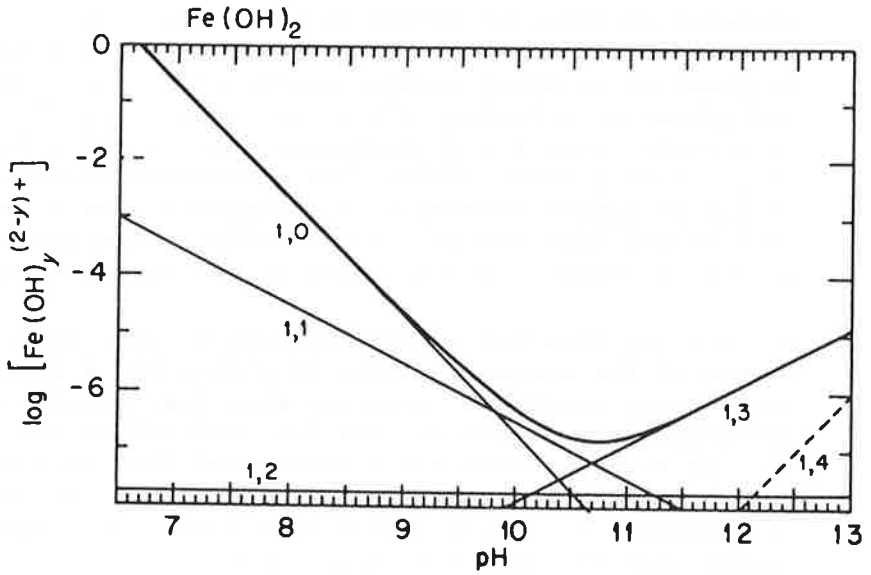

Fig. 88: Distribution of iron(II)-hydroxo complexes in equilibrium with iron(II) hydroxide as a function of pH at 25°C. No polynuclear complexes occur /11/.

However, the reducing environment in a repository is different to the conditions in ventilated soils. There is no known work on the reaction of magnetite with bentonite but Linn and Whittig /93/ show that iron(II) plays a role under reducing conditions. As shown in Figure 88, the $FeOH^+$ complex can make up a significant percentage of the available divalent iron and can be preferentially sorbed by montmorillonite. Polynuclear complexes of iron(II) are unknown. Possible (e.g. radiolytic) oxidation of emplaced iron(II) could lead to hydroxide layers.

No specific information on the behaviour of montmorillonite in a repository can be derived from Gerstl and Banin's work /57/ on Fe(II)/Fe(III) transformations in clay minerals.

The reactions between bentonite and magnetite must therefore be investigated experimentally with reference to a repository. The formation of iron-rich clay minerals such as greenalite and cronstedtite which have a structure similar to kaolinite cannot be ruled out /63/. The effects of possible chloritisation or formation of new phases on the efficiency of the bentonite barrier have also to be assessed from the point of view of the bentonite/magnetite quantity ratios (ca. 10:1 as volume proportions).

6.6 Resistance to radiation

After the steel canister has been corroded through, nuclides will be released from the glass, pass through the canister corrosion products and then be sorbed by the bentonite. The montmorillonite structure can be destroyed by the decay of these nuclides at their sorption positions.

The α-doses required for metamictisation have been investigated in connection with the solidification of high-level waste in crystalline materials /59/. These are in the order of 10^{19} disintegrations per cm^3 *). An expansion of a few percent is usually linked with loss of the lattice periodicity.

---

*) Metamictisation is understood to mean the crystalline amorphous transformation. The structural damage in high-level waste is caused almost exclusively by α-particles and their recoil nuclei.

Corresponding investigations of clay minerals are scant. When assessing the possible effects of metamictisation of montmorillonite, the following points are to be taken into account:

- some of the α-emitters decay before reaching the bentonite
- there are 32.7 m^3 of bentonite for 150 litres of glass
- the total sorption capacity of the bentonite is not blocked by actinides
- even if the montmorillonite structure is destroyed, the amorphous alteration product still has a sorption capacity.

It appears from investigations with sorbed Es-253 on montmorillonite, kaolinite and attapulgite /60/ that a dose of around $4 \cdot 10^{18}$ α/g completely destroys the structure. It was, however, observed that the remaining amorphous material continues to sorb the einsteinium.

The percentage of metamictised montmorillonite can now be estimated for a Swiss repository on the basis of this critical dose. For each glass canister (0.15 m^3), there are $8.8 \cdot 10^4$ kg of bentonite with a montmorillonite content of ca. 70% /102/. It can further be deduced from /179/ that the cumulative α-dose in the waste in 10^6 years will be approximately $5 \cdot 10^{25}$ α/m^3 or $7.5 \cdot 10^{24}$ disintegrations per 150 litres glass. This is sufficient to metamictise $1.9 \cdot 10^3$ kg of montmorillonite which corresponds to only 3% of the material present.

In reality, the central areas of the backfill would naturally be more extensively damaged than the peripheral zones. However, this does not alter the conclusion that the expected damage hardly affects the bentonite at all.

With an expected canister lifetime of more than 1000 years, the effect of β- and γ-radiation on the backfill is negligible. Besides, these types of radiation affect the properties of clay minerals only very slightly. A γ-dose of $3 \cdot 10^{10}$ rads (Co-60, corresponding to around 10^{20} β-disintegrations per cm^3) causes no detectable (by X-ray) structural alterations in the bentonite (p.42 in /7/). During irradiation, significant quantities of carbon dioxide and hydrogen form from organic impurities and sorbed water. It is noted that radiolytically induced reduction of iron(III) could lead to formation of interstratifications in smectite.

According to investigations by Spitsyn /151/, γ-radiation and accelerated electrons cause an increase in cation exchange capacity and a reduction of the crystallographic c-axis (Table 18). The expandability remains the same after irradiation. Finally, reference should be made to the fact that γ-radiation with Co-60 up to $9.5 \cdot 10^9$ rads has no significant influence on the water permeability of compacted bentonite.

Table 18: The effect of γ- and electron radiation on the sorption capacity and position of the (001)-lattice parameter of montmorillonite /151/.

Radiation	Conditions	Absorbed dose (rad)	Sorption capacity (meq/100g)	d(001) Å
-	-	-	35.0	14.255
γ	air-dried	10^7	35.0	14.255
γ	"	10^8	41.0	13.598
γ	"	10^9	43.2	13.392
γ	"	10^{10}	44.6	12.627
γ	in solution (Sr^{2+}	10^7	35.0	14.310
γ	"	10^8	36.4	13.897
γ	"	10^9	43.0	13.801
e	air-dried	10^7	35.0	14.250
e	"	10^8	39.1	14.029
e	in solution (Sr^{2+}	10^7	35.0	14.312
e	"	10^8	36.0	14.100

7 MODIFICATION OF THE BACKFILL MATERIAL

Although bentonites largely fulfil the requirements mentioned in the introduction for a backfill material, there remains the question whether individual properties of the backfill require to be improved by specific additions.

Modification of the physico-mechanical properties - for example by addition of silica sand or crushed break-out material /72, 158/ - is not dealt with here. The chemical properties which can be modified are

- the buffer capacity (pH, redox potential)
- the retention capacity for specific nuclides
- the effect on corrosion of the steel canister and the glass matrix.

Since it can be assumed that the bentonite increases the pH of the inflowing groundwater /176/, improvement of the pH-buffering is not necessary. As bentonites contain mostly iron(II) (e.g. 0.6 to 1.5% in MX-80 /169/), the backfill also has a certain redox capacity. However, in the Swiss concept, a sufficiently large redox capacity is introduced into the repository by the steel canister and its corrosion products /133/. It is therefore unnecessary to modify the backfill in this respect.

Bentonites are poor sorbents for anions (TcO_4^-, I^-) and various cations such as NpO_2^+. In saline waters, Cs^+ and Sr^{2+} are only moderately sorbed. The literature therefore occasionally recommends the addition of specific sorbents to the bentonite /17, 25, 115/. The selection given in Table 19 should include activated carbon for adsorption of TcO_4^- /115/.

As can be assumed from section 5.3, the long-lived nuclides $^{99}TcO_4^-$, $^{129}I^-$ and $^{237}NpO_2^+$ could only decay within the backfill with unrealistically high K_d-values. If it is also taken into account that technetium and neptunium are reduced by the redox buffer to the better sorbed IV oxidation state, then addition of specific sorbents for these nuclides in the higher oxidation states is not efficient. This is also true for Sr-90 and Cs-137 which decay before the canister fails because of their half-lives of around 30 years.

Table 19: Possible specific sorbents for addition to the backfill material.
Ln: lanthanides. Act: actinides /17/.

Mineral	Composition	Sorbed nuclides
Apatite	$Ca_5(PO_4)_3$ (OH,F)	all Act
Monazite	$LnPO_4$	all Act
Vivianite	$Fe_3(PO_4)_2$	all Act
Calcite	$CaCO_3$	Act(III)
Dolomite	$(Ca,Mg)CO_3$	Act(III)
Baryte	$BaSO_4$	Sr^{2+}
Gypsum	$CaSO_4 \cdot 2H_2O$	Sr^{2+}
Cinnabarite	HgS	I^-
Chalkosine	Cu_2S	I^-
Galenite	PbS	I^-, IO_3^-

Under the anaerobic conditions in a sealed repository, the bentonite has no adverse effect on the corrosion behaviour of the steel canister /148/ and the expected lifetime of 1000 years /109/ should be exceeded /102/. As significant lengthening of the canister lifetime can enhance repository safety, the possibility of adding corrosion inhibitors should not be ignored. Addition of phosphate was suggested /60/. It still remains to be clarified whether or not the inhibiting effect leads to a significantly lower corrosion rate.

The dissolution rate of borosilicate glasses is increased by bentonite and by the canister corrosion products /61/ so that the addition of an inhibitor is to be considered for glass corrosion. Introduction of the inhibitor between the glass container and the steel canister is preferential to addition to the bentonite /61/.

8 SUMMARY OVERVIEW

Bentonites are clays with a high montmorillonite content. They are selected as a backfill material because of their swelling capability and their sorption behaviour with respect to cations. The properties to be discussed are closely linked with the montmorillonite layer structure. The extent of the layer charge and the nature of the interlayer cations can vary these properties widely.

8.1 Clay/water systems

- Bentonite affects the water composition by saturation of the water with montmorillonite and by ion-exchange. These reactions lead to an increase in pH with values in the range 8 to 10 to be expected. Illite formation and the oxidation of organic and sulphidic impurities in the bentonite will tend to lower the pH. If these reactions occur slowly, the acid formed can be buffered by the bentonite.

- Swelling of montmorillonite in a restricted volume causes a swelling pressure to build up which is in the same order as the lithostatic pressure in the repository. Under these conditions, the water content of the bentonite is below 30%. This corresponds to a water uptake of at most four interstitial water layers or an interlayer spacing of 1 nm.

  A simple correlation between swelling pressure and water activity can be derived on a thermodynamic basis and allows swelling pressure to be estimated from water vapour adsorption isotherms. The link between swelling pressure and the relatively easily determinable heat of immersion is more complex because it contains an entropy term which cannot be ignored. These relationships are of practical use because they avoid costly swelling pressure measurements.

  According to this thermodynamic concept, physical qualities of macroscopic clay/water systems are used to assess swelling pressure. Other models describe the swelling pressure as the difference in osmotic pressure between the outer solution and the interlayer fluid or as superposition of a repulsion of the electrical double layer and a van der Waals attraction (DLVO model). These models are not suitable for describing the swelling in the case of small interlayer spacing. The DLVO model fails completely because it does not take account of the solvation forces which become effective at $\lambda < 5$ nm. A semi-empirical model which describes the swelling pressure as a function of layer charge density and layer spacing could be used as a rough approximation. Its applicability to swelling pressures above 7 bars has not yet been confirmed.

- The water activity of the expanded bentonite in the repository will be significantly lower than 1. This can have an effect on the kinetics of chemical reactions and on ionic equilibria.

8.2 The sorption behaviour of montmorillonite

Cation adsorption on montmorillonite can only partly be described as exchange of interlayer ions. To some extent, cation adsorption also occurs through complexation with surface OH groups. The relevant model which was developed on oxidic surfaces also forms the basis for understanding adsorption of anions and weak acids. If adsorption occurs as cation exchange, its extent depends strongly on the salinity of the water.

The interpretation of literature sorption data (K_d values) from a theoretical viewpoint is rarely completely possible. The result of this is that conservative sorption data have to be used for safety analyses /101/. The estimation of the temperature-dependence of adsorption also causes difficulties because of the contradictions in the data material.

8.3 Diffusion in compacted bentonite

Diffusion through a porous medium retarded by sorption can, in principle, be determined from the diffusivity of a non-sorbable ion and the K_d value determined by batch test. This procedure can lead to false results, for which there are basically two reasons:

- The classic pore model (diffusion in pore-water, adsorption on pore walls) is inadequate because an additional surface diffusion is to be taken into account in compacted bentonite.

- K_d values are generally dependent on the solid/solution ratio. The data from diluted suspensions cannot be applied to a system with a very high solid content without additional checking.

For these reasons, direct diffusion measurements on compacted bentonite are preferred. The apparent diffusivities determined in non-stationary tests lie in the range of $10^{-10} m^2 \cdot s^{-1}$ for non-sorbable materials down to $10^{-14} m^2 \cdot s^{-1}$ for tri- and quadrivalent actinides.

Anions show abnormal diffusion behaviour, which is again linked to the montmorillonite structure.

The electrical conductivity and gas permeability of the bentonite are of interest from the point of view of canister corrosion. The conductivity at $10^{-4} \Omega^{-1} cm^{-1}$ (30% water content) is in a favourable range. Special investigations have shown that the hydrogen produced by corrosion can escape without an unacceptably high pressure build-up in the repository.

8.4 The stability of montmorillonite

- The thermal stability of dry bentonite is assured over geological time periods at a repository temperature of around 60°C. The interlayer water is given off at temperatures of 100 to 200°C. With the exception of special cases which are not relevant for a repository, this reaction is reversible. The splitting-off of water from structural OH ions occurs only at temperatures over 300°C. Irreversible alteration of swelling capability and cation exchange capacity during a dry phase in the initial period ($T \leqq 150°C$) is therefore not to be expected.

- The ranges of thermodynamic stability of the expandable layer silicates rule out large variations in water composition. The composition of granitic waters often lies outwith these limits (Figure 73). On the other hand, the composition of pore-waters from clay formations adhere closely to the montmorillonite/illite and the montmorillonite/kaolinite stability limits (Figure 75). However, the prevailing conditions in the repository are practically stagnant and complete restructuring of the montmorillonite is not to be expected ("self-buffering" according to /54/).

- The reaction series of smectite alteration with a high clay/water ratio lead, depending on the nature of the interlayer ions and the dissolved ions, in the direction of mica or chlorite structures. No external aluminium source is necessary for increasing the layer charge (illitisation) and formation of aluminium hydroxide interlayers similar to chlorite. The aluminium is provided by dissolved montmorillonite fractions.

- For illitisation of montmorillonite, the tetrahedral layer charge must be increased by isomorphic substitution and potassium must also be present. If only one of these conditions is fulfilled, there is no irreversible layer collapse at repository temperature.

  If the potassium supply is taken to be rate-determining for illite formation, it can be estimated for the conditions to be expected in a Swiss repository that considerably more than 10^6 years would be necessary for complete alteration of the montmorillonite.

  Evaluation of natural analogie investigations also leads to the conclusion that a drastic alteration in cation exchange capacity, expandability and hydraulic conductivity of the repository backfill is not to be expected at 60°C during times in excess of 10^6 years. Although formation of illite/smectite interstratifications cannot be ruled out, they will not lead to a drastic drop in backfill quality.

  Kinetic data on the smectite-illite alteration obtained from laboratory experiments vary to a marked extent and uncertainties exist about the reaction mechanism. Large discrepancies exist in the activation energies which makes extrapolation to repository temperatures impossible. Compared with data from

natural analogues, kinetic data from laboratory tests are rather conservative.

Experimental investigations also show in particular that calcium and magnesium inhibit illitisation. Calcium-bentonite would therefore be more suitable than sodium-bentonite. Experiments also show that complete illitisation is not to be expected: the alteration products contain interstratifications.

The layer charge in iron-containing montmorillonite can be increased by reduction of the iron. It is therefore recommended that bentonites with as low an iron content as possible should be used as a backfill. This point is also of interest from the point of view of interactions between bentonite and the canister corrosion products.

- The formation of hydroxide interlayers similar to chlorite in montmorillonite is a problem which has not yet been dealt with in disposal literature. Such chloritisation could - in the same way as illitisation - impair the expandability, cation exchange capacity and hydraulic conductivity of the backfill. Partial chloritisation by aluminium is quite common in soils but this phenomenon does not appear to be significant at bentonite deposits. It is, however, possible that anomalies in the swelling behaviour of particular bentonites could be explained by partial chloritisation. It can be concluded overall that chloritisation will not have a long-term detrimental effect on the properties of the repository backfill. Excluded from this are disposal sites where the water has a significantly higher magnesium content than shown to date by analysis. Chlorite could be formed in such a case. The question remains open whether chloritisation of montmorillonite can be caused by iron from the canister corrosion products. This problem should be investigated experimentally.

- Radioactive decay is not expected to have a detrimental effect on the backfill. Although metamictisation of montmorillonite as a result of α-disintegrations cannot be ruled out, it is estimated that only 3% of the material used will be affected. The amorphous reaction products still act as sorbents.

8.5 Modification of the backfill material

Additions to bentonite to increase or improve the buffer capacity (pH, redox potential) and the sorption behaviour do not appear necessary in the light of the current repository concept. Although the bentonite accelerates glass corrosion, there is no reason to add an inhibitor to this reaction to the backfill. Since the canister corrosion products also speed up the glass corrosion rate, such an inhibitor could advantageously be placed between the glass container and the steel canister. On the other hand, additives which inhibit steel corrosion can be expected to further lengthen the canister lifetime.

9 CONCLUSIONS AND RECOMMENDATIONS

9.1 Conclusions

Because of low water flow and the high solid/water ratio, the bentonite will modify the composition of the inflowing groundwater. The most important change is an increase in the pH. Isolated indications of a possible drop in pH should be given further attention.

The properties of the backfill will not alter markedly during a period of around 10^6 years. In particular, irreversible alteration of the montmorillonite during the initial dry period with increased temperature is not expected. The formation of illite/smectite interstratifications cannot be ruled out on the long term but complete illitisation of montmorillonite is highly unlikely on kinetic grounds and because of the limited potassium supply from the groundwater. Smectites with I/S interstratifications still have good swelling and sorption properties. Alteration of montmorillonite to non-expandable chlorite is only possible in magnesium-rich waters such as have not yet been encountered in the Nagra boreholes.

With the given quantity ratios, radioactive decay can be ruled out as having a negative effect on the bentonite. However, the possibility remains of the montmorillonite being altered by reactions with the canister corrosion products, in which case the high bentonite/iron ratio is to be taken into account.

Under repository conditions, the swelling of montmorillonite on uptake of water is primarily innercrystalline; osmotic swelling is insignificant. Although there is as yet no quantitative microscopic model for evaluating swelling pressure, this can be estimated from the heat of immersion or from water vapour adsorption isotherms with the aid of thermodynamic relationships. The water activitiy in expanded bentonite is significantly lower than 1. The sorption and retention behaviour of the bentonite can be explained qualitatively by the combined action of ion exchange and reactions with surface OH groups. For a better quantitative understanding, it would be desirable to have more parameter studies rather than accumulation of empirical distribution coefficients. The result of this would presumably be that less conservative K_d-values could be used in the safety considerations. The effect of temperature on sorption appears to be small but literature data are, to some extent, contradictory.

In a later planning stage, a choice will have to be made between a Ca-bentonite and an Na-bentonite. Apart from the better availability of Ca-betonites in Europe, Ca-montmorillonite has a lower tendency to illitisation than the Na variant. As swelling under repository conditions is purely innercrystalline, Na-montmorillonite offers no advantages in this respect. However, when selecting a bentonite, the contents of organic and sulphidic impurities and the iron content of the montmorillonite should also be taken into account.

9.2 Recommendations for further work

Open questions still remain, particularly with reference to reactions of bentonite with the canister corrosion products and alteration of the groundwater pH by the bentonite. These two aspects should be investigated experimentally. It should be possible, to a large extent, to combine these investigations with the current experiments on steel corrosion in bentonite.

There should also be further investigation of how the decreased water activity affects the modelling of chemical equilibria in bentonite.

Further investigations of the sorption behaviour of bentonite should place more emphasis on the basic understanding of measured phenomena. This is important because, in contrast with formation of surface complexes, sorption through ion-exchange depends strongly on the salinity of the water.

10 LITERATURE REFERENCES

1. P. Aagard, H.C. Helgeson: Activity/Composition Relations Among Silicates in Aqueous Solution II. Clays and Clay Minerals 31 (1983) 207.

2. B. Allard, J. Rydberg, B. Torstenfelt: Disposal of Radioactive Waste in Granitic Bedrock. In /52/, p.47.

3. L.L. Ames, J. E. McGarrah, B.A. Walker: Sorption of Trace Constituents from Aqueous Solutions onto Secondary Minerals. I: Uranium. Clays and Clay Minerals 31 (1983) 321; II: Radium. Ibid. p.325.

4. L.L. Ames, J.E. McGarrah, B.A. Walker: Sorption of Uranium and Radium by Biotite, Muscovite and Phlogopite. Clays and Clay Minerals 31 (1983) 343.

5. D.M. Anderson, P.F. Low: The Density of Water Adsorbed by Lithium-, Sodium- and Potassium-Bentonite. Soil Sci. Soc. Proc. 22 (1958) 99.

6. D.M. Anderson (Compiler): Smectite Alteration. KBS TR 83-03 (1983).

7. D.M. Anderson (Compiler): Smectite Alteration II. KBS TR 84-11 (1984).

8. K. Anderson, B. Allard: Sorption of Radionuclides on Geologic Media - a Literature Survey. I: Fission Products. KBS TR 83-07 (1983).

9. K. Anderson, B. Torstenfelt, B. Allard: Sorption of Radionuclides in Geologic Systems. KBS TR 83-63 (1983).

10. M.A. Anderson, A.J. Rubin (Eds.): Adsorption of Inorganics at Solid-Liquid Interfaces. Ann Arbor Science (1981).

11. C.F. Baes, R.E. Mesmer: The Hydrolysis of Cations. J. Wiley & Sons (1976).

12. L.M. Barclay, R.H. Ottewill: Measurements of Forces Between Colloidal Particles. Spec. Disc. Farad. Soc. 1 (1970) 138; I.C. Callaghan, R.H. Ottewill: Interparticle Forces in Montmorillonite Gels. Farad. Disc. Chem. Soc. 57 (1974) 110.

13. I. Barshad: Thermodynamics of Water Adsorption and Desorption on Montmorillonite. Clays and Clay Minerals 8 (1960) 84.

14. G.W. Beall, B. Allard: Chemical Factors Controlling Actinide Sorption in the Environment. Trans. Am. Nucl. Soc. 32 (1979) 164.

15. G.W. Beall et al.: Sorption Behaviour of Trivalent Actinides and Rare Earth on Clay Minerals. In /52/, p.201.

16. G.W. Beall, B. Allard: Sorption of Actinides from Aqueous Solutions Under Environmental Conditions. In /166/, p.193.

17. G.W. Beall, B. Allard: Chemical Aspects Governing the Choice of Backfill Materials for Nuclear Waste Repositories. Nuclear Technology 59 (1982) 405.

18. M.M. Benjamin, N.S. Bloom: Effects of Strong Binding of Anionic Adsorbates on Adsorption of Trace Metals on Amorphous Iron Oxyhydroxide. In /166/, p.41.

19. P.R. Bloom, M.B. McBride, B. Chadbourne: Adsorption of Aluminium by a Smectite. I: Surface Hydrolysis During Ca^{2+}-Al^{3+} Exchange. Soil Sci. Soc. Amer. J. 41 (1977) 1068.
M.B. McBride, P.R. Bloom: II: An Al^{3+}-Ca^{2+} Exchange Model. Ibid. p.1073.

20. Z.Borovec: The Adsorption of Uranyl Species by Fine Clay. Chemical Geology 32 (1981) 45.

21. A.C.M.Bourg, P.W. Schindler: Ternary Surface Complexes. Chimia 32 (1978) 166; 33 (1979) 19.

22. T.S. Bowers, K.J. Jackson, H.C.Helgeson: Equilibrium Activity Diagrams for Coexisting Minerals and Aqueous Solutions at Pressures and Temperatures to 5 kb and 600°C. Springer (1984).

23. G.W. Brindley, G. Brown (Eds.): Crystal Structure of Clay Minerals and their X-Ray Identification. Mineralogical Soc. Monograph No.5. Mineralogical Soc., London (1980).

24. B.G. Brodda, E. Merz: Zur Wirksamkeit von Tonmineralien als Rückhaltebarriere bei der Endlagerung radioaktiver Abfälle in Salzgesteinen. Z. dt. Geol. Ges. 134 (1983) 453.

25. D.G. Brookins: Geochemical Aspects of Radioactive Waste Disposal. Springer (1984).

26. F. Bucher et al.: Herstellung und Homogenität hochverdichteter Bentonitproben. NTB 82-05 (1982).

27. F. Bucher, U. Spiegel: Quelldruck von hochverdichteten Bentoniten. NTB 84-18 (1984).

28. R. Calvet: Adsorption dipolaire et conductivité de l'eau absorbée sur la montmorillonite calcique. Proc. Int. Clay Conf. (1972) 519.

29. H.T. Chan: A Progress Report on Laboratory Studies of Clay Type Grouting (Sealing) Materials. AECL-TR-188 (1982).

30. N.A. Chapman, I.G. McKinley, J. Smellie: The Potential of Natural Analogues in Assessing Systems for Deep Disposal of High-Level Radioactive Waste. NTB 84-41 (1984).

31. L. Carlson, P. Bo: Sorption of Radionuclides on Clay Minerals. In IAEA-SM-257: Environmental Migration of Long-Lived Radionuclides. IAEA (1982).

32. F. Casteels et al.: Corrosion of Materials in Clay Environment. In R. Odoj, E. Merz (Eds.): Internat. Seminar on Chemistry and Process Engineering for High-Level Liquid Waste Solidification. Jül-Conf. 42, Vol.2 (1981).

33. D. Craw: Ferrous-Iron Bearing Vermiculite-Smectite Series Formed During Alteration of Chlorite to Kaolinite, Otago Schist, New Zealand. Clay Minerals 19 (1984) 509.

34. J.A. Davis: Adsorption of Natural Organic Material from Freshwater Environments by Aluminium Oxide. In R.A. Baker (Ed.): Contaminants and Sediments Vol.2, p.279. Ann Arbor Science Publ. (1980).

35. J.B. Dixon, M.L. Jackson: Properties of Intergradient Chlorite-Expansible Layer Silicate of Soils. Soil Sci. Soc. Amer. Proc. 26 (1962) 358.

36. J. Dresselaers. F. Casteels, H. Tas: Corrosion of Construction Materials in Clay Environments. In S.V. Topp (Ed.): Scientific Basis for Nuclear Waste Management IV. Elsevier (1982).

37. J.I. Drever: The Geochemistry of Natural Waters. Prentice-Hall, Englewood Cliffs (1982).

38. D. Eberl, J. Hower: Kinetics of Illite Formation. Geol. Soc. of America Bull. 87 (1976) 1326.

39. D. Eberl, J. Hower: The Hydrothermal Transformation of Sodium and Potassium Smectite into Mixed-Layer Clay. Clays and Clay Minerals 25 (1977) 215.

40. D. Eberl: The Reaction of Montmorillonite to Mixed-Layer Clay: The Effect of Interlayer Alkali and Alkaline Earth Cations. Geochim. Cosmochim. Acta 42 (1978) 1.

41. D. Eberl: Reaction Series for Dioctahedral Smectites. Clays and Clay Minerals 26 (1978) 327.

42. C.H. Edelmann, J.Ch.L. Favejee: On the Crystal Structure of Montmorillonite and Halloysite. Zeitschr. f. Kristallographie 102 (1940) 417.

43. C.H. Edelmann: Relation entre les proprietées et la structure de quelques mineraux argilleux. Verre, Silicates, Ind. 12 (1947) 3.

44. T. Eriksen, A. Jacobsson: Ion Diffusion Through Highly Compacted Bentonite. KBS TR 81-06 (1981).

45. T.E. Eriksen, A. Jacobsson: Ion Diffusion in Compacted Sodium and Calcium Bentonite. KBS TR 81-12 (1981).

46. T.E. Eriksen, A. Jacobsson: Diffusion of Hydrogen, Hydrogen Sulfide and Large Molecular Weight Anions in Bentonite. KBS TR 82-17 (1982).

47. T.E. Eriksen, A. Jacobsson: Diffusion in Clay - Experimental Techniques and Theoretical Models. KBS TR 84-05 (1984).

48. C.A. Faucher, H.C. Thomas: J. Chem. Phys. 22 (1954) 258; G.R. Grysinger, H.C. Thomas: Ibid 64 (1960) 224.

49. A.P. Ferries, W.B. Jepson: The Exchange Capacities of Kaolinite and the Preparation of Homoionic Clays. J. Colloid and Interface Sci. 51 (1975) 245.

50. E. Forslind, A. Jacobsson: Clay-Water Systems. In F. Franks (Ed.): Water - A Comprehensive Treatise Vol.5, p.173. Plenum Press (1975).

51. F. Franks: Polywasser - Betrug oder Irrtum in der Wissenschaft? Vieweg (1984).

52. S. Fried (Ed.): Radioactive Waste in Geologic Storage. ACS Symposium Series No.100. Amer. Chem. Soc. (1979).

53. J.J. Fripiat et al.: Thermodynamic Properties of Adsorbed Water Molecules and Electrical Conduction in Montmorillonites and Silicas. J. Phys. Chem. 69 (1965) 2185.

54. B. Fritz, M. Kam, Y. Tardy: Geochemical Simulation of the Evolution of Granitic Rocks and Clay Minerals Submitted to a Temperature Increase in the Vicinity of a Repository for Spent Nuclear Fuel. KBS TR 84-10 (1984).

55. R.M. Garrels, C.L. Christ: Solutions, Minerals and Equilibria. Harper & Row (1965).

56. R.M. Garrels: Montmorillonite/Illite Stability Diagrams. Clays and Clay Minerals 32 (1984) 161.

57. Z. Gerstl, A. Banin: Fe^{2+}-Fe^{3+} Transformation in Clays and Resin Ion-Exchange Systems. Clays and Clay Minerals 28 (1980) 335.

58. W.F. Giggenbach: Construction of Thermodynamic Stability Diagrams Involving Dioctahedral Potassium Clay Minerals. Chemical Geology 49 (1985) 231.

59. R. Grauer: Kristalline Stoffe zur Verfestigung hochradioaktiver Abfälle. NTB 84-08 and EIR-Bericht No. 508 (1984).

60. R. Grauer: Behältermaterialien für die Endlagerung hochradioaktiver Abfälle: Korrosionschemische Aspekte. NTB 84-19 and EIR-Bericht No. 523 (1984).

61. R. Grauer: Synthesis of Recent Investigations on Corrosion Behaviour of Radioactive Waste Glasses. NTB 85-27 and EIR-Bericht No. 538 (1985).

62. D.J. Greenland: Interaction Between Humic and Fulvic Acids and Clays. Soil Science 111 (1971) 34.

63. R.E. Grim: Clay Mineralogy. McGraw-Hill (1968).

64. R.E. Grim, N. Güven: Bentonites. Geology, Mineralogy, Properties and Uses. Developments in Sedimentology 24. Elsevier (1978).

65. P. Grossenbacher: Die Komplexbildung von Fulvinsäure mit Schwermetallen. Diss. Universität Bern (1979).

66. G.C. Gupta, F.L. Harrison: Effect of Humic Acid on Copper Adsorption by Kaolin. Water, Air and Soil Pollution 17 (1982) 357.

67. R.G. Haire, G.W. Beall: Consequences of Radiation from Sorbed Transplutonium Elements on Clays Selected for Waste Isolation. In /52/; see also p.9 in /7/.

68. H.C. Helgeson, T.H. Brown, R.H. Leeper: Handbook of Theoretical Activity Diagrams Depicting Chemical Equilibria in Geologic Systems Involving Aqueous Phase at one Atm. and 0° to 300°C. Freeman, Cooper & Co., San Francisco (1969).

69. H.C. Helgeson et al: Summary and Critique of the Thermodynamic Properties of Rock Forming Minerals. Am. J. Sci. 278 (1978) 1 - 229.

70. P.C. Hiemenz: Principles of Colloid and Surface Chemistry. Marcel Dekker (1977).

71. C.H. Ho, N.H. Miller: Effect of Humic Acid on Uranium Uptake by Hematite Particles. J. Colloid and Interface Sci. 106 (1985) 281.

72. P. Holopainen, V. Pirhonen, M. Snellman: Crushed Aggregate-Bentonite Mixtures as Backfill Material for the Finnish Repositories of Low- and Intermediate-Level Radioactive Wastes. YJT 84-07 (1984).

73. J.J. Howard, D.M. Roy: Development of Layer Charge and Kinetics of Experimental Smectite Alteration. Clays and Clay Minerals 33 (1985) 81.

74. J. Hower et al.: Mechanism of Burial Metamorphism of Argillaceous Sediment: 1. Mineralogical and Chemical Evidence. Geol. Soc. of America Bull. 87 (1976) 725.

75. C.P. Huang, Y.T. Lin: Specific Adsorption of Co(II) and Co(III) EDTA - Complexes on Hydrous Oxide Surfaces. In /166/, p.61.

76. J.N. Israelachvili, G.E. Adams: Measurements of Forces Between Two Mica Surfaces in Aqueous Electrolyte Solutions in the Range of 0 - 100 nm. J. Chem. Soc. Farad. Trans. I, 74 (1978) 975.

77. R.M. Johnston: The Conversion of Smectite to Illite in Hydrothermal Systems. A Literature Review. AECL-7792 (1983).

78. R.M. Johnston, H.G. Miller: The Effect of pH on the Stability of Smectite. AECL-8366 (1984).

79. G. Kahr, M. Müller-Vonmoos: Unveröffentlichte Messungen (1984).

80. G. Kahr, R. Hasenpatt, M. Müller-Vonmoos: Ionendiffusion in hochverdichtetem Bentonit. NTB 85-23 (1985).

81. G. Kahr et al.: Wasseraufnahme und Wasserbewegung in hochverdichtetem Bentonit. NTB 86-14 (1986).

82. R. Keren, I. Shainberg: Water Vapor Isotherms and Heat of Immersion of Na/Ca-Montmorillonite Systems. I: Homoionic Clays. Clays and Clay Minerals 23 (1975) 193.

83. J.W. Kijne: On the Interaction of Water Molecules and Montmorillonite Surfaces. Soil Sci. Soc. Amer. Proc. 33 (1969) 539.

84. D.G. Kinniburgh, M.L. Jackson: Cation Adsorption by Hydrous Metal Oxides and Clay. In /10/, p.91.

85. G. Lagaly, R. Fahn: Ton und Tonminerale. In Ullmanns Encyklopädie der technischen Chemie, 4. Aufl., Band 23, p.311. Verlag Chemie (1982).

86. G. Lagaly, D. Klose, E. Heinerth: Silicate. In Ullmanns Encyklopädie der technischen Chemie, 4. Aufl., Band 21, p.365. Verlag Chemie (1982).

87. T.M. Lai, M.M. Mortland: Self-Diffusion of Exchangeable Cations in Bentonite. 9th Nat. Conf. Clay and Clay Minerals.

88. D. Langmuir: Uranium Solution-Mineral Equilibria at Low Temperatures with Application to Sedimentary Ore Deposition. Geochim. Cosmochim. Acta 42 (1978) 547.

89. F. Lanza, C. Ronsecco: Influence of a Backfilling Material on Borosilicate Glass Leaching. In W. Lutze (Ed.): Scientific Basis for Nuclear Waste Management V, p.125. Elsevier (1982).

90. D. Laske, C. Caflisch, K.H. Wiedemann: Untersuchungen zum Sorptionsverhalten von Cs-137 und Sr-90 in verschiedenen Gestein/Lösungs-Systemen. NTB 83-09 (1983).

91. A. Lerman: Geochemical Processes. p.345. J. Wiley & Sons (1979).

92. P. Liechti: Adsorption von Metallionen an der Grenzfläche Kaolinit-Wasser. Diss. Universität Bern (1982).

93. W.C. Linn, L.D. Whittig: Alteration and Formation of Clay Minerals During Clay Formation. Clays and Clay Minerals 14 (1966) 241.

94. P.F. Low, D.M. Anderson: Osmotic Pressure Equation for Determining Thermodynamic Properties of Soil Water. Soil Sci. 86 (1958) 251.

95. P.F. Low, J.F. Margheim: The Swelling of Clay. I: Basic Concepts and Empirical Equations. Soil Sci. Soc. Am. J. 43 (1979) 473.

96. P.F. Low: The Swelling of Clay. II: Montmorillonites. Soil Sci. Soc. Am. J. 44 (1980) 667.

97. P.F. Low: The Swelling of Clay. III: Dissociation of Cations. Soil Sci. Soc. Am. J. 45 (1981) 1074.

98. F.T. Mackenzie: Sedimentary Cycling and Evaluation of Seawater. In J.P. Riley, G. Skirrow (Eds.): Chemical Oceanography, 2nd Ed., Vol.1, p.309. Academic Press (1975).

99. J. Mamy, J.P. Gaultier: Evolution de l'ordre cristallin dans la montmorillonite en relation avec la diminution d'échangibilité du potassium. Proc. Int. Clay Conf. 1975, Mexico City, p.149. Applied Publishing Ltd., Wilmette, Ill., USA (1975).

100. J.A. Marinsky: The Complexation of Eu(III) by Fulvic Acid. KBS TR 83-14 (1983).

101. I.G. McKinley, J. Hadermann: Radionuclide Sorption Data Base for Swiss Safety Assessment. NTB 84-40 and EIR-Bericht No. 550 (1984).

102. I.G. McKinley: The Geochemistry of the Near-Field. NTB 84-48 (1985).

103. D. Meyer, J.J. Howard (Eds.): Evaluation of Clay and Clay Minerals for Application to Repository Sealing. ONWI-486 (1983).

104. M. Mosslehi, A. Lambrosa, J.A. Marinsky: The Interaction of Bentonite and Glass with Aqueous Media. KBS TR 83-33 (1983).

105. Mott, Hay & Anderson, Consulting Engineers: The Backfilling and Sealing of Radioactive Waste Repositories, Vol. 1 + 2. EUR 9115 EN (1984).

106. M. Müller-Vonmoos, G. Kahr: Bereitstellung von Bentoniten für Laboruntersuchungen. NTB 82-04 (1982).

107. M. Müller-Vonmoos, G. Kahr: Mineralogische Untersuchungen von Wyoming Bentonit MX-80 und Montigel. NTB 83-12 (1983).

108. M. Müller-Vonmoos, G. Kahr: Langzeitstabilität von Bentonit unter Endlagerbedingungen. NTB 85-25 (1985).

109. Nagra: Projekt Gewähr 1985. Endlager für hochaktive Abfälle; Das System der Sicherheitsbarrieren. NGB 85-04 (1985).

110. I. Neretnieks: Diffusivities of Some Dissolved Constituents in Compacted Wet Bentonite Clay MX-80 and the Impact on Radionuclide Migration in the Buffer. KBS TR 82-27 (1982); Nuclear Technology 71 (1985) 458.

111. I. Neretnieks: Some Aspects of the Use of Iron Canisters in Deep Lying Repositories for Nuclear Waste. NTB 85-35 (1985).

112. H.W. Nesbitt, G.M. Young: Prediction of some Weathering Trends of Plutonic and Vulcanic Rocks and Kinetic Considerations. Geochim. Cosmochim. Acta 48 (1984) 1523.

113. B.W. Ninham: Long-Range vs. Short-Range Forces. The Present State of Play. J. Phys. Chem. 84 (1980) 1423.

114. E.J. Nowak: Radionuclide Sorption and Migration Studies of Getters for Backfill Barriers. SAND 79-1110 (1980).

115. E.J. Nowak: Composite Backfill Materials for Radioactive Waste Isolation by Deep Burial in Salt. In J.G. Moore (Ed.): Scientific Basis for Nuclear Waste Management III, p.545. Plenum Press (1981).

116. C.H. Obihara, E.W. Russell: Specific Adsorption of Silicate and Phosphate by Soils. J. Soil Sci. 23 (1972) 105.

117. J.L. Oliphant, P.F. Low: The Relative Partial Specific Enthalpy of Water in Montmorillonite-Water Systems and Its Relation to the Swelling Pressure of These Systems. J. Colloid and Interface Sci. 89 (1982) 366.

118. U. Olofsson, B. Allard: Complexes of Actinides with Naturally Occuring Substances. Literature Survey. KBS TR 83-09 (1983).

119. H. van Olphen: Interlayer Forces in Bentonite. Clays and Clay Minerals 2 (1954) 418.

120. H. van Olphen: Unit Layer Interaction in Hydrous Montmorillonite Systems. J. Colloid Sci. 17 (1962) 660.

121. H. van Olphen: Thermodynamics of Interlayer Adsorption of Water in Clays. I: Sodium Vermiculite. J. Colloid Sci. 20 (1965) 822. II: Magnesium Vermiculite. Proc. Int. Clay Congress, Tokyo 1969, Vol.1, p.649, Jerusalem, Israel UP (1969).

122. H. van Olphen: An Introduction to Clay Colloid Chemistry. J. Wiley & Sons (1977).

123. J.D. Oster, P.F. Low: Activation Energy for Ion Movement in Thin Water Films on Montmorillonite. Soil Sci. Soc. Proc. 27 (1963) 369.

124. G.D. Parfitt: Fundamental Aspect of Dispersion. In G.D. Parfitt (Ed.): Dispersions of Powders in Liquids, p.81. Elsevier (1969).

125. R.M. Pashley: Hydration Forces Between Mica Surfaces in Aqueous Electrolyte Solutions. J. Colloid and Interface Sci. 80 (1981) 153; DLVO and Hydration Forces Between Mica Surfaces. Ibid. 83 (1981) 531.

126. E. Pery, J. Hower: Burial Diagenesis in Gulf Coast Pelitic Sediments. Clays and Clay Minerals 18 (1970) 165.

127. R.M. Pollastro: Mineralogical and Morphological Evidence for the Formation of Illite at the Expense of Illite/Smectite. Clays and Clay Minerals 33 (1985) 265.

128. R. Pusch: Required Physical and Mechanical Properties of Buffer Masses. KBS TR 33 (1977).

129. R. Pusch: Highly Compacted Na-Bentonite as Buffer Substance. KBS TR 74 (1978).

130. R. Pusch: Water Uptake, Migration and Swelling Characteristics of Unsaturated and Saturated Highly Compacted Bentonite. KBS TR 80-11 (1980).

131. R. Pusch: Swelling Pressure of Highly Compacted Bentonite. KBS TR 80-13 (1980).

132. R. Pusch: Stability of Deep-Sited Smectite Minerals in Crystalline Rock - Chemical Aspects. KBS TR 83-16 (1983).

133. R. Pusch: Use of Clays as Buffers in Radioactive Repositories. KBS TR 83-46 (1983).

134. R. Pusch, Th. Forsberg: Gas Migration Through Bentonite. KBS TR 83-71 (1983).

135. R. Pusch, L. Ranhagen, K. Nilsson: Gas Migration Through MX-80 Bentonite. NTB 85-36 (1985).

136. R.C. Reynolds, J. Hower: The Nature of Interlayering in Mixed-Layer Illite-Montmorillonites. Clays and Clay Minerals 18 (1970) 25.

137. C.I. Rich: Hydroxy Interlayers in Expansible Layer Silicates. Clays and Clay Minerals 16 (1968) 15.

138. H.E. Roberson, R.W. Lahann: Smectite to Illite Conversion Rates: Effect of Solution Chemistry. Clays and Clay Minerals 29 (1981) 129.

139. R.A. Robie, J.R. Fisher: Thermodynamic Properties of Minerals and Related Substances at 298.15 K and 1 bar Pressure and at Higher Temperatures. U.S. Geol. Surv. Bull. 1452 (1978).

140. B.L. Sawhney: Selective Sorption and Fixation of Cations by Clay Minerals: A Review. Clays and Clay Minerals 20 (1972) 93.

141. P. Schindler et al.: Ligand Properties of Surface Silanol Groups. J. Colloid and Interface Sci. 55 (1976) 469.

142. P. Schindler: Surface Complexes at Oxide-Water Interfaces. In /10/, p.1.

143. F. Schreiner, S. Fried, A.M. Friedman: Measurements of Radionuclide Diffusion in Ocean Floor Sediments and Clay. Nuclear Technology 59 (1982) 429.

144. R.J. Serne, D.J. Bradley: Methods Used to Estimate Geochemical Aspects of Radionuclide Migration from Waste Repositories. Trans. Am. Nucl. Soc. 32 (1979) 161.

145. I. Shainberg, E. Bresler, Y. Klausner: Studies on Na/Ca-Montmorillonite Systems. 1: The Swelling Pressure. Soil Sci. 111 (1971) 214.

146. S.Y. Shiao, P. Rafferty, E. Meyer: Ion-Exchange Equilibria Between Montmorillonite and Solutions of Moderate to High Ionic Strength. In /52/, p.297.

147. R. Siever, N. Woodford: Sorption of Silica by Clay Minerals. Geochim. Cosmochim. Acta 37 (1973) 1851.

148. J.P. Simpson: Experiments on Container Materials for Swiss High-Level Waste Disposal Projects. Part I: NTB 83-05 (1983); Part II: NTB 84-01(1984).

149. J.R. Sims, F.T. Bingham: Retention of Boron by Layer Silicates, Sesquioxides and Soil Materials. I: Layer Silicates. Soil Sci. Soc. Am. J. 31 (1967) 728; II: Sesquioxides. Ibid. 32 (1968) 364; III: Iron and Aluminium Coated Layer Silicates and Soil Materials. Ibid. 32 (1968) 369.

150. M. Snellman: Chemical Conditions in a Repository for Spent Fuel. YJT 84-08 (1984); see also YJT 84-11 (1984).

151. V.I. Spitsyn et al.: Influence of Irradiation with Gamma-Quanta and Beam of Accelerated Electrons on the Sorption Parameters of Clay Minerals of the Montmorillonite Group. In S.V. Topp (Ed.): Scientific Basis for Nuclear Waste Management IV, p. 703. Elsevier (1982).

152. G. Sposito: Thermodynamics of Swelling Clay-Water Systems. Soil Sci. 114 (1972) 243.

153. G. Sposito: Thermodynamics of Soil Solutions. Clarendon Press (1981).

154. G. Sposito, R. Prost: Structure of Water Adsorbed on Smectites. Chemical Reviews 82 (1982) 553.

155. G. Sposito: The Surface Chemistry of Soils. Oxford University Press (1984).

156. J. Środoń: Mixed-Layer Illite-Smectite in Low-Temperature Diagenesis: Data from the Miocene of the Carpathian Foredeep. Clay Minerals 19 (1984) 205.

157. F.J. Stevensons: Micronutrients in Soil 79 (1982). Quoted after /65/.

158. J. Studer et al.: Verfüllen und Versiegeln von Stollen, Schächten und Bohrlöchern, Band 1 und 2. NTB 84-33 (1984).

159. W. Stumm, H. Hohl, F. Dalang: Interaction of Metal Ions with Hydrous Oxide Surfaces. Croatica Chem. Acta 48 (1976) 491.

160. W. Stumm, R. Kummert, L. Sigg: A Ligand Exchange Model for the Adsorption of Inorganic and Organic Ligands at Hydrous Oxide Interfaces. Croatica Chem. Acta 53 (1980) 291. L. Sigg, W. Stumm: The Interaction of Anions and Weak Acids with the Hydrous Goethite Surface. Colloids and Surfaces 2 (1981) 101.

161. W. Stumm, J.J. Morgan: Aquatic Chemistry (in particular Chapter 10: The Solid-Solution Interface). J. Wiley & Sons 1981.

162. J.W. Stucki, D.C. Golden, C.B. Roth: Effects of Reduction and Reoxidation of Structural Iron on the Surface Charge and Dissolution of Dioctahedral Smectites. Clays and Clay Minerals 32 (1984) 350.

163. J.W. Stucki et al.: Effect of Oxidation State of Octahedral Iron on Clay Swelling. Clays and Clay Minerals 32 (1984) 357.

164. Y. Tardy, B. Fritz: An Ideal Solid Solution Model for Calculating Solubility of Clay Minerals. Clays and Clay Minerals 16 (1981) 361.

165. Y. Tardy, R.M. Garrels: A Method for Estimating Gibbs Energies of Formation of Layer Silicates. Geochim. Cosmochim. Acta 38 (1974) 1101. See also /164/.

166. P.H. Tewari (Ed.): Adsorption from Aqueous Solutions. Plenum Press (1981).

167. E. Tipping, J.R. Griffith, J. Hilton: The Effect of Adsorbed Humic Substances on the Uptake of Copper(II) by Geothite. Croatica Chem. Acta 56 (1983) 613.

168. B. Torstenfelt et al.: Radionuclide Diffusion and Mobilities in Compacted Bentonite. KBS TR 83-34 (1983).

169. B. Torstenfelt et al.: Iron Content and Reducing Capacity of Granites and Bentonites. KBS TR 83-36 (1983).

170. R.C. Turner, J.E. Brydon: Effect of Length of Time of Reaction on some Properties of Suspensions of Arizona Bentonite, Illite and Kaolinite in which Aluminium Hydroxide is Precipitated. Soil Sci. 103 (1967) 111.

171. C.E. Veawer, L.D. Pollard: The Chemistry of Clay Minerals. Developments in Sedimentology 15. Elsevier (1973).

172. B. Velde: Clays and Clay Minerals in Natural and Synthetic Systems. Developments in Sedimentology 21. Elsevier (1977).

173. B. Velde, A.M. Brusewitz: Metasomatic and Non-Metasomatic Low Grade Metamorphism of Ordovician Meta-Bentonites in Sweden. Geochim. Cosmochim. Acta 46 (1982) 447.

174. B.E. Viani, C.B. Roth, P.F. Low: Direct Measurement of the Relation Between Swelling Pressure and Interlayer Distance in Li-Vermiculite. Clays and Clay Minerals 33 (1985) 244.

175. K. Vogt, H.M. Köster: Zur Mineralogie, Kristallchemie und Geochemie einiger Montmorillonite aus Bentoniten. Clay Minerals 13 (1978) 25.

176. H. Wanner: The Effect of Sodium Bentonite on the Chemical Composition of Groundwater. EIR internal report TM-45-85-03 (1985); see also TM-45-85-17.

177. H. Wanner: EIR internal report AN-45-85-33 (1985).

178. B.P. Warkentin, G.H. Bolt, R.D. Miller: Swelling Pressure of Montmorillonite. Soil Sci. Soc. Am. Proc. 21 (1957) 495.

179. W.J. Weber, F.P. Roberts: A Review of Radiation Effects in Solid Nuclear Waste Forms. Nuclear Technology 60 (1983) 178.

180. A. Weiss et al.: Ueber das Anionenaustauschvermögen der Tonmineralien. Z. anorg. allgem. Chem. 284 (1956) 247.

181. A. Weiss: Die innerkristallinie Quellung als allgemeines Modell für Quellvorgänge. Chem. Ber. 91 (1958) 487.

182. A. Weiss: Ueber das Kationenaustauschvermögen der Tonminerale I: Vergleich der Untersuchungsmethoden. Z. anorg. allgem. Chem. 297 (1958) 232.

183. A. Weiss: Ueber das Kationenaustauschvermögen der Tonminerale II: Der Kationenaustausch bei den Mineralen der Glimmer-, Vermikulit- und Montmorillonitgruppe. Z. anorg. allgem. Chem. 297 (1958) 257.

184. A. Weiss: Ueber das Kationenaustauschvermögen der Tonminerale III: Der Kationenaustausch bei Kaolinit. Z. anorg. allgem. Chem. 299 (1959) 92.

185. Westinghouse Electric Corporation: Engineered Waste Package Conceptual Design. Appendix D: Backfill Considerations. ONWI-438 (1983).

186. J.H. Westsick et al.: Water Migration Through Compacted Bentonite Backfills for Containment of High-Level Nuclear Waste. Nuclear and Chemical Waste Management 4 (1983) 291.

187. E.J. Wheelwright et al.: Development of Backfill Materials as an Engineered Barrier in the Waste Package System - Interim Topical Report. PNL-3873 (1981).

188. B.J. Wood: Backfill Performance Requirements - Estimates from Transport Models. Nuclear Technology 59 (1982) 390.

189. T.T. Yokoyama, T. Nakazato, T. Tarutani: Polymerisation of Silicic Acid on Iron(III) Hydroxide. Bull. Chem. Soc. Jpn. 53 (1980) 850.

190. R.N. Yong, B.P. Warkentin: Soil Properties and Behaviour. Elsevier (1975). Quoted after /131/.

191. A.C. Zettlemoyer, G.J. Young, J.J. Chessik: Studies of the Surface Chemistry of Silicate Minerals III: Heat of Immersion of Bentonite in Water. J. Phys. Chem. 59 (1955) 962.